THESIS FOR THE DEGREE OF DOCTOR OF PHILOSOPHY

Electronic Control of Flexural Nanowire Vibrations

FABIO SANTANDREA

GÖTEBORGS UNIVERSITET

Department of Physics
University of Gothenburg
SE-412 96 Göteborg, Sweden 2011

Electronic Control of Flexural Nanowire Vibrations
FABIO SANTANDREA
ISBN: 978-91-633-5863-0
Electronic version available at:
http://hdl.handle.net/2077/25321

Doktorsavhandling vid Göteborgs Universitet

Condensed Matter Theory
Department of Physics
University of Gothenburg
SE-412 96 Göteborg
Sweden
Telephone +46 (0)31 786 9178

Typeset in LaTeX

Figures created using MATLAB, KPaint, KCircuit and POV-Ray.

Chalmersbibliotekets reproservice
Göteborg, Sweden 2011

FABIO SANTANDREA
Condensed Matter Theory
Department of Physics
University of Gothenburg

ABSTRACT

"Nanoelectromechanical systems" (NEMS) are nanometer-sized mechanical structures coupled to electronic devices of comparable size. The coupling between mechanical and electronic degrees of freedom, combined with their mesoscopic size, provide these systems with some unique properties that make them interesting from both the fundamental and technological point of view.

In this thesis, we present theoretical work about a specific kind of NEMS, that is a suspended doubly clamped carbon nanotube in which extra charge is locally injected through the DC voltage-biased tip of a scanning tunneling microscope (STM).

The analysis presented here indicates that, in the classical regime, under the conditions of weak dissipation or sufficiently strong electromechanical coupling, the equilibrium configuration of the suspended nanotube becomes unstable and the system evolves towards a state of self-sustained periodic oscillations that is reminescent of the single-electron "shuttle" regime in Coulomb blockade nanostructures. Furthermore, combining the conditions for the onset of the electromechanical instability with the local character of the charge injection provided by the STM, it seems possible to generate a selective excitation of the bending vibrational modes of the nanotube.

Instead of pumping energy into the suspended nanotube, the electromechanical coupling can be also exploited to remove energy from it. Even though the tunneling electrons represent a strongly nonequilibrium environment interacting with the mechanical subsystem, the analysis presented in this thesis shows that the dynamics of the nanotube in the regime of weak coupling is formally equivalent to that one of a quantum harmonic oscillator coupled to an equilibrium thermal bath characterized by an effective temperature that can be much lower than the environmental (i.e. thermodynamic) temperature.

This nonequilibrium cooling effect studied here has an intrinsic quantum mechanical nature, since it is based on the (bias voltage controlled-) destructive interference between the probability amplitudes associated to those inelastic tunneling processes characterized by the emission of quantized vibrational excitations. When the transport of charge is thermally activated, this mechanism provides a simple procedure to drive the oscillating nanotube to nearly its quantum ground state.

Keywords: NEMS, carbon nanotubes, Coulomb blockade shuttle instability, ground-state cooling, nonequilibrium thermodynamics.

Research publications

The work presented in this thesis is an introduction to and summary of the work presented in the following research articles, referred to as paper I, II, III and IV.

PAPER I

Self-organization of irregular nanoelectromechanical vibrations in multimode shuttle structures
L. M. Jonsson, F. Santandrea, L. Y. Gorelik, R. I. Shekhter and M. Jonson
Phys. Rev. Lett. **100**, 186802 (2008).

PAPER II

Selective excitations of transverse vibrational modes of a carbon nanotube through a "shuttle-like" electromechanical instability
F. Santandrea
Physics Research International vol. 2010, 493478. doi:10.1155/2010/493478.

PAPER III

Cooling of nanomechanical resonators by thermally activated single-electron transport
F. Santandrea, L. Y. Gorelik, R. I. Shekhter and M. Jonson
Phys. Rev. Lett. **106**, 186803 (2011).

PAPER IV

Suppression of stochastic fluctuations of suspended nanowires by temperature-induced electronic tunneling
F. Santandrea, L. Y. Gorelik, R. I. Shekhter and M. Jonson
arXiv:1105.1738.

These papers are appended at the end of the thesis.

Related scientific work by the author not included in the thesis:

Nonequilibrium and quantum coherent phenomena in the electromechanics of suspended nanowires
R. I. Shekhter, F. Santandrea, G. Sonne, L. Y. Gorelik and M. Jonson
Low Temperature Physics **35** (8-9) 662.

Electromechanical instability in suspended nanowire-based NEMS
F. Santandrea
Licentiate thesis, University of Gothenburg (2009).

Ground state cooling of nanomechanical vibrations based on quantum interference effects.
F. Santandrea
Technical report number 186 - Proceedings The Linneaus Summer School in Quantum Engineering, Hindås 2010 Department of Microtechnology and Nanoscience - MC2, Chalmers.

TABLE OF CONTENTS

Research publications I

Table of Contents IV

Preface V

1 NEMS 1
- 1.1 General remarks . . . 1
- 1.2 Dissipation in micro- and nano-mechanical systems . . . 5
  - 1.2.1 Zener theory of anelasticity . . . 6
- 1.3 Single electron shuttle transport . . . 9
- 1.4 Quantum limit of macroscopic mechanical systems . . . 17

2 Carbon nanotube-based NEMS 23
- 2.1 Carbon nanotubes . . . 23
- 2.2 Electromechanics of carbon nanotubes . . . 25
- 2.3 Scanning Tunneling Spectroscopy of carbon nanotubes . . . 28

3 Electromechanical instability in suspended nanowire-based NEMS 32
- 3.1 Nanotube dynamics in the classical regime . . . 34
- 3.2 Charge transport in the Coulomb blockade regime . . . 37
- 3.3 Electrostatic interaction . . . 45
- 3.4 Multimode shuttling of single electrons . . . 47
- 3.5 Geometrical scanning of nanotube bending modes . . . 51
- 3.6 Appendix A . . . 55

4 Cooling of nanomechanical resonators by thermally activated electron transport 58
- 4.1 Nanotube dynamics in the quantum limit . . . 59
- 4.2 Cooling by destructive interference . . . 63
- 4.3 Cooling in the zero-bias limit . . . 71
- 4.4 Appendix B . . . 76

5 Summary 79

Preface

I have seen all the works that are done under the sun; and, behold, all is vanity and vexation of spirit.
That which is crooked cannot be straight: and that which is wanting cannot be numbered.
I communed with mine own heart, saying, Lo, I am come to great estate, and have gotten more wisdom than all they that have been before me in Jerusalem: yea, my heart had great experience of wisdom and knowledge.
And I gave my heart to know wisdom, and to know madness and folly: I perceived that this also is vexation of spirit.
For in much wisdom is much grief: and he that increaseth knowledge increaseth sorrow.

Ecclesiastes, chap. 1

Je voudrais pas crever / Avant d 'avoir connu / Les chiens noirs du Mexique / Qui dorment sans rêver / Les singes à cul nu / Dévoureurs de tropiques / Les araignées d'argent / Au nid truffé de bulles [. . .]

Je voudrais pas crever / Sans savoir si la lune / Sous son faux air de thune / Aun côté pointu / Si le soleil est froid / Si les quatre saisons / Ne sont vraiment que quatre

Je voudrais pas mourir / Sans qu On ait inventé / Les rosés éternelles / La journée de deux heures / La mer à la montagne / La montagne à la mer / La fin de la douleur / Les journeaux en coleur / Tous les enfants contents / Et tant de trucs encore / Qui dorment dans les crânes / Des géniaux ingénieurs / Des jardin iers joviaux / Des soucieux socialistes / Des urbains urbanistes /Et des pensifs penseurs [. . .]

Je voudrais pas crever, Boris Vian†

Since the autumn of 2006 I have been working as a Ph. D. student in the Condensed Matter Theory group at the department of Physics of the University of Gothenburg. The material presented in this Ph. D. thesis is based on the results of my research work, which in general has been focused on the physical properties of nanoelectromechanical systems (NEMS). The thesis is organized in four chapters and an appendix which consists of four scientific papers, referred to as Paper I, II, III and IV.

The first chapter is a "not-so-general" introduction to the field of NEMS. The reason why it cannot be defined as "general" is that, even though this area of research is rather new, the pace at which its development proceeds is so fast and the spectrum of competencies involved (in physics as well as in engineering) is so broad that it is clearly impossible to condense all the interesting material in a single chapter. Rephrasing a very often quoted sentence by R. Feynman, we can say that there is much work to do "both at the top and at the bottom". The topics have been chosen consistently with the directions along which my research work as Ph. D. student has developed. Therefore, the material presented in the first two introductory chapters turns out to be the most closely related to the analyses presented in the appended research papers, e.g. energy dissipation in nanometer-sized mechanical systems, single-electron transport, physical properties of carbon nanotubes and quantum limit of NEMS).

If any claim of exhaustivity must be abandoned *a priori*, on the other hand, the viewpoint from which the whole work hs been conceived can be stated without ambiguity. In this thesis, as well as in the appended papers, the *fundamental* physical aspects of NEMS have been considered, rather than the *technological* reasons that make them interesting and challenging at the same time.

The third and fourth chapters are conceived specifically to provide the background underlying the works presented in Paper I and II and Paper III and IV, respectively. Some effort has been put in order to avoid unnecessary repetitions wherever possible. Finally, in chapter (5) the results contained in the papers are summarized.

CHAPTER 1

NEMS

"Nanoelectromechanical systems" (NEMS) are a class of nanometer-sized mechanical structures (for instance beams, cantilevers, gears, membranes) coupled to an electronic device of comparable dimensions. For a number of reasons, they can be considered as the natural result of scaling down to the nanometer scale the currently well developed technology of "micro-electromechanical systems" (MEMS), which concerns devices whose typical sizes range from 10 μm to 1 mm.

In this chapter we will review some of the general physical properties of NEMS. The viewpoint adopted here focuses more on the fundamental rather than the technological aspects. The material presented here is very far from being an exhaustive review of the field of NEMS. The criterion that has guided the selection of the topics treated here is their relevance in connection to the research activity of the author, whose main results are presented in the papers appended to the thesis. More detailed overviews of the field of NEMS can be found in the reviews by Blencowe [1,2] and Ekinci and Roukes [3].

1.1 General remarks

The application of fabrication techniques originally developed for semiconductor electronic devices (such as photolithography, electron beam lithography and reactive ion etching) has been decisive for the large-scale manifacturing of MEMS and the growth of the industry related to them. Part of these technologies constitutes also the bulk of one of the main methodologies elaborated for the fabrication of NEMS (the so-called *top-down* approach). Nowadays different categories of MEMS have found vast application in commercial products, for example as accelerometers, pressure sensors, components of displays and sensors for the detection and analysis of biological and chemical samples. The general structure and performance of NEMS is not in principle dissimilar from that of MEMS and it can be understood theoretically from the scheme shown in Fig. (1.1), which is taken from [3]. Typically, a nanoeletromechanical device comprises one or more movable elements, such as suspended beams, cantilevers or membranes, with at least one characteristic length in the nanometer range. The vibrational modes of this mechanical structure can

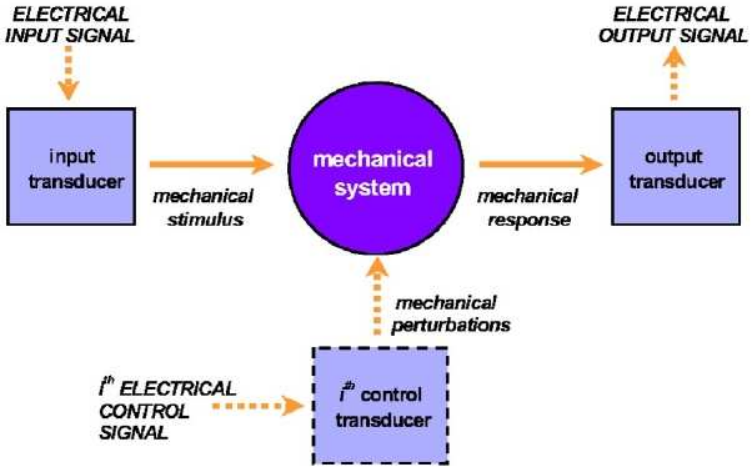

Figure 1.1: General scheme of a NEMS device [3].

excited through electrical signals, which are converted to mechanical perturbations through some suitable transducer device.

The readout of the NEMS mechanical response (i.e. the displacement of the movable element) is achieved through another transducer, that is responsible to transform the mechanical state back to an electrical signal. The signal produced by the output transducer can be eventually amplified for further elaboration. Additional electrical/mechanical perturbations can be included in order to modify some of the NEMS properties or for measurement purposes.

However, even though the scheme in Fig. (1.1) is appropriate to delineate the common traits of MEMS and NEMS functioning, the simple picture of NEMS as miniaturized versions of MEMS does not correspond exactly to reality. The possibility to control the motion of nano-sized objects and the charge transport through them allows to envisage a rich variety of novel applications, but at the same time the development of NEMS poses several fundamental and technical problems that can be safely considered irrelevant in the field of MEMS. As examples of such issues that need to be reconsidered at the nanometer scale, we mention: the dissipation of mechanical energy (and therefore the heat flow), the effects of charge quantization on the electronic transport, the role of nonlinear mechanical effects and the conditions under which the dynamics of mechanical systems comprising several thousands of atoms obeys quantum mechanical instead of classical rules.

From a technical point of view, the problem of transduction in nanoelectromechanical devices is still critical, since the sensitivity required to detect the mechanical displacement increases as the size of the movable part is reduced. Furthermore, the actuation and transduction processes, i.e. the input and output operations should be performed by devices that are coupled to the mechanical part of the NEMS in such a way that the interaction produces a readable signal without perturbing excessively the dynamics.

Most of the techniques developed to handle this kind of problems in the field of MEMS cannot be straightforwardly scaled down to the nanometer-scale. For instance, electronic and optical transduction methods, that are widely employed in MEMS, become unpractical at the nanometer scale because of the presence of parasitic capacitances and the diffraction limit.

The most promising approach, in order to overcome these difficulties, consists in coupling the nanomechanical element to some electronic device of comparable size such as a single-electron transistor (SET) [4, 5] or a superconducting Cooper-pair box [6]. The interest in studying this kind of coupled systems goes beyond what could be motivated by their being a potential solution to a technical problem. The coupling between mechanical and electronic degrees of freedom at the nanometer scale gives raise to a variety of peculiar physical effects, some of which have been investigated theoretically in the papers included in this thesis.

The most common geometries considered for NEMS both in theoretical and experimental works are characterized by a vibrating structure such as a cantilever or a doubly clamped beam. The typical frequencies of this nano-sized mechanical oscillators can be estimated through simple models based on classical elasticity theory. For example, the frequency of the fundamental flexural mode of doubly clamped beams with rectangular cross section is given by [7]:

$$\nu \equiv \frac{\omega}{2\pi} = 1.05 \frac{t}{L^2} \sqrt{\frac{E}{\rho}} \tag{1.1}$$

where L is the length of the beam, t its thickness, E is the Young modulus of the material, ρ its mass density and the numerical prefactor depends on the specific geometry. For some realistic choices of the values of the parameters E, ρ and typical lengths L, t ranging from the micro- to the nanometer scale, Eq. (1.1) suggests that NEMS vibrational frequencies fall between the MHz and the GHz scale, that is the interval of radio frequencies. A natural question that arises is then: to what extent theoretical predictions derived from "macroscopic" theories such as Eq. (1.1) can be considered accurate or even only meaningful for nanometer-sized mechanical systems?

Models based on classical elasticity theory are used extensively in the literature about NEMS and the predictions based on them turn out in a (perhaps surprisingly) good agreement with the experimental results. Simulations [8] and some experimental work [9] indicate that the breakdown of continuum mechanics should occur for structures on the order of a few tenths of lattice constants in cross section.

It is worth to remark that for real nanomechanical resonators expressions like Eq. (1.1) provide only an order-of-magnitude estimate of the frequency of their vibrational modes. Vibrating systems at the nanometer scale are particularly sensitive to the mechanical stresses that can result from the coupling with the external environment (including the mesoscopic electronic devices

which could be used for actuation or detection of their motion) or the presence of structural defects (particularly in multi-layered structures). In some cases the shift of the eigenfrequencies introduced by these perturbations can be controlled experimentally and provide a practical tool to gain information about the motion of the mechanical system, as it has been demonstrated for suspended carbon nanotubes-based NEMS.

Another relevant property that contributes to increase the vibrational frequencies of NEMS is the smallness of their masses, which are generally characterized in terms of effective values determined partly by material properties and partly by the geometry of the device. The possibility to combine high resonance frequencies and low masses ($\lesssim 10^{-15}$ g) makes the NEMS ideally suited to work as extremely sensitive mass sensing devices. Some rather impressive experimental results [10] suggest that the sensitivity of such devices could reach the level that would allow the detection of fews small molecules, which means masses of the order of $\sim 10^{-22}$ g. However, from the practical point of view the small effective mass of NEMS represent also a serious inconvenience to large scale manufacturing of devices, since it compromises the reproducibility of the results of the fabrication procedures.

Many of the envisaged applications involving NEMS depend crucially on the robustness of the nanomechanical oscillations against the damping induced by all the possible dissipative mechanisms which can play a significant role in a real device. The parameter which characterizes the resistance of an oscillator against any possible internal or external source of damping is the quality factor (usually denoted as Q), that is defined as the ratio between the maximum energy stored and the energy dissipated over one cycle.

The refinement of the nanofabrication procedures has made possible to observe, in the relatively short time interval of a few years, a remarkable trend of growth of the Q factors achievable for nanomechanical oscillators (from $\sim 10^2$ to $\sim 10^5$). From the theoretical point of view, there are no arguments that suggests the existence of some fundamental limit to the maximum Q factor of a nanomechanical resonator.

Large Q factors affect the NEMS dynamical behavior in several ways that are desirable for applications. For example, NEMS with large Q necessitate of lower power consumption to operate. The minimum operation power for a NEMS, P_{min}, can be estimated as the energy (per unit time) that has to be pumped into the system in order to drive it to oscillate with amplitudes of the same order of thermal fluctuations of the displacement, that is $P_{min} \simeq k_B T\omega/Q \sim 10^{-17}$ W at room temperature for $\omega \sim 100$ MHz and $Q \sim 10^4$. This estimated power is much smaller than the typical power dissipated in digital circuits, which is of the order of $\sim$ W. That might be of particular interest for electronic applications of NEMS, since the requirements of efficiency and sustainability in energy management is becoming more and more urgent for novel technologies.

Another useful feature related to the possibility of large Q factors is that,

in the linear regime, they sharpen the response of the device resonant external perturbations, which makes possible to resolve small shifts in the vibrational frequency that can carry useful information about the system and therefore provide the basic ingredient for highly performant sensing devices. Besides the interests for applications, dissipation in nanometer-sized mechanical systems is an interesting problem in itself from the fundamental point of view (see Sec. 1.2).

1.2 Dissipation in micro- and nano-mechanical systems

The question of energy dissipation and heat transport at the nanometer scale is extremely relevant for all the fundamental and practical application involving NEMS. In this section we describe briefly some of the physical processes which can be responsible for the dissipation of energy in NEMS and review a general method (Zener's theory of anelasticity) which can be used to include dissipative effects in mechanical models.

A natural question that arises is: what are the most relevant dissipative processes that limit the quality factor of nanomechanical oscillators? Perhaps it is impossible to answer this question in general, because all the geometric, structural and material (and, in some circumstances, even the *dynamical*) properties of the devices contribute to the irreversible exchange of energy between the mechanical degrees of freedom of the NEMS and the surrounding environment (that is, all the other *internal* and *external* degrees of freedom).

Furthermore, the quantitative agreement between theoretical models and experimental data is hindered by the fact that some physical properties at the nanometer-scale differ dramatically from the corresponding bulk values and even their definition itself is somewhat questionable because of the nearly-molecular or even atomic scale of many characteristic lengths of many NEMS. In other terms, the scaling of many physical properties with the size can be non monotonous as a consequence of the non negligible surface-to-volume ratio that is a distinctive feature of systems at the nanometer scale.

The damping of the vibrations of a nanomechanical oscillator originates from a variety of physical processes. Some of them can be significantly suppressed by clever design and careful manifacturing of the device. For example, the losses of energy due to clamping to the lateral supports in NEMS with suspended parts as movable elements are a major limitation to the mechanical Q factor [11, 12].

Among the dissipative effects related to the coupling of the oscillator with the external environment, we can mention the damping that could be introduced by a nearby electrical system used as a transducer [13] and the friction due to the pressure of the surrounding gas, if the NEMS does not operate in vacuum [14, 15]. In addition to these external sources of damping, the dis-

sipation of mechanical energy occur also through several processes that depend on the internal structure of the resonator (for example because of the presence of impurities and defects in the crystall lattice [16]) and/or on fundamental processes such as thermoelasticity [17,18] and phonon-phonon [19] and electron-phonon interactions [7].

The analytical modeling of these dissipative mechanisms leads to different approximate expressions for the Q factor, which in general is some function of the geometric and material properties of the oscillator, as well as of some environmental parameter such as pressure and temperature. If more than one mechanism contributes to the damping of the oscillations, the total quality factor by summing up the various contributions in the following way:

$$\frac{1}{Q_{tot}} = \frac{1}{Q_1} + \frac{1}{Q_2} + \dots . \tag{1.2}$$

1.2.1 Zener theory of anelasticity

The theory of anelasticity introduced by Zener [20] is an attempt to formulate a general phenomenological model for the description of the large variety of dissipative processes that take place in solids. In this section we briefly discuss Zener's approach since it has been applied in the analysis of the STM-carbon nanotube system presented in Paper II.

The "elastic solid" is a model for the mechanical behavior of solid-state systems based on the celebrated Hooke's "law", that is a linear relationship between the stress σ affecting a deformed body and its strain u, which reads:

$$\sigma = Mu \tag{1.3}$$

or equivalently, $u = J\sigma$, where $J \equiv 1/M$ is the modulus of compliance, while M is the modulus of elasticity of the material [21]. For an arbitrary deformation, the stress and strain are expressed as second-rank tensors and Eq. (1.3) must be intended as a set of linear equations expressing each component of the stress tensor in terms of all the components of the strain tensor (or vice versa). The physical picture of solid bodies underlying Eq. (1.3) can be summarized by the following properties:

1. the strain that results from any applied stress (and vice versa) has a unique equilibrium value;

2. within the natural limits imposed by the finite velocity of sound in the material, the strain (stress) is assumed to equilibrate instantaneously in response to an applied stress (strain);

3. the response to an applied stress (strain) is linear.

The uniqueness of the equilibrium values of stress and strain guarantees the possibility to consider these two physical quantities as suitable variables to describe the thermodynamic state of the system. Most important for the issue of dissipation in NEMS is property (2), since the istantaneous character of the mechanical response of an elastic solid implies that it behaves as a conservative system. The dissipation of mechanical energy is not taken into account in theoretical models based exclusively on Eq. (1.3).

Relaxing one or more of the three conditions underlying the theory of elasticity, it becomes possible to describe systems whose behavior deviates from the predictions of the simple elastic model. For example, some materials are characterized by the presence of multiple equilibrium values for stress and strain, which means that a certain initial state cannot be completely recovered by simply releasing the applied stress or strain (*plastic* or *viscoelastic* behavior).

Zener instead focused his attention on property (2), which is clearly an approximation since the mechanical response of a system to an applied stress (or strain) cannot be istantaneous. The physical origin of this retardation effect is the coupling of the mechanical system (which is described by the u and σ) with a large number of microscopic degrees of freedom (which could characterize, for example, impurities and defects in the crystal lattice of the system, or the molecules of a surrounding fluid). When the macroscopic variables u and σ are perturbed from their equilibrium values, the mechanical energy is transferred to these microscopic degrees of freedom, which, by means of irreversible kinetic processes such as diffusion, evolve towards the configuration of local equilibrium imposed by the new equilibrium values of u and σ. It is clear then that the dissipation of mechanical energy is fundamentally dependent on the time needed for the microscopic degrees of freedom to adjust themselves to the new equilibrium situation. The longer it takes, the more energy is transferred to them from the mechanical system.

Zener introduced the term "anelasticity" to indicate the behavior of solid-state systems which manifest retardation in the response to mechanical stimuli. It should be remarked that this retarded response does not replace completely "instantaneous" elastic behaviour described by Eq. (1.3), because every solid can be considered elastic to some (and often large) degree. The presence of anelasticity adds a small time-dependent contribution to the response of the system to mechanical perturbations.

In order to formulate a quantitative description of anelasticity, Zener considered the most general first-order linear differential equation with constant coefficients involving stress and strain:

$$\sigma + \tau_\epsilon \dot{\sigma} = M_R(\varepsilon + \tau_\sigma \dot{\varepsilon}) \tag{1.4}$$

The physical meaning of the three parameters τ_σ, τ_ε, M_R in Eq. (1.4) can be understood as follows. If a constant stress is applied to the solid, the strain relaxes exponentially to its equilibrium value and the characteristic time in which this process occurs is given by τ_σ. The same behaviour is found for

the stress and τ_ϵ is the stress relaxation time for a constant strain imposed to the solid. The parameter M_R is the proper elastic modulus associated to the deformation when all the relaxation processes have concluded.

In a typical experimental situation, the movable part of NEMS is a mechanical element vibrating at some frequency ω, that corresponds to the situation in which stress and strain are periodic functions of time, $\sigma = \sigma_0 e^{i\omega t}$, $\varepsilon = \varepsilon_0 e^{i\omega t}$, where σ_0 and ε_0 are constant. In order to understand how the damping of nanomechanical oscillations is taken into account in Eq. (1.4), it is convenient to discuss qualitatively two limiting cases, that are defined by different values of the ratio between the mechanical frequency and the stress and strain relaxation times (supposed to be independent of frequency).

First we consider the case of "fast" relaxation, that occurs if the vibrational frequency is much lower than the rates of stress and strain relaxation, i.e. $\omega \ll 1/\tau_\sigma$, $1/\tau_\varepsilon$). In this situation the stress and strain are basically at their equilibrium values at all times (at least with the time resolution determined by the period of the oscillations, $\sim 1/\omega$) and the system behaves basically like an elastic solid, $\sigma \approx M_R \varepsilon$ and the energy dissipated per cycle is negligible.

On the other hand, if the frequency of oscillations is much larger than the effective relaxation rates, $\omega \gg 1/\tau_\sigma$, $1/\tau_\varepsilon$, then the stress and strain have no time to relax, that is the kinetic processes that would realize the removal of energy from the mechanical system are basically "frozen" over the time scale defined by the period of the oscillations (adiabatic vibrations). On the basis of these considerations, the dissipation of energy turns out to be small also in this regime, which can be formally expressed by a relationship between stress and strain that is the same as for the elastic (i.e. non dissipative) solid, except for the elastic modulus that in this case assumes an "effective" or "unrelaxed" value, $\sigma \approx M_U \varepsilon$, where $M_U \neq M_R$.

In the intermediate regime, $\omega \sim 1/\tau_\sigma$, $1/\tau_\varepsilon$, the relationship between stress and strain is frequency-dependent and it can be found from Eq. (1.4) by Fourier transform. Eq. (1.4) becomes $\sigma(\omega) = E(\omega)\varepsilon(\omega)$, where the response function $E(\omega)$ is given by:

$$E(\omega) = \left(\frac{1 + \omega^2 \tau^2}{1 + \omega^2 \tau_\varepsilon^2} - \frac{i\omega\tau}{1 + \omega^2 \tau_\varepsilon^2} \Delta_E \right) E_R \equiv E_1(\omega) + iE_2(\omega). \tag{1.5}$$

In Eq. (1.5) the mean relaxation time $\tau \equiv \sqrt{\tau_\sigma \tau_\varepsilon}$ and the "relaxation strength" of the elastic modulus, $\Delta_E \equiv (E_U - E_R)/E_R$, where $E_{R,U} \equiv 1/M_{R,U}$ have been defined. Depending on the specific context in which Zener model is applied, these parameters can be expressed as functions of temperature and material and geometric properties of the system.

A general form to parametrize the effective relaxation time can be found if the rate at which the relaxation occurs is limited by the probability to overcome an energy barrier or an energy gap between two microscopic states (transitions between the states can be activated by absorbing energy from the mechanical vibrations, see [16]). In this case the relaxation rate $1/\tau$ can be

expressed by an Arrhenius-like form: $\tau^{-1} = \nu_0 \exp(-w/k_B T)$, where ν_0 is a frequency factor intrinsic to the process, T is the temperature and w is the height of the energy barrier.

The expression for $E(\omega)$ in Eq. (1.5) indicates that the stress has a component that is $\pi/2$ out of phase with respect to the strain. The work done by the stress over one period of oscillation, which corresponds to the energy dissipated in one cycle, is given be the time integral of the real part of $\sigma d\varepsilon/dt$ and the only non-zero contribution to it is proportional to $E_2\varepsilon_0$.

The ratio between the energy dissipated and the energy stored over one cycle defines the quality factor of an oscillating system, a dimensionless parameter which is useful to evaluate the robustness of the oscillator against the damping induced by all the possible sources of dissipation. In the case of Zener model this quantity is equivalent (up to a factor π) to the ratio between the imaginary and real parts of $E(\omega)$. Therefore, from Eq. (1.5) and assuming $\Delta \ll 1$, we can derive the Zener quality factor:

$$Q_Z(\omega)^{-1} \equiv \frac{E_2(\omega)}{E_1(\omega)} = \Delta_E \frac{\omega\tau}{1+(\omega\tau)^2} \tag{1.6}$$

The inverse quality factor defined in Eq. (1.6) has a Lorentzian dependence on the quantity $\omega\tau$. That is consistent with the physical considerations presented above, for which the dissipation is expected to be small in the limits $\omega\tau \ll 1$ and $\omega\tau \gg 1$. The peaks expected from Eq. (1.6) for $\omega\tau \sim 1$ have been actually bserved in a number of experimental situations, characterized by different relaxation processes, involving for example point-defects (in this are the peaks are known in the literature as "Snoek peaks"), reorientaton of defect pairs ("Zener peaks"), dislocations ("Bordoni peaks"), grain boundaries and thermoelasticity (for a comprehensive review see [21]).

We conclude this section by pointing out that the structure of Eq. (1.5) implies that Zener model of anelasticity can be easily included in the mechanical models derived from elasticity theory in order to describe the motion of nanomechanical systems. For example, in the theory of linear flexural oscillations of a doubly clamped beam, the effect of dissipation can be taken into account by replacing the ordinary Young modulus of the beam (that corresponds to the "relaxed" value in the terminology introduced above) with the complex-valued function shown in Eq. (1.5), that can be re-written as $E(\omega) = E_1(\omega) = [1 + i/Q_Z(\omega)]$. This approach has been followed in the work on the STM-carbon nanotube system described in Paper II.

1.3 Single electron shuttle transport

The phenomenon of Coulomb blockade is a remarkable example of how the electronic transport in tunneling nanostructures is crucially affected by the accumulation of charge in small parts of the devices. However, the presence of

uncompensated electric charges characterizes also other aspects of the physics of nanometer-sized devices. The electrostatic forces among such accumulated charges can induce significant mechanical deformations of the movable parts of the systems. This issue is not adressed in the standard theory of Coulomb blockade, however that is a central problem in the physics of NEMS.

The investigation of the consequences of adding mechanical degrees of freedom in a nanostructure in which the transport of charge is heavily influenced by Coulomb repulsion led Gorelik *et al.* to predict that, under certain conditions, the mechanical equilibrium state can be unstable [22]. The analysis that they performed on the system sketched in Fig. (1.2), that is a movable metallic grain situated between two voltage-biased bulk electrodes, showed that if the conditions for the electromechanical instability are attained the system dynamics evolves towards a steady regime characterized by self-sustained (since no external periodic driving is present) oscillations. During each cycle electrons are transferred from the left to the right electrode by the movable island and that supported the authors of [22] to introduce the terms "shuttle instability" and "shuttle transport of charge".

The physics of the shuttle instability has been theoretically explored in several regimes (e.g. quantum/classical and coherent/stochastic for what concerns the mechanical motion and the tunneling process, respectively) and both in normal and superconducting systems. For a thorough introduction and a guide to the vast literature on this subject, the reader is refered to the review papers [23, 24].

In this section we discuss the main features of the shuttle instability and the related regime of charge transport. The presentation is oriented towards the physical aspects of the mechanism (including some experimental results) rather than on the details of its theoretical description and it is thought to serve as introduction to the analysis of the electromechanical instability in NEMS, which is the main theme of the first part of this thesis.

The idea of the shuttle instability emerged originally from the theoretical study of nanostructures containing metallic grains or molecular clusters embedded in a self-assembled dielectric substrate of organic molecules between two DC-voltage biased electrodes. The model on which Gorelik *et al.* based their analysis is depicted in Fig. (1.2).

One of the reasons of interest in this kind of devices is the fact that they manifest Coulomb blockade effects at room temperature. Moreover, the dielectric layer of organic molecules between the leads is mechanically compliant, which implies that the metallic island can move under the effect of an external force. The combination of large Coulomb repulsion and mechanical compliance of the embedding substrate implies that the transfer of charge from one lead to the other across the central island can give rise to a significant deformation of these structures in response to the electrostatic force caused by the bias voltage. For what concerns the electronic transport properties, the system can be thought as a double tunnel junction. We consider first the usual

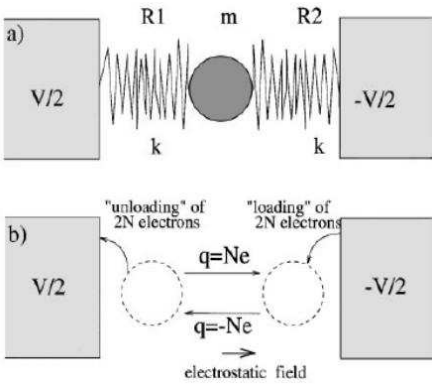

Figure 1.2: (a) Simple model of a soft Coulomb blockade system in which a metallic grain (center) is linked to two bulk electrodes by elastically deformable organic molecular links. (b) The static equilibrium state for the grain becomes unstable if the bias voltage is sufficiently large. When the grain is slightly shifted from the center of the system, it receives some extra charge of the same sign of the closest electrode and then it is accelerated towards the other electrode by the electrostatic force. The sign of the net grain charge alternates leading to an oscillatory grain motion and a novel "electron shuttle" mechanism for charge transport [22].

static situation, in which the motion of the center of mass of the grain is totally suppressed (or, more precisely, restricted to thermal fluctuations) and a constant bias voltage V is applied between the leads. In this case the net charge Q of the grain would be determined only by the current balance between the grain and the leads.

The possibility for the grain to move perturbs the current balance and hence the net charge of the island varies in time. The crucial observation is that whenever the grain is close to one of the leads, the charge exchange with the other electrode is almost completely suppressed, because the tunnel resistance of each junction depends exponentially on the distance between the grain and the corresponding lead. Therefore the value of the extra charge on the grain when it approaches one of the electrodes is determined by the polarization of the nearest lead at that moment. In other words, the extra charge on the grain at any given time t depends on which electrode the island has been close to at recent times $t' < t$. It turns out from these considerations that the extra charge that appears on the grain as a consequence of its center of mass motion, $Q(t)$, responds with some *retardation* to the variation in time of the grain position, $x(t)$. Within the framework of linear response theory, the non-instantaneous nature of the charge response can be expressed in the form: $Q(t) = \int \chi(t - t')x(t')dt'$, where $\chi(t)$ is a suitable response function, which is appreciably different from zero within a certain characteristic time interval.

Once that the grain is charged by electron tunneling at one of the leads, the electrostatic force due to the bias voltage pulls it towards the opposite lead. If the bias is simmetrically distributed as shown in Fig. (1.2), the extra

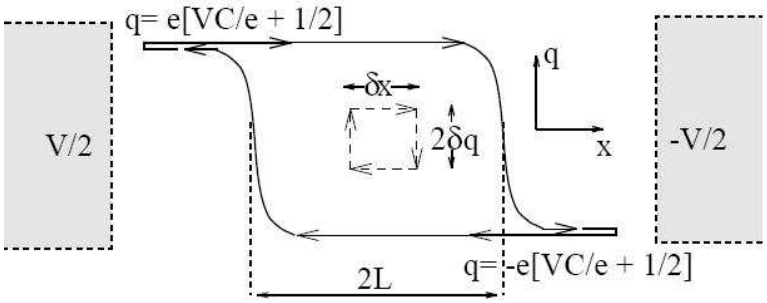

Figure 1.3: Charge response to a cyclic grain motion. The dashed lines describe a simple trajectory in the charge-position plane for which the work done on the grain by the electrostatic field can be easily calculated and shown to be positive. The electrostatic force always acts along the same direction of the grain displacement, hence pumping energy into the mechanical vibrations and leading to an instability (see text). The solid lines describe more realistically the charge response at large oscillation amplitudes [22].

charge is positive at the turning point near the positively charged electrode and negative at the turning point near the negatively charged electrode. The sign change of the grain charge occurs mainly in the proximity of the turning points, while for most of the trajectory between the leads the sign of the extra charge remains constant.

If we now consider the simple trajectory in the (x, Q) plane shown in the middle of Fig. (1.3) it becomes clear that the work W_{el} performed by the electrostatic force during one cycle is positive, which means that some energy is transferred from the electrostatic field to the moving island.

In other words, the charged grain is accelerated by the electrostatic force and, moreover, it finds itself in the right place at the right time to be accelerated since the electrostatic force is always applied along the same direction of the grain displacement (instead of the opposite one).

By virtue of the general properties of response functions [25] the sign of the electrostatic work done on the island does not depend on the trajectory, therefore the result $W_{el} > 0$ has a general validity (even for the more realistic trajectory represented by solid lines in Fig. (1.3). As a consequence of the pumping of energy from the electrostatic field, the metallic island starts to perform oscillations around the static equilibrium position with increasing amplitude. In absence of any form of dissipation of the mechanical energy, this increase would occur at arbitrarily low voltages and would continue without limits.

However, in any real system mechanical oscillations are actually damped by a variety o mechanisms (see Sec. (1.2)), therefore the positive electrostatic work performed on the grain is balanced by the negative work done by all the dissipative forces that can play a role in the system. If the net energy balance $W_{el} - W_{diss}$ per cycle turns out to be positive then the energy of the mechanical

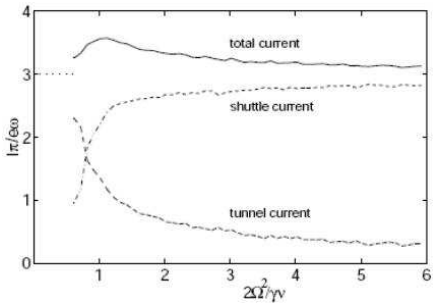

Figure 1.4: The total time-averaged current through the system sketched in Fig. (1.2) consists of two contributions, the shuttle current and the tunneling current. As the dissipation of mechanical energy (expressed through the damping rate γ) decreases, the shuttle current saturates to a constant value that is proportional to the frequency of the oscillations. At the same time, the tunneling current is proportional to the fraction of the oscillation period that the grain spends in the middle region, defined by $|x| < \lambda$. This fraction is inversely proportional to the oscillation amplitude, and hence the tunneling current decreases as γ^{-1} increases (from [22]).

vibrations increases and the static equilibrium position of the grain (defined by $x = 0$, $Q = 0$) becomes unstable. The necessary conditions for the onset of this electromechanical instability can be expressed equivalently in terms of a maximum value of dissipation that can be tolerated or a threshold value for the bias voltage (more generally, for the coupling between mechanical and electronic degrees of freedom) that needs to be overcome.

The analysis performed by Isacsson *et al.* in Ref. [26] elucidates the dynamics of the system once that the conditions for the instability are attained. After a transient regime, the moving island reaches a steady state characterized by finite-amplitude periodic motion (so called *limit cycle* oscillations [27]). During each cycle electrons are transferred from the left to the right lead by the oscillating island. This "shuttle-like" mechanism performs the transport of charge across the system in a radically different way from the sequence of tunneling process that characterize a static double junction system, as can be seen from Fig. (1.4).

The hallmarks of the shuttle mechanism of charge transfer has been investigated in several NEMS and molecular electronic devices. However, in most of the cases the experimental set-up presents striking differences from that usually considered in the theoretical works.

A variety of movable elements has been considered to play the role of the oscillating island: a macroscopic (radius $\sim$ 2 mm) metallic sphere [28], colloidal Au particles attached to a vibrating probe [29, 30], a metallic grain supported by a metallic or silicon cantilever (a sort of nanomechanical pendulum, [31–33]). Furthermore, all these devices were driven by an AC voltage, instead of DC as in the theoretical model. An alternative example of mechanical single-electron transistor has been fabricated and characterized in

the experiment of Koenig *et al.*, where a gold nanoparticle attached to a doubly clamped silicon nitride beam can act as an electron "shuttle" when the beam is actuated by piezoelectrically-generated ultrasonic waves [34].

Some effects due to the mechanical degrees of freedom appeared in the measured current-voltage characteristics of all these systems. However, no direct evidence for the development of the shuttle instability was found.

The "shuttle-like" transport of charge has also been considered as possible mechanism for explaining the current-voltage curve measured for the C_{60} single-electron transistor fabricated by Park [35]. In this device, a single C_{60} molecule was deposited in a gap 1 nm wide between two gold electrodes and a bias voltage was applied between them. The C_{60} molecule is trapped in the gap by van der Waals and electrostatic interactions with the gold electrodes. The current flowing across the molecule was found to increase sharply for certain values of the bias voltage. The step-like behaviour can be interpreted in terms of promotion of the tunneling (which implies that the current increases) due to the excitation of some quantized vibrational modes of the molecules.

In order to attribute this feature to the shuttle mechanism, it ought to be proved that the center-of-mass motion of the C_{60} is more involved in the transport of charge than the other vibrational modes. The peculiar shape of the current-voltage characteristic in Park's experiment can be interpreted also on the basis of the quantum mechanical theory of phonon-assisted tunneling and therefore the experimental evidence for the shuttle instability Park's experiment is not at all conclusive.

The results of a recent experiment performed by Moskalenko *et al.* [36] have been consistently interpreted according to the theoretical predictions of the single-electron shuttle model. The geometry of the device fabricated in this work is similar to that one considered in Park's experiment, but the material and the size of the components are different.

In the work of Moskalenko *et al.*, a gold nanoparticle with diameter of about 20 nm is embedded in the gap between two electrodes and attached to them through a monolayer of flexible organic molecules (octanedithiol). The electrodes are fabricated with rounded edges in order to reduce the difficulties that could arise because of small variations in the nanoparticle diameter. The whole device is realized on top of a silicon wafer coated with a ~ 1 μm SiO_2 layer. Planar 30-nm-thick gold electrodes separated by a gap of 10-20 nm are produced using electron-beam lithography followed by lift-off. Then the electrodes are covered with a monolayer of organic molecules, which have a length of about 1.2 nm each. Finally the gold nanoparticle is adsorbed by immersion of the device into acqueous gold solution.

Current-voltage characteristics are measured at room temperature after putting the device in a shielded dry box in order to protect it from moisture and decrease the electromagnetic noise.

The experimental current-voltage curves are shown in figure (1.6). The sharp rise in the current is attributed by Moskalenko *et al.* to the onset of

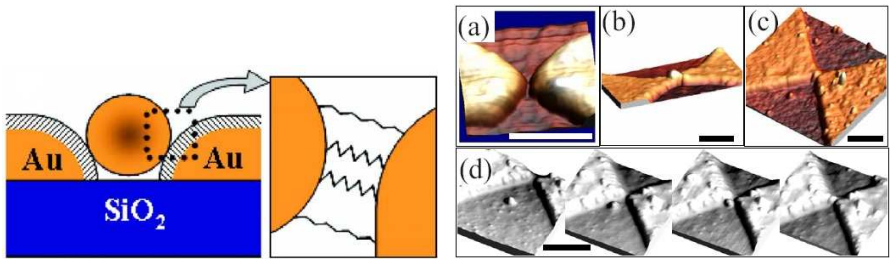

(a) (b)

Figure 1.5: (Left) Sketch of the experimental realization of the shuttle junction. The device consists of a 20 nm gold nanoparticle attached to two gold electrodes through monolayers of octanedithiol molecules acting as springs. The inset shows how the nanoparticle is attached to the monolayer; due to the curvatures of the nanoparticle and the electrode, some molecules are overstretched within the gap. (Right) (a) A pseudo-three-dimensional atomic force microscope (AFM) image of electrodes used for fabrication of a shuttle junction; (b) and (c) images of fabricated shuttle junctions; and (d) sequence of AFM images taken during manipulation of a 20 nm nanoparticle into the gap between two electrodes. Scale bars are (a) 100 and (b)-(d) 200 nm [36].

shuttle oscillations. In order to check that the transfer of charge across the device is really due to the nanoparticle, the current measured in presence of the nanoparticle has been compared to that one measured after removing it with an AFM tip, see Fig. (1.7). The qualitative features of the dynamics of the gold nanoparticle and its effects on the transport properties of the device are captured by the theoretical model reviewed in this section. However, the measured threshold voltage at which the instability develops is much higher than that one predicted by the theory. That has been explained with the tendency of the nanoparticle to get pinned somewhere between the leads, which can be due, for example, to van der Waals forces, whose effect on the shuttle mechanism has been investigated in [37]. At low voltages, the gold nanoparticle is trapped and the current through the device is due to sequential tunneling from one electrode to the other one, as in an ordinary double tunnel junction. The nanoparticle can escape from its locked position and start to oscillate if the electrostatic force (i.e. the bias voltage) is sufficiently strong. The amplitude of the vibrations initially increases and then saturates at some finite value determined by the balance between the energy adsorbed from the electrostatic field and the energy dissipated to the environment. The damping can prevent the island to get close enough to the electrodes in order to be loaded with the maximum number of electrons allowed by electrostatic repulsion, $N_{\max} = [CV/e + 0.5]$, therefore the effective electrostatic force acting on the island fluctuates and the measured current can be lower than the one expected from the simplest model. Furthermore, if the electrostatic force is not strong enough, the nanoparticle which succeeds to escape from the pinning trap, is immediately re-trapped and the oscillations are quickly suppressed.

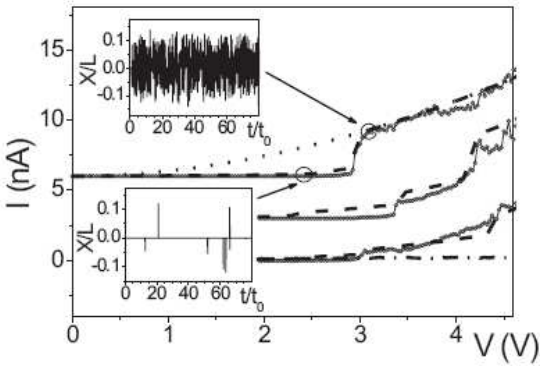

Figure 1.6: Experimental (symbols) and simulated (dotted and dashed lines) current-voltage characteristics of shuttle junctions. The dotted line corresponds to oscillations in the case of zero pinning and the dashed lines to the case of finite pinning in the system. The insets show the displacement of the gold nanoparticle as a function of time in two different bias voltages: one smaller and one larger than the threshold value that characterizes the transition into the shuttle regime. The leakage current through the monolayer of octanedithiol molecules is shown by dashed-dotted line (from [36]).

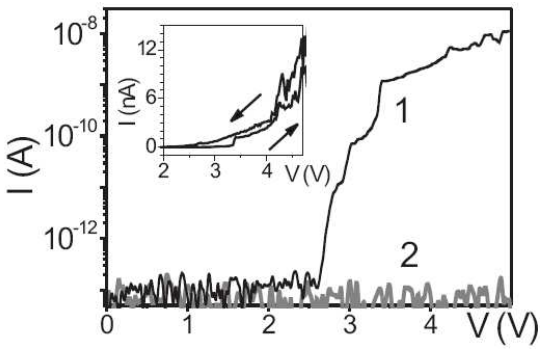

Figure 1.7: The current flowing through the device in presence of the gold nanoparticle in the shuttling regime (curve 1) and after removing the nanoparticle with an AFM tip (curve 2). The inset shows the hysteretic behaviour of the current-voltage curves obtained for a working shuttle junction in regimes of increasing and decreasing the applied voltage (from [36]).

Before ending this section, it is worth to mention the possible connection of the shuttle mechanism to something completely different, which is suggested by the very recent experimental results reported by Ristenpart *et al.* in [38].

They investigated the motion of charged water drops in a container filled half with water and half with oil unnder the effect of an applied DC voltage. What is usually expected is that once the drops (which are injected in the part filled with oil and charged by one of the two electrodes inserted in the container) reach the oil/water interface, they merge into the water. That is what actually happens for a large range of the applied voltage.

However, if the voltage is increased over a certain threshold value, then instead of merging, the water drops bounce on oil/water interface and reverse their velocity. They move back to the electrode, get charged and the turn again towards the oil/water interface. A steady periodic motion is established by applying a DC bias voltage, the same phenomenon that should characterize the single-electron shuttle. The mechanism of charge transfer is evidently different in the two cases (ionic transport for the liquid system and electron tunneling for the solid-state one), however the dynamics of the movable part of the system is qualitatively the same in the two systems.

1.4 Quantum limit of macroscopic mechanical systems

A considerable effort in the research field on NEMS has been recently devoted to explore the theoretical and experimental conditions to observe quantum (i.e. coherent) features in NEMS dynamics. At first sight, NEMS are quite different from the physical systems that we are accustomed to describe as "quantum mechanical", like for example atoms, molecules (microscopic) or superconductors and superfluids (macroscopic).

Under which conditions NEMS dynamics is expected to manifest quantum features? From a certain point of view, it is not immediate to address this point, since that would require to answer the following more general question: what *physical* conditions define the transition between classical and quantum physics? We know that it is not just a matter of length scale or number of constituents of a given system (see [39] for a thorough discussion of this point). What is usually indicated as "classical" or "semiclassical" limit in textbooks on quantum mechanics, that is letting $\hbar$ go to zero in order to recover some classical expressions from their quantum counterparts seems nothing more than a formal procedure.

In many circumstances classical mechanics is an adequate theoretical framework to explain the experimental results regarding nanometer-sized mechanical resonators. A possible attitude towards the problem of defining the conditions under which the classical description is expected to be no longer valid consists in focusing the attention on the precision of the measurement that is

performed on the resonator to detect its displacement. When this precision reaches the so-called "standard quantum limit" [40], then the dynamics of the resonator should present quantum instead of classical features. In general, any apparatus that can be used to measure the position of a movable object produces some perturbation on the motion of the system that is under measurement. That is what is intended as the "back-action" related to the measurement process. The measured root-mean-square fluctuations of the center-of-mass position of a mechanical oscillator, $\Delta x = \langle x^2 \rangle^{1/2}$, which represent the spread of the measurements of the center-of-mass position around the equilibrium value, contains always some contributions due to the back-action caused by the measurement system. They can be of fundamental or technical nature.

Quantum mechanics imposes a fundamental lower bound to the effect of the measurement-induced back-action, which can be expressed through the so-called "zero-point amplitude", $\Delta x_{gs} = (\hbar/2M\omega)^{1/2}$, where M is the oscillator mass and ω its angular frequency. According to the experimentally-oriented epistemological attitude expressed in, for example, Ref. [40] (which is closely related to the so-called "Copenaghen interpretation" or "non-interpretation" of quantum mechanics), if it turns out that $\Delta x \sim \Delta x_{gs}$, then the quantum-mechanical nature of the oscillator is manifested (see [41] and references therein).

In recent years, the investigation of the "standard quantum limit" of mechanical resonators has attracted a considerable amount of theoretical and experimental work nanoelectromechanical (and also optomechanical) systems. In general, the experimental detection of the zero-point motion of a mechanical oscillator must face two types of problems:

1. the development of a procedure through which it is possible to drive the oscillator to its vibrational ground state;

2. the need for a sensitive displacement detection scheme.

In the context of NEMS, point (2) is a general problem which is encountered in many circumstances, as we already mentioned in Sec. (1.1). The design of a sufficiently accurate position detection scheme is one of the main challenges in NEMS fabrication. The essential difficulty is based on the fact that, for a variety of reasons, most of the methods developed for MEMS cannot be straightforwardly applied to NEMS.

For example, optical techniques cannot be used because the diffraction of light cannot be avoided in nanostructures which are of the comparable size or even smaller than the wavelength of visible light. Piezoelectric methods typically heat the device so that it becomes impossible to work below a certain temperature, that, on the other hand, is requested for many applications. Moreover, as the oscillator frequency approaches the GHz range, the performance of magnetomotive detection deteriorates significantly because of parasitic capacitances. Finally, the efficiency of most of the microwave-based

transduction schemes is not sufficient to overcome the noise introduced by the amplification system that follows the transducer.

For all these reasons, the possibility to exploit parametric amplification or to couple the nanomechanical resonator to mesoscopic devices such as quantum dots, quantum point contacts and single-electron transistors, represent promising alternatives to the conventional, more "macroscopic". approaches to the problem of measuring the displacement of mechanical objects with high precision.

Regarding point (1), a common way to estimate how far a mechanical oscillator is from the quantum limit consists is based on the evaluation of the average number of quantized vibrational excitations (phonons) are expected to be in the system when it is in thermal equilibrium with the surrounding environment at a certain temperature T. It is known from statistical mechanics that this number is given by: $n_{th} = [\exp(\hbar\omega/k_B T) - 1]^{-1}$.

Therefore, when $k_B T \ll \hbar\omega$, then $n_{th} \ll 1$, which means that the only populated state is the ground state. For $\omega \sim 1$ GHz the quantum limit is reached for $T < 50$ mK, a temperature that is attainable with current dilution refrigerators. A quite sophisticated experiment, in which the ground-state cooling of an high-frequency (and quite big) mechanical resonator has been demonstrated by using a superconductive qubit, has been reported in [42].

However, apart from the technical difficulties related to the control of high-frequency resonators, there is a fundamental issue that limits in principle the performance of the *passive* (or thermodynamic) approach to cooling.

In the regime in which the populations of the excited vibrational states are smaller than the ground-state population (and quantum effects are expected to emerge), thermal conductance turns out to be quantized and that limits the rate at which a nanometer-sized system can reach thermal equilibrium with the environment [43]. In principle one could think of possible ways to optimize the heat transfer preserving the quantum nature of the vibrations, however a much simpler way to overcome this difficulty is offered by those methods that allow a systematic removal of the energy from the oscillator, based on the exploitation of experimentally controllable interactions *active cooling*.

In spite of the impressive variety of elecro- and opto-mechanical systems in which the problem of active cooling of mechanical degrees of freedom has been investigated, we can extrapolate the general features that are common to all the proposed schemes.

The basic ingredients of any scheme for active cooling can be summarized as follows:

- a two level system;
- some mechanical degrees of freedom coupled to the two level system;
- an environment inducing transitions between the two levels that involve the *irreversible* transfer of energy to/from the mechanical subsystem.

A comprehensive review of all the mechanisms that have been designed is too far beyond the scope of this thesis, however we will present here some general considerations that turn out to be useful in order to clarify the differences and the similarities between the cooling mechanism described in Paper III and IV and those ones proposed in the vast literature on the subject.

Several proposals [44] for ground-state cooling are based on the same physical principles underlying the laser-based methods developed for the cooling of trapped ions (illustrated, for example in [45]).

Other schemes strive to reproduce the electromagnetically-induced cooling by means of inelastic electronic transitions occurring in mesoscopic device coupled to the oscillator, such as tunnel junctions [46] quantum dots [47–49] or superconducting Cooper-pair boxes [50, 51]. The results about the cooling mechanism described in Paper III and IV can be collocated within this area of research.

In this context, cooling the mechanical degrees of freedom (being them the center-of-mass motion of ions confined in electromagnetic traps or of extended mechanical structures such as beams and cantilevers) is understood as the removal of energy from the mechanical system by means of another system (which we will often refer to as "the environment") which is far from thermodynamic equilibrium. Clearly, this definition deviates from the thermodynamic concept of cooling, which is based on the possibility for the system to reach *thermal equilibrium* (i.e. the same temperature) with a heat bath at lower temperature.

The removal of mechanical energy in active cooling scheme is performed by electronic transitions driven by coherent electromagnetic radiation (i.e. laser) in the optomechanical systems (including trapped ions) and by inelastic tunneling processes in the electromechanical devices. In both cases, the absorption of mechanical energy by the nonequilibrium environment (which can be the bosonic bath represented by the laser field or the fermionic (electronic) current flowing through a conducting movable structure) takes place because of the energy conservation constraint that governs the transitions between discrete, sharply defined electronic states.

The general features of the mechanism through which effective cooling can be achieved are well captured by the diagram shown in Fig. (1.8), which actually is taken from a review on laser cooling of atoms.

The "refrigerator" is represented as a quantum system with two electronic states, $|0\rangle$ (ground) and $|1\rangle$ (excited), separated by an energy gap given by $E_1 - E_0 = \hbar\omega_0$. Transitions between the two levels are promoted by an external time-varying field. When the frequency of the external field, ω_L, matches the gap between the electronic states (resonance condition), the electron "jumps" from the ground to the excited state, from which it decays (coming back to the ground) because of spontaneous emission (or analogous mechanisms in optomechanical and solid-state systems), that occurs at rate Γ.

In laser cooling of ions, this sequence of transitions manifests itself experi-

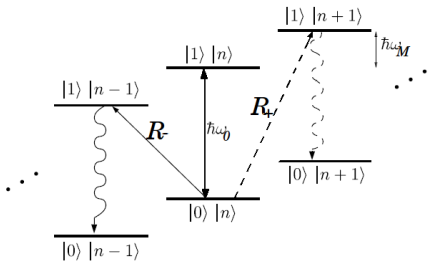

Figure 1.8: Electronic transitions leading to effective cooling ($|0n\rangle \rightarrow |0n-1\rangle$) and heating ($|0n\rangle \rightarrow |0n+1\rangle$) of the mechanical system. The processes that preserve the number of vibrons are not shown.

mentally as a Lorentzian curve centered at ω_0 with half width Γ in the dipole absorption spectrum of the ion, which shows the intensity of the light absorbed by the trapped ion as a function of the frequency of the driving laser.

The spatial confinement provided by the harmonic trap (or, in general, the mechanical degrees of freedom) generates a series of additional peaks in the dipole absorption spectrum, which are simmetrically located around ω_0. These peaks are centered at frequencies $\omega_j = \omega_0 \pm j\omega_M$, $j = 0, 1, 2 \ldots$ where $\hbar\omega_M$ is the quantum of vibrational energy. These additional lines due to the motion of the ion inside the trap form the so-called motional "sideband" spectrum. Analogous signatures of elastic and inelastic electronic transitions are detected experimentally also in solid-state systems, for example through scanning tunneling spectroscopy of suspended carbon nanotubes (see Sec. (2.3)).

The dynamics of electronic and mechanical degrees of freedom of the system is characterized by two sequences of states, $|0n\rangle$ and $|1n\rangle$, where n is the number of quantized vibrational excitations (vibrons). The external electromagnetic field induces transitions between the ground and excited states that can both preserve the number of vibrational excitations (elastic processes) and increase or reduce it (inelastic processes).

The mechanical degrees of freedom are effectively cooled if the rate that characterizes the cooling process (i.e. $|0n\rangle \rightarrow |0n-1\rangle$), is larger than the rate at which the heating processes (i.e. $|0n\rangle \rightarrow |0n+1\rangle$) occur. At leading order in the coupling constant, only single-vibron processes have to be considered and the cooling/heating rates can be written as $R_- = nA_-$ and $R_+ = (n+1)A_+$ (heating) where the rate coefficients $A_\pm$ depend on the parameters of the system. The effective cooling/heating dynamics can be characterized through a sequence of electronic transitions like: $|0n\rangle \rightarrow |1n \pm 0, 1\rangle \rightarrow |0n-1\rangle$.

In many cases, the performance of the cooling mechanism can be analysed in terms of rate equations for the populations of the vibronic states, $P(n,t)$, that express the probability to have n (vibrons) at time t. Under some conditions, these equations can be simply written down by considering the balance between the heating and cooling processes that make increase or decrease the number of vibrons by one, respectively.

Alternatively, the dynamics of the system can be analyzed in terms of the time-evolution of the average number of vibrons, $\langle n \rangle = \sum_{k=0}^{\infty} kP(k,t)$, which is determined by the following equation of motion:

$$\frac{d}{dt}\langle n \rangle = (\langle n \rangle + 1)A_+ - \langle n \rangle A_-. \tag{1.7}$$

A steady state solution of Eq. (1.7), $\overline{n} = A_+/(A_- - A_+)$, exists if the condition $A_- > A_+$ is fulfilled, that is when, per unit time, there are more processes leading to cooling rather than to heating.

Regarding the issue of what limits the efficiency of laser-based-like schemes for effective cooling (that is what prevents to reach an arbitrarily low number of vibrons), it should be stressed that the "sharpness" of the electronic levels plays a crucial role, especially to reach ground-state cooling (corresponding to $\langle n \rangle \ll 1$). If the broadening of the excited states Γ (i.e. the rate of spontaneous emission in the trapped ions cooling case) is of the same order or larger than the mechanical frequency (which determines the difference in energy between different sidebands), i.e. $\Gamma \gtrsim \omega_M$, then the cooling procedure is intrinsically less efficient, since some of the blue sidebands (corresponding to vibron emission processes) are excited together with the red sideband (that correspond to the one-vibron absorption process). In different contexts, this case is known as "Doppler cooling", "weak confinement" or "bad cavity" regime. On the other hand, if $\Gamma \ll \omega_M$, and the driving external field is "red-detuned", that is the condition $\omega_L - \omega_0 = -\omega_M$, then the cooling process is resonantly enhanced, whereas the heating is well off resonance. In this situation, known as "resolved sideband", "strong confinement" or "good cavity" regime, the average number of vibrons turns out to be $\overline{n} \approx (\Gamma/\omega_M)^2 \ll 1$, therefore ground-state cooling can be achieved.

As a final remark, we would like to point out that the theoretical framework outilined here has been applied to characterize active cooling schemes proposed for a broad variety of physical systems, including the nanoelectromechanical system considered in this thesis, as it will be illustrated in Chap. (4). For example, the expression of the average number of vibrons in the stationary state that results from Eq. (1.7) has the same structure of that one presented in Eq. (4.25) in Chap. (4).

In conclusion to this section, we would like to mention that, once that the quantum regime of NEMS could be readily accessible, a rich variety of applications are envisaged. For example, the control of the coherent motion of nanomechanical oscillators and the combination with devices that work effectively as quantum two-level systems (i.e. qubits), suggests the possibility to perform experiments that could help to shed new light (or new darkness) on the many questions related to the foundations of quantum mechanics (most of which originated by its linear character, that in principle does not prevent the superposition of states of "micro-" and "macroscopic" systems, such as in the celebrated case of "Schrödinger's cat paradox') [52].

CHAPTER 2

Carbon nanotube-based NEMS

In this section we will briefly present some general features of carbon nanotubes and outline the main motivations that make them a promising material for the realization of many applications involving NEMS. A comprehensive discussion of the physical properties of carbon nanotubes and their possible applications can be found in the vast literature existing on this subject, that nowadays amounts to a large number of review papers [53] and several books [54].

2.1 Carbon nanotubes

The choice of materials in the fabrication of NEMS plays a decisive role to determine the properties of the device. The most widely used materials for NEMS are those for which the fabrication methods in semiconductor technology are better developed, for example silicon, gallium arsenide/ aluminium arsenide (GaAs/AlGaAs) and silicon carbide (SiC).

However, alternative materials are constantly under study in order to improve the NEMS performances and explore new phenomena at the nanometer scale. Among the most promising materials for the development of NEMS are carbon nanotubes. Carbon nanotubes are quasi 1-dimensional (due to the large aspect ratio) cylindrical structures with diameters that range from half to a few nanometers. They can be seen as the result of rolling up one (for the single walled) or more (for the multi walled) 2-dimensional atomic layers of graphite (graphene) around a certain direction.

The orientation of the hexagonal carbon ring in the honeycomb lattice with respect to the axis can be taken almost arbitrarily, without any distortion of the hexagons except for that one due to the curvature of the nanotube. This geometric feature (named "chirality") of the carbon nanotube structure is related to the electronic properties of the nanotube, that is its being metallic or semiconducting.

Carbon nanotubes have been the subject of a remarkable research effort along many directions, since a paper by Iijima in 1991 [1] reported on their syn-

[1] Experimental observations of carbon nanotubes appeared even before Iijima's paper and that has generated some controversy to establish the priority in their discovery [55]

thesis during electric arc experiments to produce fullerenes [56].

As a result of their extraordinary mechanical and electronic properties, carbon nanotubes are expected to find use in a wide range of applications in material reinforcement, chemical sensing, drug delivery, solar cells, hydrogen storage and nanoelectronics. While most of research activities on carbon nanotubes are still at the fundamental level, there is an increasing number of commercial products which take benefit of the peculiar properties of these nanostructures. The industrial applications of carbon nanotubes are expected to increase after the development of practical methods for the large scale production of carbon nanotubes which make feasible to control some relevant properties, such as diameter and chirality.

The combination of peculiar mechanical and electronic properties make carbon nanotubes ideally suited for the realization of NEMS. Their high stiffness (Young modulus $\sim 10^{12}$ Pa), small cross-section, low density and defect concentration are all relevant characteristics for the fabrication of high-frequency mechanical oscillators. Furthermore, semiconducting carbon nanotubes can behave as transistors and that can be efficiently exploited for sensing the nanotube motion.

Experimental fitting to mechanical measurements of the Young modulus and elastic constants of nanotubes have been mostly made by modeling the nanotubes as elastic beams. The nanotube diameter is only a few times larger than the length of the bond between carbon atoms, therefore it is not evident that physical concepts and models developed for bulk systems should be valid to describe these nanostructures. However, continuum models of carbon nanotubes (such as beam theory for small deformations and shell theory in the case of larger and more complicated distortions) have been proven to provide a good description of their mechanical properties under many circumstances.

Due to their small size and typically low concentration of impurities and lattice defects, carbon nanotubes are ideal systems in order to investigate how atomic structure gives rise to the properties predicted by continuum elasticity theory which is usually applied to macroscopic objects. In many works the results of numerical methods based on an "atomic" perspective, such as molecular dynamics, density functional theory and tight-binding have been compared to those obtained by continuum models.

The remarkable mechanical and electronic properties of carbon nanotubes are a direct consequence of the peculiar electronic configuration of carbon and with its capability to combine with other elements in many different configurations. The electronic configuration of carbon in terms of atomic (hydrogen-like) orbitals is: $1s^2 2s^2 2p^2$. The two electrons in the $1s^2$ orbital are strongly bound and they do not significantly contribute to determine the properties of carbon in the crystalline phase.

The bond structure in graphite, that coincides with that in carbon nanotubes, can be explained in terms of the mechanism of sp^2 hybridization of atomic orbitals [54].

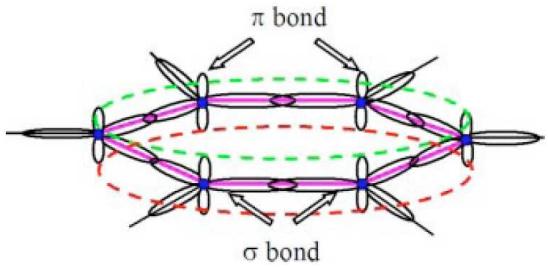

Figure 2.1: Basic hexagonal bonding structure for one graphite layer (the *graphene sheet*); carbon nuclei are shown as filled circles, out-of-plane π-bonds are represented as *delocalized* (dotted line), and σ-bonds connect the C nuclei in-plane [53].

In sp^2 hybridization one $2s$ orbital and two $2p$ orbitals combine to form three hybrid sp^2 orbitals at 120 °to each other within a plane (see Fig. (2.1)). The overlap of these in-plane states associated with neighbouring atoms determines the chemical bond between them and it is referred to as a σ-bond. This is a strong covalent bond that binds the atoms in the plane, and gives rise to the high stiffness and high strength of carbon nanotubes.

The remaining $2p$ orbital is perpendicular to the plane of the σ-bonds. In graphite the superposition of these out-of-plane orbitals associated with different layers results in a chemical bond between neighbouring layers which is referred to as π-bond. The π-bonds provide a very small contribution to the elastic properties of carbon nanotubes, which are mainly determined by the much stronger σ-bonds, however they play a decisive role to determine the electronic properties.

2.2 Electromechanics of carbon nanotubes

The considerations on the chemical bonds in carbon nanotubes are useful in order to understand the stability of the honeycomb lattice, however they provide only a static picture of these nanostructures. In reality, carbon atoms are not rigidly fixed at the lattice sites, but they can move to some degree in response to inter-atomic forces as well as to external perturbations.

The study of the lattice dynamics makes possible to understand the dynamical behaviour of the carbon nanotubes and it can be performed through standard methods of solid state physics (see [57] and [54] for the application to carbon nanotubes). The information obtained by this analysis are complementary to the predictions of macroscopic models derived from continuum elasticity theory. The mechanical state of the $2N$ atoms in the lattice unit cell can be represented as a linear combination of $6N$ normal modes of vibration, each of which represent a certain way of collective periodic motion of the atoms in the lattice. All the possible vibrational modes are characterized by a certain dispersion relation, $\omega_i(\mathbf{k})$, that is the function that describes how their frequency

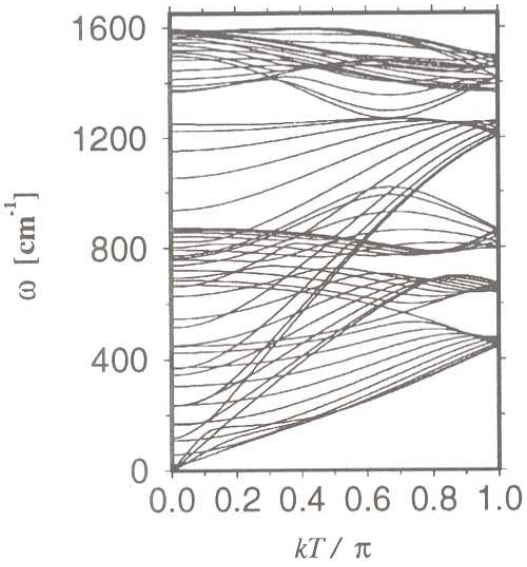

Figure 2.2: The calculated phonon dispersion relations of a carbon nanotube with chirality (10,10). The number of degrees of freedom is 120 and the number of distinct phonon branches is reduced to 66 after taking into account the simmetries of the unit cell [54].

depends on the wavevector (or wavelength).

An example of theoretical vibrational spectrum for carbon nanotubes is shown in Fig. (2.2) where, in the lowest part, four acoustic modes, defined by the condition $\omega_i(\mathbf{k} = \mathbf{0})$ are visible. They represent ways of atomic oscillations occuring along the same direction of the nanotube axis (longitudinal mode), perpendicular to it (transverse mode, which is doubly degenerate) and around it (twisting mode).

All the other $6N - 4$ curves in the vibrational spectrum of carbon nanotubes correspond to optical modes, such as the "radial breathing mode", in which the carbon atoms oscillate along the radial direction. The application of different experimental techniques makes it possible to detect many of the carbon nanotube vibrational modes. The radial breathing mode, corresponding to optical phonon branches, has been extensively studied by means of Raman spectroscopy [59]. In addition to this optical method, the local injection of extra electrons into a suspended nanotube from the tip of a scanning tunneling microscope has been shown to work as an effective probe for the radial breathing mode [60]. Longitudinal vibrations, corresponding to stretching modes of a bulk beam, have been detected through low-temperature transport spectroscopic methods [61].

The lowest energy part of the nanotube vibrational spectrum consists in the transverse (or bending or flexural) modes [61–66]. They have been experimentally investigated in several ways. Treacy *et al.* reconstructed their presence from the analysis of the blurring of images taken with a tunneling electron

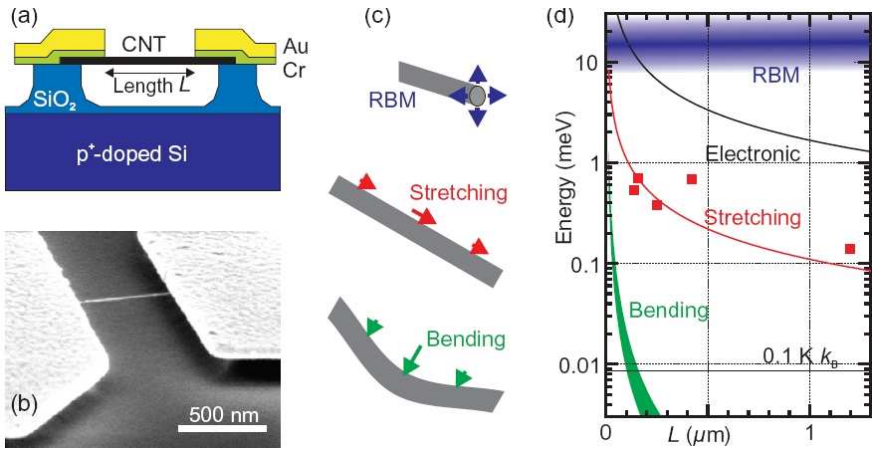

Figure 2.3: Side-view sketch (a) and scanning electron micrograph (b) of the geometry of a typical three-terminal nanoelectromechanical suspended single carbon nanotube device. (c) Schematic drawing of the vibrational modes and (d) predicted corresponding oscillator energy scales $\hbar\omega$ of suspended nanotube segments, taking into account the characteristic material properties of single-walled carbon nanotubes. The radial breathing mode scales with $1/d$ (d being the nanotube diameter), and the transversal bending mode is both diameter and tension dependent. Data points indicate observations of harmonic excitation spectra, i.e. quantized vibration modes, in low-energy transport spectroscopy experiments [58].

microscope (TEM) [67]. In the work of Garcia-Sanchez *et al.* instead, their dynamics was investigated by analyzing the motion induced on the tip of an atomic force microscope [68]. Besides these approaches, flexural oscillations of nanotube have been probed experimentally also by techniques based exclusively on electronic transport measurements, exploiting the set up sketched in Fig. (2.3) [62,64].

In this device a carbon nanotube is doubly clamped between two metallic leads (i.e. "source" and "drain") and suspended above a third electrode situated on the substrate (the "gate"). When a potential difference is applied over the nanotube, the system resembles the configuration of a Single Electron Transistor, with the nanotube playing the role of the central island. The reference to the SET has a concrete physical reason, since several works have reported the observation of the signatures of charging effects (the so-called Coulomb diamonds) in the transport characteristics of this system.

However, the mechanical degrees of freedom of the suspended nanotube add a further ingredient to the physics of this device, which has been demonstrated to be a quite suitable system to test the theoretical predictions about the effects generated by the coupling between motion and charge transport in nanostructures [69,70].

2.3 Scanning Tunneling Spectroscopy of carbon nanotubes

In this section we describe briefly the experimental results known about the nanoelectromechanical system that inspired the formulation of the theoretical model analyzed in this thesis.

In several works, LeRoy *et al.* have reported the results of transport measurements on suspended carbon nanotubes performed by the local injection of current from the tip of a scanning tunneling microscope (STM) [60]. This experimental technique turns out to be particularly effective in revealing the fingerprints of the mechanical degrees of freedom on the transport characteristics of the nanotube. The choice to study freely hanging carbon nanotubes combined with the atomic-scale spatial resolution of the STM make possible to accurately investigate such effects as Coulomb blockade and Luttinger liquid behaviour that are usually not observable in proximity of an highly conductive substrate (required by the STM). The fabrication procedure can be summarized as follows:

1. dry etching of 200 nm deep and 100 nm wide trenches on a substrate of SiO_2; the spacing between trenches is about 1μm;
2. deposition of a 100 nm thick film of Pt by evaporation over the whole sample in order to make it conductive;
3. deposition of square areas (5 μm side) of Fe:Mo catalyst;
4. chemical vapour deposition (CVD) at 100 °C for ten minutes in order to make the carbon nanotubes grow.

The nanotubes grow in random directions, some of them turn out to be suspended over the trenches for a distance of about 100 nm. Further details about the fabrication procedure can be found in [71].

LeRoy *et al.* performed low temperature transport measurements on the suspended carbon nanotubes, e.g. current-voltage characteristic and differential conductance curve. As a result of their measurements, sharp peaks appear in the differential conductance curve, which can be interpreted as the signatures of elastic electron tunneling events, in which the energy of the electronic state of the nanotube involved in the transport of charge matches the electrochemical potential in the STM tip. The difference in the energies corresponding to the peaks provides a measurement of the energy required to add one electron to the nanotube.

Furthermore, increasing the tunneling current across the nanotube, a number of less pronounced peaks appeared on the sides of the Coulomb peaks. This additional features of the differential curve can be attributed to *inelastic* tunneling processes, that take place when the transfer of charge is accompanied by the emission or absorption of quanta of mechanical energy (phonons).

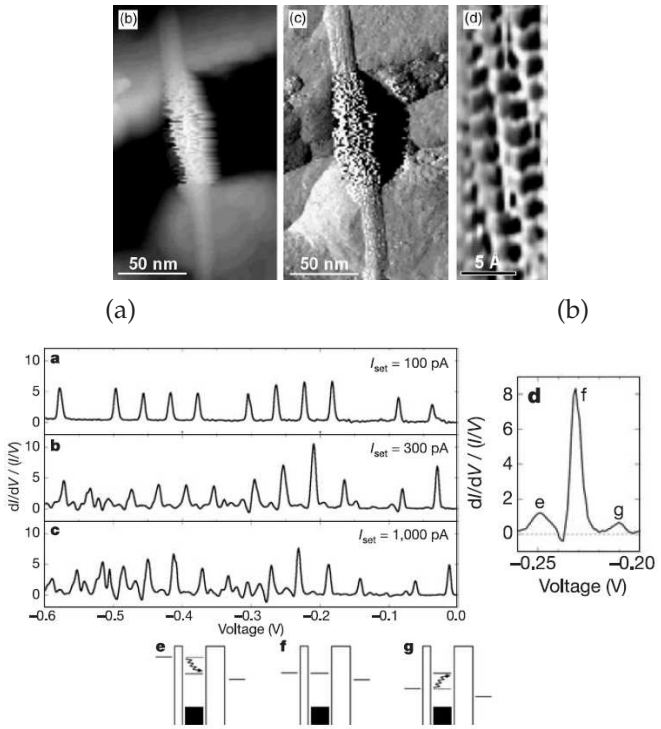

Figure 2.4: STM topography of a nanotube crossing a trench showing the freely suspended portion of the tube; STM current image showing current spikes on the suspended portion of the nanotube; high-resolution topography on a suspended portion of the nanotube showing the atomic structure. (Fig. from [71]) (a) Normalized differential conductance of a metallic single-wall carbon nanotube as a function of sample voltage taken with a low setpoint current I_{set} at -0.6 V. The tip is located at the centre of the suspended nanotube. A series of sharp peaks is visible due to the Coulomb staircase as the Fermi level of the substrate aligns with unoccupied states of the SWCNT. (b,c), Same as (a) with increasing setpoint current. A series of side peaks has appeared near the main Coulomb staircase peaks due to absorption and emission of phonons. (d) Zoom-in on one of the peaks showing side peaks corresponding to the emission (E) and absorption (G) of phonons. (e) Energy diagram for emission of a single phonon showing that an increased energy is needed for electron tunnelling. The distance between the solid black line and the top of the black box represents the Coulomb charging energy. (f) Energy diagram for elastic tunneling where a level in the nanotube is aligned with the leads. (g) Energy diagram for absorption of a phonon, which decreases the energy needed for tunneling. (h) Plot of the energy of the side peaks as a function of inverse diameter, showing a linear relationship. (Fig. from [60])

The peaks at energies above that one of the main peaks are due to electrons emitting a phonon during tunneling, while peaks at energies below are due to electrons absorbing a phonon during tunneling.

This interpretation is strongly supported by the fact that the side peaks appear at the same distance (in energy) from the main peaks. If this energy difference is interpreted as the energy carried by a single phonon, $\hbar\omega$, where ω is the mechanical frequency, LeRoy *et al.* identify the vibrational mode involved in the transport of charge as the radial breathing mode.

The presence of strong absorption peaks in the differential conductance curves shown in [60] is particularly surprising because at equilibrium, when no current is injected into the carbon nanotube, the thermal population of phonons at such low temperatures (~ 5 K) is expected to be very small. This observation indicates that the tunneling current induces a nonequilibrium phonon distribution in the suspended carbon nanotube.

CHAPTER 3

Electromechanical instability in suspended nanowire-based NEMS

In section (1.3) we reviewed the main features of the electromechanical instability known as "shuttle instability" and the related mechanism of charge transport. The nanoelectromechanical system in which this phenomenon has been originally investigated consists of a small (i.e. nanometer-sized) metallic particle embedded in soft dielectric layer between two electrodes. The only relevant mechanical degrees of freedom in this nanostructure are the center of mass position and velocity. All the dynamical variables related to the structure of the particle were ignored.

Hence, a natural question now arises: does the "shuttle" instability persist in mechanical systems whose dynamics is characterized by several mechanical degrees? The results presented in Paper I and II (together with some related works by other authors) that are discussed in this chapter address precisely this issue. The NEMS that is investigated for this purpose is a suspended carbon nanotube in which extra charge is injected from the tip of a scanning tunneling microscope (STM). The general description and some relevant experimental results regarding this system have been presented in Sec. (2.3).

The movable element in this NEMS is a doubly clamped metallic single wall carbon nanotube. The tip of the STM is positioned at some point along the nanotube axis. Extra charge is then locally injected into the nanotube by applying a bias voltage between the STM and the supporting leads. The nanotube can perform transverse oscillations over the trench between the leads and these mechanical oscillations are coupled to the tunneling current across the system because the width of the potential barrier that characterizes the STM-nanotube junction depends on the time-varying distance between the nanotube and the STM.

A number of theoretical studies performed on this system [72–75] indicate that an electromechanical instability, similar to the "shuttle-instability" predicted in mechanically-compliant Coulomb blockade nanostructures, can take place also in suspended nanowire-based NEMS.

In this chapter we will describe in detail the model analyzed to obtain the results presented in Paper I and II. The dynamics of the oscillating nanotube is assumed to be classical here, however some features of the model will be

retained also in the analysis of the quantum dynamics, which is presented in the next chapter.

Before introducing any model, we would like to discuss briefly some physical arguments on the basis of which it is possible to understand the onset of the electromechanical instability as plausible effect.

The tunneling of electrons to and from the nanotube is responsible for the time variation of the net charge on the nanotube, $Q(t)$, which is necessarily quantized, i.e. $Q(t) = -N(t)e$, where $N(t)$ denotes the number of extra electrons on the nanotube at time t. At any given time, the probability of electron tunneling through the STM tip-nanotube junction is strongly (exponentially) affected by the distance between the nanotube and the tip, whereas the probability of tunneling from the nanotube to the leads is constant. If the nanotube could be "frozen" very close or very far from the tip, the amount of net charge on it would be basically determined by the charge exchange with only the tip or the electrodes, respectively, and therefore it would depend uniquely on its position.

However, if we now consider the nanotube oscillating at some frequency ω, then, since the net charge on the nanotube cannot adjust itself instantaneously to the equilibrium value determined by the nanotube position, it follows that the amount of net charge of the nanotube at any time depends on its distance from the STM tip at earlier times. This effect of retardaded response has been already discussed in Sec. (1.3) for the shuttle system and it is particularly prononunced if the charge exchange rates between the nanotube and STM and the nanotube and the leads are comparable to the frequency of the mechanical oscillations.

Furthermore, when a bias voltage is applied between the STM and the electrodes, the nanotube is affected by an electrostatic force F which depends on the bias voltage, the extra charge that has tunneled to the nanotube and the position of the nanotube relative to the tip of the STM. The retardation that characterizes the response of the electronic degrees of freedom of the nanotube to the mechanical displacement implies that the electrostatic force performs a nonvanishing work on the nanotube.

If this work over one period of oscillation is positive, a net amount of energy is pumped into the mechanical system every cycle, which means that the amplitude of the oscillations increases. On the other hand, if the work turns out to be negative, some energy is removed from the nanotube, making the amplitude of the oscillations decrease. If the retardation is negligible, then the total work done during one cycle would be zero, since the electrostatic field is conservative.

In this chapter we will focus on the case of positive work, that resembles the situation of the ordinary point-like shuttle system. As a consequence of the pumping of energy into the mechanical vibrations, the equilibrium configuration of the nanotube becomes unstable. Because of the inevitable presence of dissipative processes that compete with the pumping mechanism and tend to

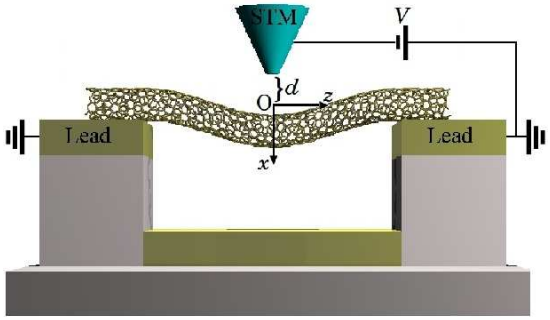

Figure 3.1: Sketch of the NEMS studied in this thesis. A metallic doubly clamped single wall carbon nanotube is suspended between two metallic electrodes and any deviation from the equilibrium configuration is described by the displacement along the $x-$axis, $u(z,t)$. An STM tip is put over the point $(0,0,z_0)$ along the nanotube axis and a bias voltage $V > 0$ is applied between the STM tip and the supporting leads. The distance between the nanotube and the STM tip at equilibrium is d, while R is the effective radius of the STM tip and L is the length of the nanotube.

bring the system to thermal equilibrium the, a finite threshold value for the electromechanical coupling is required for the instability to develop.

3.1 Nanotube dynamics in the classical regime

We already pointed out in section (2.1 that the application of continuum elasticity theory to describe the mechanical properties of carbon nanotubes has turned out to be successful in many cases. We will follow this approach here and model the suspended carbon nanotube as an elastic beam with clamped ends. Unless otherwise stated, we will use hereafter the notation defined in figure (3.1) [1]. The nanotube is modeled as an homogeneuos beam, with the origin of the reference frame at the midpoint and the z coordinate along the neutral axis (i.e. the line that undergoes nor compression neither extension during the flexure of the beam). The cross section is supposed to be uniform and situated in the xy plane. We indicate with $(0,0,z_0)$ the position of the STM tip, while d is the distance between the nanotube and the STM tip at equilibrium.

Suppose that the nanotube is deformed from its static equilibrium configuration by a bending force perpendicular to the $z-$axis. After that the force ceases to be applied, the nanotube starts to oscillates in the xz plane. In the limit of small amplitudes of oscillation, the deformation of the cross section can be neglected and the nanotube dynamics is fully described by the displacement of the neutral axis along the x direction, which in the following

[1] in which the $x-$axis points "downwards", which is the same orientation of the $x-$axis chosen in Paper I and II. However, in Chapter (4) the $x-$axis will be assumed to point upwards, consistently with the notation used in Paper III and IV.

will be denoted as $u(z,t)$.

Within the framework of elasticity theory, the simplest model through which we can describe the dynamics of the nanotube mechanical degrees of freedom is the Euler-Bernoulli equation [7]

$$\rho S\frac{\partial^2 u}{\partial t^2}+EI\frac{\partial^4 u}{\partial z^4}=F[Q(t),u,z,z_0] \tag{3.1}$$

where E is the Young modulus of the nanotube ($\sim$ 1 TPa), I is the cross-sectional area moment of inertia, ρ is the mass density and S is the cross section area. At the right-hand-side of Eq. (3.1) there is the bending force per unit lenght, F, that in general varies along the nanotube axis and depends on many factors: the time-varying extra charge on the nanotube, $Q(t)$, the distance between the nanotube and the STM tip and on the position of the STM tip. The boundary conditions corresponding to the case of a beam clamped at both ends are: $u(-L/2,\cdot)=u(L/2,\cdot)=\partial u/\partial z(-L/2,\cdot)=\partial u/\partial z(L/2,\cdot)=0$, where L is the length of the suspended part of the nanotube.

It can be shown [7] that Eq. (3.1) can be derived from the balance of the internal and external forces acting on each element of the beam when this is slightly bent. Alternatively, Eq. 3.1 (in absence of the force at the right-hand-side) results through the variational approach, which looks for the extremal condition of the action based on the lagrangian

$$\mathcal{L}[u,\partial_z^2 u,\dot{u}]=\int_{-L/2}^{L/2}dz\left[\rho S\frac{\dot{u}}{2}-\frac{EI}{2}\left(\frac{\partial^2 u}{\partial z^2}\right)^2\right]. \tag{3.2}$$

Defining the momentum density canonically conjugated to the displacement in the standard way $\pi(z,t)\equiv\delta\mathcal{L}/\delta\dot{u}$ and performing the Legendre transformation $\mathcal{H}[u,\partial_z^2 u,\pi]=\int_{-L/2}^{L/2}dz\pi\dot{u}-\mathcal{L}$, we can obtain the Hamiltonian corresponding to the lagrangian (3.2), that is

$$\mathcal{H}[u,\partial_z^2 u,\pi]=\int_{-L/2}^{L/2}dz\left[\frac{\pi}{2\rho S}+\frac{EI}{2}\left(\frac{\partial^2 u}{\partial z^2}\right)^2\right]. \tag{3.3}$$

The considerations developed in this thesis are based on the analysis of the beam dynamics (that is, of Eq. (3.1)) in terms of its normal modes. This approach amounts to expand the displacement field and the force per unit length over a complete set of orthogonal functions. A convenient choice of such a set is provided by $\{\varphi_j(z)\}$, i.e. the eigenfunctions of the differential operator $\frac{d^4}{dz^4}$ which is Hermitian if supplied with the clamped-clamped boundary condi-

tions. The normal-modes decomposition of $u(z,t)$, $\pi(z,t)$ and F reads

$$u(z,t) = \sum_j x_j(t)\varphi_j(z) \tag{3.4a}$$

$$\pi(z,t) = \sum_j \pi_j(t)\varphi_j(z) \tag{3.4b}$$

$$F[Q(t),u,z,z_0] = \sum_j f_j[Q(t),\mathbf{x},\ldots,z,z_0]\varphi_j(z) \tag{3.4c}$$

where $x_1(t),\ldots,x_j(t),\ldots \equiv \mathbf{x}$ and $\{f_j[Q(t),\mathbf{x},z,z_0]\}$ are time-dependent coefficients with the dimensions of length and force per unit length, respectively. The eigenfunctions $\{\varphi_j(z)\}$ define the spatial profiles of the normal modes of oscillation for the doubly clamped beam and they are given by:

$$\varphi_j(z) = C_1\left[\cos\left(\sqrt{c_j}\frac{z}{L}\right) - \cosh\left(\sqrt{c_j}\frac{z}{L}\right) + C_2\left(\sin\left(\sqrt{c_j}\frac{z}{L}\right) - \sinh\left(\sqrt{c_j}\frac{z}{L}\right)\right)\right], \tag{3.5}$$

where $C_2 \equiv (\cos\sqrt{c_j} - \cosh\sqrt{c_j})/(\sin\sqrt{c_j} - \sinh\sqrt{c_j})$, and C_1 is a constant determined by the normalization of the eigenfunctions (which is arbitrary). Here we choose to have dimensionless eigenfunctions, so that C_1 is fixed by the condition $\int_0^L dz\varphi_j(z)\varphi_k(z) = L\delta_{jk}$ [2]. The numerical coefficients $\{c_j\}$ in Eq. (3.5) can be calculated by solving the equation $\cos\sqrt{c_j}\cosh\sqrt{c_j} = 1$, which is derived by imposing the boundary conditions, and their values for the first few modes are: $c_j = 22.4, 61.7, 120.9, 199.9, 298.6$ (they increase roughly as n if n is the mode number).

The three bending modes with the lowest frequencies are plotted in figure (3.2), from which it is evident that they can be well approximated by the functions $\{\sin j\pi z/L\}$. This remark is useful to realize that these vibrational modes have definite symmetry properties related to the operation of spatial inversion along z with respect to the midpoint of the nanotube. The mode profiles $\varphi_j(z)$ whose index j is even turn out to be antisymmetric with respect to the nanotube midpoint, $\varphi_j(-z) = -\varphi_j(z)$, while those ones labeled by odd numbers are symmetric, $\varphi_j(-z) = \varphi_j(z)$. For the moment, we assume that the STM tip is positioned over the midpoint of the nanotube (i.e. $z_0 = 0$). In this way, the electromechanical coupling between the STM and the odd modes is negligible. The role played by the position of the STM tip in optimizing the coupling for different modes has been considered in Paper II and it will be discussed below.

Inserting the normal-modes expansions of $u(z,t)$ and F (3.4) into Eq. (3.1), it turns out that the beam dynamics is equivalent to the dynamics of a set of

[2] The eigenfunctions shown in Eq. (3.5) and Fig. (3.2) are actually obtained by imposing the double-clamping boundary conditions at $z = 0$ and $z = L$ rather than at $z = -L/2$ and $z = L/2$. That might be confusing, however it does not affect the results presented here. A similar inconvenience in the notation occurs in Figs. 2 and 3 of Paper II, in which the values of z_0/L on the horizontal axis should range between $-1/2$ and $1/2$ instead of 0 and 1.

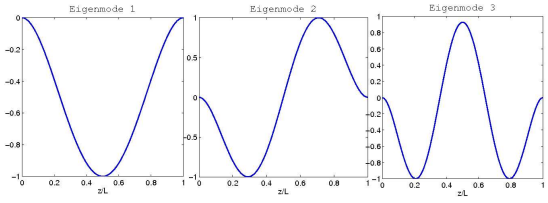

Figure 3.2: The first three bending modes of a doubly clamped beam.

coupled harmonic oscillators $\mathbf{x} \equiv \{x_1, x_2, \ldots\}$ with frequencies $\{\omega_j\}$, where $\omega_j = \frac{c_j}{L^2}(YI/\rho S)^{1/2}$, under the effect of the forces $\{f_j\}$

$$\ddot{x}_j + \gamma_j \dot{x}_j + \omega_j^2 x_j = L f_j[Q(t), \mathbf{x}, z, z_0] \tag{3.6}$$

We introduced in equation (3.6) a phenomenological damping force for each mode amplitude, $-\gamma_j \dot{x}_j$, where γ_j has the dimension of inverse time and represents the rate at which the mechanical energy is dissipated to the environment. The general aspects of the problem of dissipation in nanomechanical resonators have been introduced in section (1.2). In Paper I and II both a frequency-independent and Zener model-based damping coefficients have been considered.

In order to study the dynamics of the suspended carbon nanotube, an expression for the electrostatic force F must be specified. Furthermore, the extra charge on the nanotube varies in time because of tunneling and therefore an equation of motion for $Q(t)$ (which takes into account the variation of the width of the STM tip-nanotube tunneling barrier with the nanotube displacement) is needed to characterize the coupled dynamics of the mechanical and electronic degrees of freedom.

We will discuss the charge transport through the system in section (3.2) and derive an expression for the force in Sec. (3.3).

3.2 Charge transport in the Coulomb blockade regime

The quantization of the electron charge turns out to play a crucial role in the transport characteristics of small circuits containing tunnel junctions. The addition of one extra electron to a charged metallic body requires a finite amount of energy in order to overcome the electrostatic repulsion of the electrons that are already present. For systems whose size is between the nanometer and the micrometer scale this "charging energy" can be of the same order or even larger than the average thermal energy, which means that the transport of charge at low temperatures and low bias voltages is blocked. This suppression of the current due to electrostatic interactions is known as "Coulomb blockade" and it has been the subject of an intense stream of theoretical and

experimental research since the 70s ([76] and see [77] for a comprehensive review). It is worth to stress that a necessary condition for the manifestation of Coulomb blockade is that the electrical circuit under consideration contains tunnel junctions. While in an ordinary metal the polarization charge can assume any value (even fraction of the elementary charge e), since it is related to the displacement of the cloud of conduction electrons with respect to the positive background charge of the ions in the crystalline lattice, the tunneling through a potential barrier requires the transfer of one charged particle at the time.

Furthermore, the picture presented above is qualitatively correct to explain Coulomb blockade effects only in *metallic* systems that are not "too small". When the typical size of the system is in the range of few tenths of nanometers or below, the quantization of the electronic energy spectrum (which is not taken into account in metallic systems) is no longer negligible . As it can be readily understood by a simple "particle-in-the-box" calculation, the difference in energy between two electronic states scales with the size of the system. In general, the scale of the energy needed to add one extra electron, E_a, can be estimated as the sum of two contributions [78]:

$$E_a \approx E_k + E_C, \tag{3.7}$$

where E_C is usually denoted as the "charging energy" and its order of magnitude is given by $E_C \approx e^2/C$, C being the total capacitance of the body, while E_k is the kinetic energy of the added electron. For a free electron gas in three dimensions, $E_k = V/g(E_F)$, where V is the volume within which the gas is enclosed and $g(E_F)$ the density of states at the Fermi energy.

In the case of carbon nanotubes, which can be considered as quasi-one dimensional structures, the difference between the energies of the electronic states can be estimated as $\Delta_k \approx hv_F/2L$, where h is Planck's constant and v_F the Fermi velocity. For realistic values of the parameters, this estimate gives $\Delta_k \sim 1.7$ meV/μm, which shows that the quantization of the electronic spectrum can play a decisive role in the transport properties of carbon nanotubes.

In this chapter and, partially in the next one as well, we will however consider the case in which the metallic behavior is dominant and the nanotube can be basically treated as a long and thin conductive cylinder. This approximation is appropriate for nanotubes that are not too short ($\sim 1\mu$m) and allows to describe the electron-electron interaction in the system through a simple model based on classical electrostatics. In section (last) we will concerned instead with the limit in which the quantization of the electronic spectrum is most relevant and analyze the dynamics of the system through a fully quantum-mechanical treatment.

The transport of charge through the STM-nanotube system will be treated here within the framework of the so-called "orthodox theory" of Coulomb blockade [76,79], which has been successfully applied to describe a variety of

experiments. Within this theoretical framework, given an arbitrary arrangement of conducting bodies, the transfer of charge through the barrier between the two sides of a tunnel junction is considered as a *stochastic* process which occurs at a certain rate Γ. The amount of extra charge that can be found on an isolated body connected to the rest of the system by tunnel junction (a so-called "island") is always an integer multiple of the elementary charge e, i.e. the quantum wave-like nature of the charge carriers is ignored.

This theory describes correctly the physics of charge transport in small circuits provided that the following conditions are fulfilled:

- The electron energy quantization inside the conductors is ignored, i.e. the electron energy spectrum is treated as continuous. This approximation is valid only if $E_k \ll E_C, k_B T$.

- The time of electron tunneling through the barrier is assumed to be the smallest among all the time scales that characterize the system, including the average time interval between two consecutive tunneling events. Furthermore, when a tunnel event takes place, the state of the electrons in every part of the circuit is supposed to relax to a local equilibrium distribution (i.e. a Fermi function) within a time interval that is much shorter than the time that elapses between two consecutive tunneling events.

- The phenomenon of cotunneling, that is the simultaneous tunneling of several electrons due to the coherent superposition of electronic wavefunctions is not taken into account. This approximation is plausible as long as the transparency of the tunnel junctions is well below unity. In other terms, the "tunnel resistance" of all the junctions (see below for the definition) must be larger than the quantum unit of resistance, which is given by von Klitzig's constant, $R_Q = h/4e^2 \approx 6.5$ kΩ.

For what concerns the transport properties, the STM-nanotube system considered in this thesis is equivalent (if we neglect the effects related to the mechanical degrees of freedom) to two tunnel junctions connected in series, with a central conducting "island" (the carbon nanotube) located between two bulk electrodes (the STM tip on one side and the supporting leads on the other). In this type of circuits, if the orthodox theory presented above is applicable, the net charge on the island is unambiguosly determined at any time and, if we neglect any offset possibly introduced by charged defects, [3] it is quantized in

[3]This offset charge that would shift the net charge of the island and therefore mask the quantization effect can be removed by adding a third electrode (the "gate") capacitively coupled to the island. The circuit would assume then the configuration known as "single-electron transistor". If island mechanical degrees of freedom affects the transport of charge, such as in the case of the STM-nanotube system, the coupling to the gate can have also interesting dynamical effects, as discussed in Sec. (4).

units of the electron charge, $Q = -Ne$, where N takes integer values. According to the physical picture suggested by the orhodox theory of Coulomb blockade, $N(t)$ can be seen as a discrete random variable (see [80] as an example of analysis along these lines). Instead of looking for a suitable *stochastic* differential equation to describe the dynamics of $N(t)$, it is more straightforward to introduce probability distribution function, $P_N(t)$, which gives the probability to have N extra charges on the island at time t. The transport of charge through double tunnel junction circuits (such as the STM-nanotube system considered here) can be analyzed through a *deterministic* master equation which reads

$$\frac{dP_N}{dt} = \Gamma_{N,N+1}P_{N+1} + \Gamma_{N,N-1}P_{N-1} - (\Gamma_{N+1,N} + \Gamma_{N-1,N})P_N. \tag{3.8}$$

In Eq. (3.8), $\Gamma_{N,N'}$ is the rate for a transition from state N to state N', where $|N - N'| = 1$ since the charge of the island varies by units of e. The change of the island charge can take place because of tunneling through one junction (that is, in our case, the STM-nanotube junction) or the other (i.e. the nanotube-leads junction). The rates that appear in Eq. (3.8) take into account the two possibilities and therefore are given by the sum of two contributions:

$$\Gamma_{N+1,N} = \Gamma_S^{\leftarrow}(N,\cdot) + \Gamma_L^{\rightarrow}(N,\cdot) \tag{3.9}$$

$$\Gamma_{N-1,N} = \Gamma_S^{\rightarrow}(N,\cdot) + \Gamma_L^{\leftarrow}(N,\cdot), \tag{3.10}$$

The notation $\Gamma_\alpha^{\rightarrow(\leftarrow)}$ in Eq. (3.9) indicates that the charge tunnels through the STM tip-nanotube junction ($\alpha = S$) or the nanotube-leads junction ($\alpha = L$), from the electrode to the nanotube ($\rightarrow$) or from the nanotube to the electrode ($\leftarrow$). The $\cdot$ in Eq. (3.9) stands for all the physical quantities that contribute to determine the rate of the tunneling processes. The rest of this section is devoted to clarify which form can be derived for the tunneling rates within the framework of the orthodox theory and how Eq. (3.8) should be modified in order to account for the effects due to the electromechanical coupling in the STM-nanotube system.

The condition of low transparency of the tunnel junctions can be exploited as a starting point for a perturbative calculation of the tunneling rates. The two sides of the junction are modeled as reservoirs of non-interacting electronic quasiparticles. According to standard perturbation theory, the rate of transition through a given junction α from the state characterized by (quasi)-momentum $\hbar\mathbf{k}$ to the state with (quasi)momentum $\hbar\mathbf{q}$, is given by

$$\Gamma_\alpha^{k\to q} = \frac{2\pi}{\hbar}|t_{kq}|^2\delta(E_k - E_q - \Delta E_\alpha), \tag{3.11}$$

where $E_{k,q}$ are the energies of the initial and final electronic states and $|t_{kq}|^2$ is (quantum-mechanical) probability of transmission from the state $\mathbf{k}$ localized at one side of the junction to the state $\mathbf{q}$ localized at the other side, and

ΔE_α is the difference between them. The $\delta-$function in Eq. (3.11) enforces the constraint of energy conservation that must be fulfilled by the transition. The total rate of tunneling through the junction can be obtained from the sum of the rates between every pair of states (i.e. Eq. (3.11) weighted with a statistical factor that gives the probability of occupation of the states (that is, Fermi-Dirac distributions, since in the orthodox theory the electronic reservoirs are assumed to be at equilibrium). If the electronic spectra of the sides of the junction can be treated as continuous, the sums over the quasi-momenta $\mathbf{k}$, $\mathbf{q}$ can be turned into integrals. If the transmission probability can be approximated as independent of the electron energy, so that the total rate of tunneling reads eventually

$$\Gamma_\alpha^\eta = \frac{e^2}{R_\alpha} \frac{\Delta E_\alpha^\eta}{1 - \exp\left(-\Delta E_\alpha^\eta / k_B T_\alpha\right)} \tag{3.12}$$

where the indexes α and η run over the junctions and the "forward" ($\rightarrow$) and "backward" ($\leftarrow$) processes, respectively. According to Eq. (3.12), the temperature of the electronic reservoirs in the two sides of the junction is assumed to be the same, T_α. In spite of the name, the tunnel resistance, R_α, must not be interpreted as an ohmic resistance. It encloses the quantum features of the tunneling processes and it is defined as $R_\alpha = (2\pi/\hbar)|t_\alpha|^2 g_i g_f$, where $g_{i,f}$ is the density of states in the two sides of the junction evaluated at the respective Fermi energies. In the case of the STM tip-nanotube junction, the probability amplitude of tunneling through the barrier depends exponentially on the distance between the nanotube and the STM tip, that is $t_S \equiv t_S[u(z_0,t)] = \bar{t}_S \exp[-\sum_j x_j(t)\varphi_j(z_0)]$, where $\bar{t}_S$ is a constant and λ is the tunneling length of the junction, that is the characteristic distance within which the rate of electron tunneling is appreciably different from zero.

The difference in energy between the initial and final state, ΔE, can be taken from several sources. For example, it could come from the mechanical system coupled to the tunnel junction (this would be the case of *vibron-assisted* tunneling) or from the electrostatic energy stored in the capacitance associated to the junction. Here we focus on the latter situation, and come back to the former in Chapter (4), in connection with the results presented in Paper III and IV.

The transport of charge across a tunnel junction can be considered as an irreversible thermodynamic process. The electrostatic energy that the tunneling electron takes in order to overcome the potential barrier is dissipated as heat once it has reached the other side of the junction. That can induce an effective heating or cooling of the electronic reservoirs in the two sides of a tunnel junction, see [81]).

As a consequence of the second law of thermodynamics, the process occurs spontaneously if it leads to a decrease of a suitable thermodynamic potential, or "free energy" G. Which thermodynamic potential is appropriate to describe the tunneling process? That in general depends on the physical constraints imposed to the system [82]. The set of conductors which make up the circuit is

not isolated, since it is able to exchange heat and particles (i.e. electrons) with the surroundings. A typical experiment takes place at constant temperature, therefore we can imagine that the whole circuit is in contact with a thermal bath in equilibrium at temperature T. Furthermore, the electrostatic potentials of some of the metallic bodies in the circuit are held fixed by voltage sources, which amounts to say that they are connected to large reservoirs of particles with constant chemical potential μ.

Given these constraints, the possibility for a given tunnel process is determined by the variation of the generalized Gibbs free energy:

$$G_{fin} - G_{in} \equiv \Delta G = \Delta U - W_{vs}, \tag{3.13}$$

where ΔU is the variation of the electrostatic energy, which can be expressed equivalently in terms of the net charges on the conductors, q_i, or the potentials,ϕ_i, whereas W_{vs} is the work done by the voltage sources in order to keep constant the potentials of the conductors connected to them. In the works presented in this thesis, we consider only voltage sources that do not vary in time, therefore their work can be simply expressed as $\Delta W_{vs} = \sum_i q_i \phi_i$, where the sum runs over all the conductors which are held to constant potential.

According to the considerations presented above, a tunneling process that changes the electrostatic energy from U_i to U_f takes place spontaneously if $\Delta G < 0$. The variation of the electrostatic energy for an arbitrary set of metallic bodies can be calculated as

$$U = \frac{1}{2} \sum_{ij} \mathbb{C}_{ij} \phi_i \phi_j = \sum_{ij} \mathbb{C}_{ij}^{-1} q_i q_j, \tag{3.14}$$

$\mathbb{C}_{ij}$ are the elements of "Maxwell's capacitance matrix" ($\mathbb{C}^{-1}$ being its inverse), which relates the charges and the potentials: $q_i = \sum_{j=1}^{M} \mathbb{C}_{ij} \phi_j$ [83]. The possibility to characterize the relationship between charges and potentials through a matrix is a direct consequence of the linear nature of Maxwell equations. The coefficients $\mathbb{C}_{ij}$ depend essentially on the geometry of the system, in a way that needs to be evaluated numerically or modeled analitically on the basis of some simplifying approximation.

In the following, we adopt a slightly different and more simplified approach in order to describe the electrostatics of the system. Our considerations are based on the *circuit model* shown in Fig. (3.3), rather than on Maxwell's capacitance matrix. That amounts to model the system as a network of capacitors and tunnel junctions instead of separated metallic bodies.

Regarding the difference between the two descriptions, we can point out that, by definition, the $\mathbb{C}_{ij}$ coefficients depend not only on the position of the $i-$th body with respect to the $j-$th, since they are calculated by solving Poisson equation for electrostatic potential in the geometry of the whole system. Therefore, even if the $k-$th body is grounded ($k \neq i, j$), its position affects the value of $\mathbb{C}_{ij}$ through the boundary conditions.

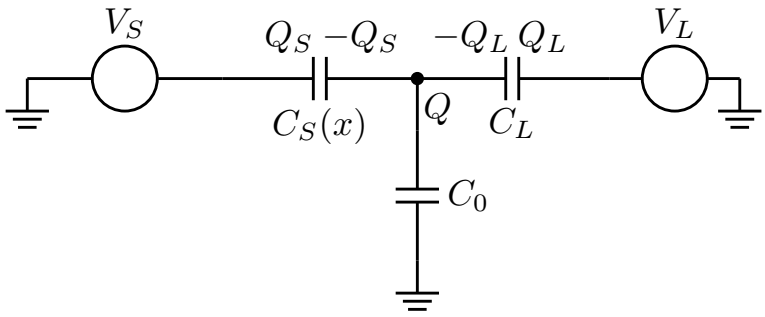

Figure 3.3: Circuit model for the STM-carbon nanotube system.

On the other hand, the circuit model simplifies the description, since it reduces the physical system to a set of junctions characterized by *effective* capacitances which depend only by the *local* geometry, that is on the area and relative distance of the model capacitors associated to the junctions. Now, we can look at the STM-nanotube system as a system of two tunnel junctions, one between the STM tip and the suspended beam and the other between the beam and the supporting leads, which are characterized by capacitances $C_S(\mathbf{x})$ and C_L and resistances $R_S[\mathbf{x}] = R_0 \exp[-\sum_i x_i \varphi_i(z_0)/\lambda]$ (R_0 being the value for the nanotube at the equilibrium distance d from the STM tip) and R_L, respectively. Both the capacitance and the resistance of the STM tip-nanotube junction are modulated by the motion of the nanotube.

The capacitance C_0 in Fig. (3.3) represents the possible capacitive coupling between the nanotube and all the (metallic) bodies in the universe other than the STM tip and the leads. In contrast to what happens in the systems in which the central island is a metallic particle, here C_0 can be not negligible due to the extended structure of the nanotube. For example, if the substrate over which the nanotube is suspended contains metallic parts, there could be some accumulation of charge in those regions of the nanotube that are far from both the STM tip and the leads. Furthermore, the capacitance C_0 would depend on the spatial configuration of the nanotube, that is, $C_0 \equiv C_0[(x)]$.

In order to simplify the model, here we assume that the supporting leads and every other body except the STM tip are grounded, so that the capacitance $C_g = C_0 + C_L$ can be interpreted as the effective capacitance of the suspended nanotube with respect to the ground. Furthermore, the $\mathbf{x}-$dependence of C_0 is neglected and the STM tip is supposed to be connected to an ideal voltage source that holds its electrical potential to a constant negative value $-V$.

One can then use Kirchhoff's laws in order to express the charges stored in the three capacitors, Q_S, Q_L, Q_0 as functions of the (quantized) extra charge on the nanotube, $Q = Q_S - Q_L - Q_0 = -Ne$, and the STM tip potential, $-V$. The electrostatic energy of the system that results from this calculation reads:

$$U = \frac{Q^2}{2C_\Sigma[\mathbf{x}]} + \frac{C_S[\mathbf{x}]C_g V^2}{2C_\Sigma[\mathbf{x}]}, \tag{3.15}$$

where $C_\Sigma[\mathbf{x}] \equiv C_S[\mathbf{x}]+C_L+C_0$. We remark that the structure of the electrostatic energy in Eq. (3.15), that shows U as the sum of a charge-dependent and a charge-independent contribution, is not affected by the particular choice of the voltages across the capacitors. For an arbitrary choice of the voltages the variation of the generalized Gibbs free energy associated to a tunneling event that transfers one elementary charge through a junction i held at voltage V_i, can be written as

$$\Delta G_i = \frac{(Q \mp e)^2}{2C_\Sigma} - \frac{Q^2}{2C_\Sigma} - eV_i\left(1 - \frac{C_i}{C_\Sigma}\right) - e\sum_{j\neq i}\frac{C_j V_j}{C_\Sigma}. \tag{3.16}$$

The $Q-$independent terms in Eq. (3.16) represent the work done by the voltage sources in order to keep the voltages constant. In particular, the $i-$th voltage source performs work to replace the charge that has tunneled through the junction (i.e. eV_i) and, like the other voltage source, to compensate the polarization charge induced by the charge tunneled on the island (i.e. $e\sum_j C_j V_j/C_\Sigma$).

The expression for ΔG_i in Eq. (3.16) might look identical to that one for an ordinary double tunnel junction (i.e. without mechanical degrees of freedom). However, it is worth to remark that since U depends on the nanotube displacement $\mathbf{x}$, the electrostatic energies of the initial and final states in Eq. (3.16) should be evaluated at the equilibrium values of $\mathbf{x}$ corresponding to the charge states Q and $Q \mp e$, which in principle are different. In the following, we will neglect the correction due to this mechanical effect.

Now we can evaluate ΔG_i for several tunneling processes in order to realize which ones play a significant role in the transport of charge across the system. For example, the probability of tunneling of one electron from the STM tip to the (initially neutral) nanotube is determined by the difference

$$\Delta G_S^{\rightarrow} = \frac{e}{C_\Sigma}\left[\frac{e}{2} - C_g V\right], \tag{3.17}$$

where C_Σ is evaluated at the equilibrium values of $\mathbf{x}$ for the neutral nanotube. Eq. (3.17) implies that the free energy decreases after the tunneling if the bias voltage is larger than the threshold value $V_C = e/2C_g$. For the tunneling of one electron from the (initially charged) nanotube to the leads, the variation of the generalized Gibbs energy is given by

$$\Delta G_L^{\rightarrow} = -\left(V + \frac{e}{2C_S}\right) \tag{3.18}$$

It can be easily checked that if the bias voltage is in the interval defined by $e/2C_g < V < e/2C_S$ (where C_S is assumed to be smaller than C_L for any value of $\mathbf{x}$) then the only two processes involved in electron transport through the system are the charging of the nanotube from the STM tip and its discharging through the nanotube-leads tunnel junction.

As mentioned at the beginning of this section, in spite of its genuinely quantum-mechanical origin, within the orthodox theory of Coulomb blockade, the tunneling of electrons is considered as a stochastic, rather than coherent process. According to this approach, the dynamics of the charge state of the nanotube is described by the distribution function $P_N(t)$, whose evolution in time is determined by the master equation (3.8).

In NEMS the coupling between mechanical and electronic degrees of freedom is typically not negligible, therefore a more general description is required to characterize the physical state of the system. For this purpose, it is convenient to introduce the function $P_N(\mathbf{x}, \pi, t)$, which represents the joint probability density of finding N extra electrons on the nanotube when its mechanical state is described by the normal-mode amplitudes and conjugated momenta ($\mathbf{x}$, π) at time t. The joint probability density $P_N(\mathbf{x}, \pi, t)$ obeys a generalized Boltzmann equation, in which the collisional integral is replaced by a term describing the tunneling processes (see section (3.4)).

However, in the limit in which the rate of tunneling is much larger than the mechanical frequency ($\omega \ll \Gamma_S, \Gamma_L$), that corresponds to the usual experimental situation for NEMS, it is only the "average" number of extra electrons that actually affects the (comparatively slow) motion of the nanotube. The time evolution of $P_N(t)$ can then be analyzed in terms of a simple kinetic equation that differs from the master equation of the orthodox theory (that is, Eq. (3.8)) only for the $\mathbf{x}-$dependence of the rate of tunneling between the STM tip and the nanotube. In the regime of strong Coulomb blockade (i.e. $N = 0, 1$ are the only possible charge states), this equation reduces to

$$\frac{dP_1}{dt} = -\Gamma_L P_1 + \Gamma_S[\mathbf{x}](1 - P_1) \tag{3.19}$$

which is the equation used in Paper I to describe the transport of charge through the STM-nanotube system.

3.3 Electrostatic interaction

Consistently with the conditions of validity of the "orthodox theory" of Coulomb blockade for metallic systems, we assume that the electron-electron interaction in our case can be adequately included through the classical concept of capacitance. The dependence of the electrostatic force on the net charge of the nanotube Q can then be determined from general considerations on the electrostatics of the system.

For a system of conductors characterized by electrostatic energy U, the force along a given direction x acting on a conductor is $-(\partial U/\partial x)_q$, where the derivative represents the rate of change of the energy when the body moves along the direction x and the suffix q indicates that the charges on the conductors are supposed to be constant.

On the other hand, if some of the conductors are supposed to be held at constant potential while changing their relative positions, then they must be connected to voltage sources and the work performed by them in order to keep the potentials constant must be taken into account. In this case, the role of U is played by the function $U-\sum_k q_k\phi_k$, where the sum over k is extended to all the conductors connected to the voltage sources [83]. This issue is usually discussed in textbooks for the simple case of a parallel plates capacitor. If one does not take into account the constraint of fixed voltage, the resulting force between the oppositely charged plates of the capacitor turns out to be repulsive instead of attractive (and, besides that, a factor $1/2$ off the correct value).

According to these considerations, the electrostatic force that affects the nanotube when it moves along the $x-direction$ under the condition that the bias voltage V is fixed, turns out to be

$$F \equiv -\frac{\partial}{\partial x}\left(U - Q_S V\right)_V \chi(z, z_0) = \frac{[Q - C_g V]^2}{2C_\Sigma^2}\frac{\partial C_S}{\partial x}, \tag{3.20}$$

where $\chi(z, z_0)$ is a function with the dimensions of an inverse length that describes the distribution of the force along the $z-$axis. It is worth to remark that the force (3.20) is always attractive, as expected for the electrostatic force between two oppositely charged plates of a capacitor.

The possibility to factorize the dependencies of the force on the x and z coordinates relies on the circuit model introduced in section (3.2), where the only the $\mathrm{x}-$dependence of the capacitance C_S is taken into account.

Regarding the distribution of the electrostatic force along the nanotube axis, we specify that, throughout this thesis and the Papers I-IV, the force is considered to be strongly localized around the position of the STM tip, i.e. $\chi(z, z_0) \sim \delta(z - z_0)$. This is clearly an approximation, since it is known that the electrostatic force between charged bodies must decay as some negative power of their relative distance. However, it is possible to show that the "delta" form for the electrostatic force is a reasonable approximation if the size of the STM tip is much shorter than the length of the nanotube, a condition that can be readily fulfilled in the geometry of the STM-carbon nanotube system. A detailed proof of the validity of this approximation can be found in Appendix A.

If a gate electrode would be inserted rode in the trench between the leads, it would coupled capacitively to the nanotube through the $\mathrm{x}-$dependent capacitance $C_G[\mathrm{x}]$. The possible effects related to this additional electrode are briefly discussed in Sec. (4.1), whereas the generalization of Eq. (3.20) that would be required in that case is presented in Appendix B.

3.4 Multimode shuttling of single electrons

The description of the STM-nanotube system that takes into account only the coupling to the fundamental bending mode of the nanotube does not introduce qualitatively new features to the physical picture that emerges from the analysis of the point-like shuttle system [72].

However, the results presented in Paper I and II indicate that this is not the case if the contributions of all the bending modes to the nanotube displacement are taken into account. The STM tip is assumed to be put over the midpoint of the nanotube ($z_0 = 0$), and this implies that all the "even" modes do not contribute to the motion of the nanotube, since the mode profiles $\varphi_j(z)$ have a node for j even.

Furthermore, the system is assumed to be in the regime of strong Coulomb blockade and that makes possible to express the electrostatic force per unit length (3.20) in the simple form $F = e\mathcal{E}P_1(t)\delta(z - z_0)$, since $N^2 = N$ if the only possible values for N are 0 and 1. The coupling between mechanical and electronic degrees of freedom originates from the dependence of the force on $P_1(t)$ that is the average probability to have one extra electron on the nanotube at time t, while the "effective electrostatic field" $\mathcal{E}$ is a positive constant with the dimensions of Volt/meter that can be calculated from Eq. (3.20) by expanding the right-hand-side around the equilibrium position and retaining only the zero-th order term in $\mathbf{x}$. Within this approximation, even though the force does not depend explicitly on the nanotube displacement, there is an implicit dependence on $\mathbf{x}$ through $P_1(t)$, because of the form of the rate of tunneling across the STM tip-nanotube junction.

We would like to point out that $\mathcal{E} > 0$ implies that the condition $e/2C_g < V < e/2C_S$ which, according to the considerations developed in Sec. (3.2) means that the only two tunneling processes that can contribute to the transport of charge through the system are the tunneling of one electron from the STM tip to the (initially neutral) neutral and the tunneling from the singly-charged nanotube to the leads.

The mechanical motion is assumed to be much slower than the rate of tunneling across both junctions ($\omega \ll \Gamma_S, \Gamma_L$), so that the transport of charge can be analyzed through the simple kinetic equation (see Eq. (3.19)). The coupled equations of motion for the normal modes-amplitudes and the average probability $P_1(t)$ read:

$$\ddot{x}_j + \gamma\dot{x}_j + \omega_j^2 x_j = eP_1\mathcal{E}/M \tag{3.21a}$$

$$\dot{P}_1 = -\Gamma_\Sigma[\mathbf{x}]P_1 + \Gamma_L[\mathbf{x}], \tag{3.21b}$$

where $\Gamma_\Sigma \equiv \Gamma_S[\mathbf{x}] + \Gamma_L$, $\Gamma_S[\mathbf{x}] = \Gamma_S \exp[-\sum_j x_j/\lambda]$ ($\varphi_j(z_0 = 0) \approx 1$ for j odd), Γ_S being the one shown in Eq. (3.12). The dissipation in the system is modeled by the linear "viscous" term $-\gamma\dot{x}_j$ in Eq. (3.21) and, since the damping rate γ is assumed to be constant, the loss of energy from the oscillating nanotube occurs in the same way for each mode.

In the limit in which the frequencies of the bending modes are smaller than the typical total rate of tunneling, $\omega_j/\Gamma_\Sigma \ll 1$, where $\Gamma_\Sigma \equiv \Gamma_S+\Gamma_L$, it is possible to find a solution for Eq. (3.21b) in the form of a power series in ω_j/Γ_Σ (see Paper I).

It is worth to remark that the condition $\omega_j/\Gamma_\Sigma \ll 1$ is far from being optimal in order to achieve the electromechanical instability. The difficulty to obtain the instability in this regime is reflected by the request of a higher quality factor than it was considered in the single-mode case (see the numerical results in Paper I).

As a consequence of the quantized nature of the tunneling current, the nanotube experiences a sequence of random "kicks" that makes it deviate from the static equilibrium configuration. We notice that the effect of each single kick is to shift the equilibrium position of the nanotube by the small amount $\Delta x_e = e\mathcal{E}\sum_j \varphi_j(z_0)/M\omega_j^2$, which can be considered as the natural parameter to evaluate the contribution to the electromechanical coupling due to the electrostatic interaction. It is worth to point out that, if the tip of the STM is put over the point $z_0 = 0$, the contribution of each mode to the electromechanical coupling, $\varepsilon_j \equiv e\mathcal{E}/M\omega_j^2$ differs from the others only for the frequency factor $1/\omega_j^2$. Even though this shift is quite small, $\Delta x_e \ll 1$, the results presented in Paper I and II reveal that, under certain conditions, the "kicks" produced by the tunneling electrons can make the equilibrium state of the nanotube unstable. The analysis of this phenomemon has been performed by means of both analytical and numerical methods.

The analytical procedure presented in Paper I is based on the observation that the conditions $\omega_j \ll \Gamma_S, \Gamma_L$ assure that any deviation of the nanotube from the equilibrium configuration will vary very slowly in time compared to typical time scale of the dynamics of the nanotube net charge, which is defined by the interval between two consecutive tunneling events. This physical argument support the possibility to seek for solutions of the equations of motion (3.21) in the form $x_j(t) = \lambda A_j(t)\sin(\omega_j t + \chi_j(t))$, where the amplitudes $A_j(t)$ and phases $\chi_j(t)$ are approximately constant over the periods of oscillation associated to the different vibrational modes, $\dot{A}_j$, $\dot{\chi}_j \ll \omega_j$.

In order to investigate how the different vibrational modes affectt dynamically each other, it is necessary to go beyond the linear approximation in $\sum_j x_j/\lambda$. The condition of weak electromechanical coupling (and therefore initially small displacement) makes possible to expand the position-dependent tunneling rate $\Gamma_S[\mathbf{x}]$ up to third order in $\sum_k x_k/\lambda$ and P_1 up to the first order in ω_j/Γ_Σ.

Combining the large separation in the characteristic timescales of mechanical and electronic degrees of freedom and the feebleness of the electromechanical coupling, we can reformulate the equations of motion in terms of the slowly-varying functions A_j, χ_j, by replacing the x_j in Eqs. (3.21) with the Ansatz $x_j(t) = \lambda A_j(t)\sin(\omega_j t + \chi_j(t))$ and averaging over the period of the first mode, which is the longest one. In this time interval the amplitudes and

phases for the different modes can be considered constant and be replaced by their average values.

The equations of motion after averaging read:

$$\dot{A}_j = \alpha_j A_j \left(\delta_j - A_j^2 - 2 \sum_{k \neq j} A_k^2 \right) \tag{3.22}$$

$$\dot{\chi}_j = 0, \tag{3.23}$$

where δ_j and α_j are given by

$$\delta_j = 16 \left(1 - \frac{4\gamma \Gamma_\Sigma \lambda}{\omega_j^2 d_j} \right) + \mathcal{O}\left(\frac{\omega_j^2}{\Gamma_\Sigma^2} \right) \tag{3.24a}$$

$$\alpha_j = \frac{\varepsilon_j \omega_j^2}{128 \Gamma_\Sigma} \left[1 + \mathcal{O}\left(\frac{\omega_j^2}{\Gamma_\Sigma^2} \right) \right] . \tag{3.24b}$$

To first order in ω_j/Γ_Σ the expressions for δ_j and α_j do not depend on the mode index j, as the product $\omega_j^2 \varepsilon_j$ is independent on j. Because of this one can replace $\delta_j \to \delta$ and $\alpha_j \to \alpha$.

The behavior of the solution of Eq. (3.22) can be readily visualized for the case of two modes n, m (the generalization to more modes is straightforward). The stationary points of the two nonlinear coupled equations can be found analytically and their stability can be determined through the evaluation of the Jacobian matrix [27].

The dynamical behavior of the system depends on the sign of the parameter δ. From Eq. (3.22) it is clear that, if $\delta < 0$ the only stationary point is the origin, that corresponds to the absence of any oscillation. The nanotube lies at rest in some static configuration determined only by the constant tunneling rates Γ_S and Γ_L. On the other hand, if $\delta > 0$ the origin becomes unstable and three more stationary points appear: a saddle point at $(\delta/3, \delta/3)$ and two stable points at $(\sqrt{\delta}, 0)$ and $(0, \sqrt{\delta})$. These different scenarios are shown in Fig. (3.4). The two new stable points represent oscillating states with finite amplitude $\sqrt{\delta}$ and frequency ω_n or ω_m, depending on the initial conditions.

The conditions $\delta > 0$ defines the onset of the shuttle instability. From $\delta = 0$ it is possible to find the expression for the threshold electric field above which the instability starts to develop, $\mathcal{E}_c \equiv 4\Gamma_\Sigma \lambda \gamma M/e$. The analysis of Eq. (3.22) indicates that, once the instability for a certain number of vibrational modes is established, the system evolves in such a way that only one of the unstable modes reaches the new stationary state, characterized by steady amplitude oscillations, i.e. the *limit cycle*.

The selection of the surviving mode is determined by the initial conditions as the mode which initially has the largest displacement from the origin (that is from the static equilibrium state), maintains its separation from the other ones and evolves into a limit cycle. Trajectories in the amplitudes space cannot cross and this result can be generalized analytically to the case of an arbitrary

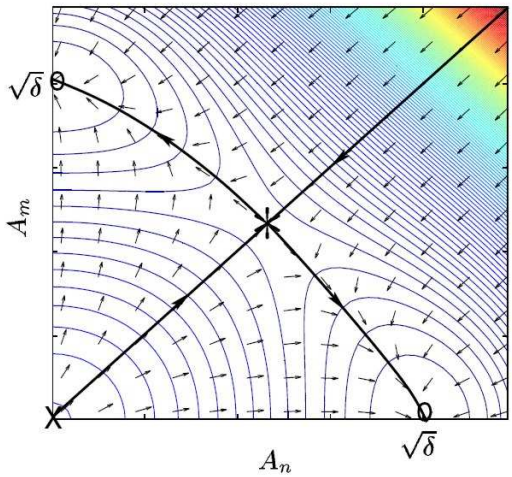

Figure 3.4: (Color online) Stationary points when two modes (n and m) are unstable. Two attractors, indicated by (**o**), correspond to a finite amplitude of one mode while the other mode is suppressed are shown. The stationary point marked with (**x**) is a repellor and the point indicated by (*) is a saddle point. The thick lines are separatrices that trajectories cannot cross. The separatrix $A_n = A_m$ ensures that if $A_n(0) > A_m(0)$, this inequality hold for all times t [74].

number of modes by studying the asymptotic behavior of the solutions of Eq. (3.22) [74].

It is worth to remark that the symmetry between modes that characterizes Fig. (3.4) is actually broken if higher order (in ω_n/Γ_Σ and ω_m/Γ_Σ) corrections to δ become relevant or if the dissipation affects each mode in a different way. Then each mode will have its own δ_n and, in general, it may happen that the selection of the survivor mode is not only based on the size of the initial displacements from the static equilibrium point.

In order to check the results obtained by the analysis of Eq. (3.22), they have been compared with the numerical solution of the equations of motion for the mode amplitudes x_j (Eqs. (3.21a) and (3.21b)), based on a fourth-order Runge-Kutta method. Fig. (3) in Paper I shows both the analytical and numerical solution for a given choice of the initial conditions. The agreement between the results obtained from the two approaches is found in the whole range of parameters for which the analytical treatment is valid.

The numerical solution of the equations of motion for the x_j illustrates also another aspect of the dynamics of the system in the regime characterized by the electromechanical instability. Since the frequencies of the different modes are not commensurable, i.e. they are not integer multiples of the fundamental mode, the initial motion of the nanotube is not characterized by a sharply defined periodicity as can be seen in the lower left panel of Fig. (3). However, when the system reaches the final stationary state and only the mode $n = 5$ (which initially had the largest deviation away from static equilibrium) has

a non zero amplitude, its oscillations are clearly periodic with frequency ω_5. The same behavior for modes n=1 or 3 is observed by simply switching the initial conditions among them.

Furthermore, the numerical analysis of Eq. (3.21a) is not necessarily limited by the requirement that the oscillation amplitude be kept small with respect to the tunneling length. The results shown in Fig. (4) of Paper I, for instance, suggest that the selective evolution promoted by the simultaneous instability of many vibrational modes can characterize also the "large amplitudes" regime.

3.5 Geometrical scanning of nanotube bending modes

The theoretical study presented in Paper I and reviewed in Sec. (3.4) suggests that the onset of the electromechanical "shuttle-like" instability in an extended object, such as a suspended nanotube, induces a selective evolution of its many mechanical degrees of freedom.

However, it should be stressed that even though the existence of many stable states characterized by periodic oscillations was proven in Paper I, there is no clear evidence of how they could be probed from the experimental point of view. The discrimination of different unstable vibrational modes cannot be *physically* performed by a careful choice of the initial conditions as it can be *theoretically* done when solving the equations of motion of the model.

The definition of a feasible method to selectively induce the electromechanical instability in the STM-nanotube system has been the basic motivation for the work that is described in Paper II. The main idea for the procedure suggested i Paper II is to exploit the spatial profiles of the modes and the possibility to accurately control the position ofthe STM tip in order to optimize the coupling for the specific mode that is chosen to be unstable.

The geometric features of the vibrational modes appear in the model through the expression of the electromechanical coupling, which has been defined as $\varepsilon \equiv e\mathcal{E}\sum_k \varphi_k^2(z_0)/M\lambda\omega_k^2$ and is therefore dependent on the spatial profiles of the modes at the position of the STM tip, $\varphi_j(z_0)$. The point $z_0 = 0$, for which $\varphi_j(z_0) = 0$ if j even and $\simeq 1$ if j odd represents a quite peculiar choice.

In general, the dynamics of the mode amplitudes x_j will be determined by the specific electromechanical coupling for the $j-$th mode, $\varepsilon_j = e\mathcal{E}\varphi_j^2(z_0)/M\omega_j^2\lambda$. Furthermore, if the bias voltage is fixed, the only other parameter that can be varied is the equilibrium distance between the STM tip and the nanotube, d, which determines the tunneling rate at equilibrium, $\Gamma_S(d)$ (denoted by $\Gamma_0(d)$ in order to keep consistency with the notation used in Paper II).

In other terms, we can investigate the stability of the STM-nanotube system as a function of the position of the STM along the z direction, which is parallel to the nanotube axis and along the x direction, which is perpendicular to it.

For what concerns the description of the coupled dynamics of the mechanical and electronic degrees of freedom of the system, in Paper II we followed the more general approach mentioned in Sec. (3.2), whose key ingredient is the joint probability density $P_N(\mathbf{x}, \pi, t)$.

We still consider the system in the strong Coulomb blockade regime and limit to one the maximum number of extra electrons on the nanotube, so that only the probability densities $P_0(\mathbf{x}, \pi, t)$ and $P_1(\mathbf{x}, \pi, t)$ should be considered.

The time evolution of P_0 and P_1 is determined by two coupled generalized Boltzmann equations in which the collisional integral is replaced by a suitable term that describes the tunneling [4]. In order to study the dynamics of the nanotube averaged over its possible charge states, it is convenient to introduce the functions $P_\pm \equiv P_1 \pm P_0$, that obey the equations of motion

$$\frac{\partial P_+}{\partial t} + (\mathcal{L}_1 + \mathcal{L}_2)(P_+ + P_-) = 0 \tag{3.25a}$$

$$\frac{\partial P_-}{\partial t} + (\mathcal{L}_1 + \mathcal{L}_2)(P_+ + P_-) = \\ = \Gamma_-[\mathbf{x}; z_0]P_+ + \Gamma_+[\mathbf{x}; z_0]P_-, \tag{3.25b}$$

where $\Gamma_+[\mathbf{x}; z_0] \equiv \Gamma_S[\mathbf{x}; z_0] + \Gamma_L$, $\Gamma_-[\mathbf{x}; z_0] \equiv \Gamma_S[\mathbf{x}; z_0] - \Gamma_L$ and the Liouvillian operators $\mathcal{L}_1$ and $\mathcal{L}_2$ are defined as follows:

$$\mathcal{L}_1 \equiv \sum_j \left[\frac{\pi_j}{M} \frac{\partial}{\partial x_j} - M\omega_j^2 x_j \frac{\partial}{\partial \pi_j} + \gamma_j \frac{\partial}{\partial \pi_j} \pi_j \right]$$

$$\mathcal{L}_2 \equiv e\mathcal{E} \sum_j \varphi_j(z_0) \frac{\partial}{\partial \pi_j}.$$

From Eqs. (3.25) we can derive the equations of motion for any dynamical variable averaged over the probability densities P_+ and P_-: $\langle (\ldots) \rangle_\alpha \equiv \int (\ldots) P_\alpha(\mathbf{x}, \pi, t) d\mathbf{x} d\pi$, where $\alpha = \pm$. The set of equations of motion for the first moments $\langle 1 \rangle_- \equiv P_-(t)$, $\langle x_j \rangle_\alpha$, $\langle \pi_j \rangle_\alpha$ is:

$$\frac{d\langle x_j \rangle_\alpha}{dt} = \frac{\langle \pi_j \rangle_\alpha}{M} \tag{3.26a}$$

$$\frac{d\langle \pi_j \rangle_\alpha}{dt} = -M\omega_j^2 \langle x_j \rangle_\alpha - \gamma_j \langle \pi_j \rangle_\alpha + e\mathcal{E}\varphi_j(z_0) P_1 \tag{3.26b}$$

$$\frac{dP_-}{dt} = \langle \Gamma_-[\mathbf{x}; z_0] \rangle_+ - \langle \Gamma_+[\mathbf{x}; z_0] \rangle_-, \tag{3.26c}$$

The dissipation in the system is introduced by the "viscous" term $-\gamma_j \langle \pi_j$ in Eqs. (3.26), where the index j reflects the fact that dissipation can be frequency-dependent, that is it affects each vibrational mode in a different way.

In Paper II, we considered the case in which the damping of the mechanical vibrations can be described in terms of the model formulated by Zener that has been described in Sec. (1.2.1): $\gamma_j = \Delta_E \omega_j \tau / (1 + (\omega_j \tau)^2)$. We do not refer

to a specific dissipative mechanism and choose values for the parameters Y and τ such that reasonable values for the effective quality factors of different modes, $Q_j \equiv \gamma_j/\omega_j$ could be obtained.

We point out that the set of equations (3.26) is not closed because the tunneling rate $\Gamma_S[\mathbf{x}; z_0]$ introduces a coupling between the first and all the other moments. However, if we just focus on the analysis of the conditions that generate a dynamical instability (without actually characterizing the steady states towards which the system evolves once the instability has started to develop) in the limit of small oscillation amplitudes we can expand $\Gamma_S[\mathbf{x}; z_0]$ to first order in x_j/λ and that reduces (3.26) to a closed set of linear equations.

The static solution of the linearized equations of motion, $\langle \pi_j \rangle_\alpha = 0$, $\langle x_j^\alpha \rangle_\alpha = \bar{x}_j^\alpha$, $p_- = \bar{p}$, where $\bar{x}_j^\alpha$ and $\bar{p}$ are constant, describes the nanotube as a slightly bent beam at rest. The stability of this solution can be investigated by substituting the expressions $\langle \xi_k \rangle_+ \equiv \bar{\xi}_k + A_k e^{\beta_k t}$ (where ξ_k is any of the dynamical variables $\langle x_k \rangle$, $\langle \pi_k \rangle$, p_- and A_k is constant) in the linearized equations of motion and solving for the exponents β_k [27].

The analytic expression of the β_k cannot generally be found since it requires the solution of an algebraic equation of degree higher than the third. However, in the regime of weak electromechanical coupling and weak dissipation we can look for exponents of the form $\beta_k \sim i\omega_k + \delta_k$, with $|\delta_k| \ll \omega_k$ and derive an analytical expression for the δ_k which up to the first order in all ε_k and γ_k reads:

$$\delta_k = -\frac{\gamma_k}{2} + \frac{\Gamma_0^*(d)\Gamma_L}{2\Gamma_+^*(d)} \frac{\omega_k^2 \varepsilon_k(z_0)}{\omega_k^2 + \Gamma_+^{*2}(d)} \left(1 + i\frac{\Gamma_+^*(d)}{2\omega_k}\right), \tag{3.27}$$

where $\Gamma_+(d)^* \equiv \Gamma_0^*(d) + \Gamma_L$ (i.e. $\Gamma_S(d) + \Gamma_L$). The sign of the real part of δ_k in Eq. (3.27) determines the stability of the static solution for the $k-$th average mode amplitude. If $\mathfrak{Re}[\delta_k] > 0$ then $\langle x_k \rangle_+$ increases exponentially in time, hence the static solution for the k-th mode is unstable. This is the signature of a "shuttle-like" electromechanical instability. On the other hand, if $\mathfrak{Re}[\delta_k] < 0$ the energy pumped into the vibrational mode by the electrostatic field is not able to compensate the loss due to dissipation and after a time interval of the order of $1/\gamma_k$ the k-th mode amplitude decays to its static value.

For fixed values of γ_k, $\mathcal{E}$ and Γ_L, the sign of $\mathfrak{Re}[\delta_k]$ becomes a function of z_0 and $\Gamma_0^*(d)$, i.e. it depends only on the position of the STM tip in the xz plane. The set of values of z_0 and $\Gamma_0^*(d)$ for which the real part of δ_k is positive defines the instability region for the k-th mode amplitude in the plane (z_0,$\Gamma_0^*(d)$).

The instability regions of the first three modes in the two limits $\omega_1\tau \gg 1$ and $\omega_1\tau \ll 1$ are shown in Fig. (3.5(a)) and Fig. (3.5(b)), respectively. The regions determined analitically by taking the real part of δ_k in Eq. (3.27) are delimited by solid lines and they are compared with the regions obtained by the numerical solution of the algebraic problem for the exponents β_k, which are delimited by markers. Two different scenarios are possible depending on the value of the parameter $\omega_1\tau$. If the relaxation time τ is longer than the characteristic time scales associated to the vibrational modes, $\tau \gg 1/\omega_j$, then

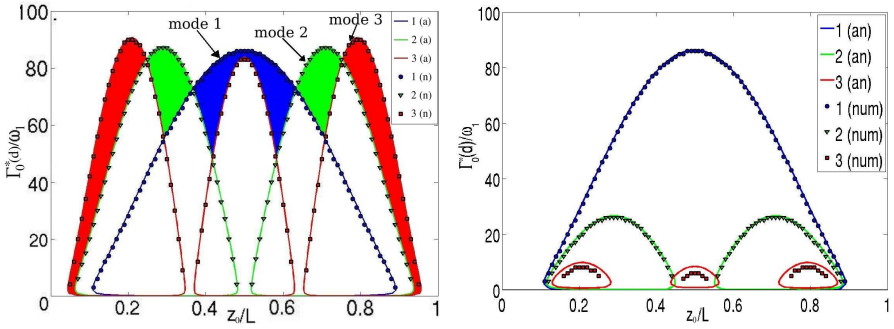

(a) (b)

Figure 3.5: Regions of instability in the parameter plane $(z_0, \Gamma_0^*(d))$ of the first three bending modes in the case of "slow" **(a)** and "fast" **(b)** dissipation-induced mechanical relaxation (see text). The regions computed from the real part of the analytic expression (3.27) (solid lines) are compared with the results obtained by the numerical solution of the linearized equations of motion (markers). The parts of the plot filled with colors correspond to the values of $(z_0, \Gamma_0^*(d))$ for which a single vibrational mode is excited. The values of the relevant parameters for **(a)** are: $1/\tau = 0.1\omega_1$. $e\mathcal{E}/(m\lambda\omega_1^2) = 0.1$, $\Gamma_L = 5\omega_1$, $Y = 10^{-4}$ and for **(b)**: $1/\tau = 10\omega_1$, $e\mathcal{E}/(m\lambda\omega_1^2) = 0.1$, $\Gamma_L = 5\omega_1$, $Y = 10^{-3}$.

it is possible to find regions in the parameter plane $(z_0, \Gamma_0^*(d))$ where only a single mode is unstable without having the other modes unstable as well (see the areas filled with colors in Fig. (3.5(a))). A selective excitation of the vibrational modes is possible in this case.

On the other hand, if the mechanical relaxation induced by dissipation is much faster than the mechanical vibrations, $\omega\tau \ll 1$, then the fundamental mode dominates over all the others and the instability of a certain mode is always accompanied by the instability of the fundamental one. The selective excitation of the vibrational modes cannot be achieved in this case.

In concluding this section, we would like to point out that the results presented in Paper II indicate that the geometric features of the STM-suspended nanotube device can play a substantial role in promoting the instability of the static equilibrium configuration. This aspect is peculiar of the STM-nanotube system (and, more generally, of all the NEMS in which the role of the movable element is played by a spatially extended structure, such as a beam or a membrane) whereas, on the other hand, in "point-like" shuttle systems the conditions for the onset of the electromechanical instability have been always expressed in terms of a bias threshold voltage that has to be overcome or a maximum damping rate that can be tolerated.

3.6 Appendix A

As long as the STM tip is not put too close to the ends of the nanotube (so that the edge effects due to the supporting leads are negligible), in good approximation the force depends only on the relative distance from the position of the STM tip, that is $\chi(z, z_0) \approx \chi(|z - z_0|)$.

The coefficients of the electrostatic force expanded on the normal-modes basis $\varphi_j(z)$ can be expressed as the sum of two contributions:

$$f_j = \int_{-L/2}^{L/2} F[Q(t), \mathbf{x}, z', z_0]\varphi_j(z')dz' \approx$$
$$\approx F[Q(t), \mathbf{x}]\varphi_j(z_0)\int_{-L/2}^{L/2}\chi(z' - z_0)dz' + F[Q(t), \mathbf{x}]\int_{-L/2}^{L/2}[\varphi_j(z') - \varphi_j(z_0)]\chi(z' - z_0)dz'. \tag{3.28}$$

The first integral from left in Eq. (3.28) is convergent since F decays faster than $|z - z_0|^{-1}$. A simple estimate of the behaviour of the $x-$component of the electrostatic force far from the STM tip can be performed by modeling the STM tip as a charged sphere of radius R at distance d above an infinite grounded metallic cylinder. From this analysis it turns out that $F \sim |z - z_0|^{-3}$ for $|z - z_0| \gg R, d$.

Since the first integral from left in Eq. (3.28) is convergent, then it just produces a finite factor that multiplies the eigenmode function below the STM tip, $\varphi_j(z_0)$. The second integral from left in Eq. (3.28) can be estimated as follows:

$$\int_{-L/2}^{L/2}[\varphi_j(z') - \varphi_j(z_0)]\chi(z' - z_0)dz' \simeq \int_{z_0-R/2L}^{z_0+R/2L}[\varphi_j(z') - \varphi_j(z_0)]\chi(\xi' - \xi_0)d\xi' \simeq$$
$$\left(\frac{d^2\varphi_j}{dz^2}\right)_{z_0}\int_{z_0-R/2L}^{z_0+R/2L}(z' - z_0)^2\chi(z' - z_0) \leq \varphi_j''(z_0)\mathrm{max}_\chi \mathrm{R}^3 = \frac{\mathrm{R}^2}{\mathrm{L}^2}\mathrm{max}_\chi \mathrm{R},$$

where max_χ is the maximum value of χ over the region where the force is significantly different from zero (which has been assumed to be symmetric with respect to z_0) and the parity of $\chi \sim |z - z_0|^{-3}$ around z_0 makes possible to get rid of the linear term in the Taylor expansion of $\varphi_j(z) - \varphi_j(z_0)$.

Since $\mathrm{max}_\chi \mathrm{R}$ is of the same order of $\int_{-L/2}^{L/2} F[Q(t), z' - z_0]dz' < \infty$ we can argue that the second term in Eq. (3.28) is $\mathcal{O}(R^2/L^2)$ with respect to the first one. Consistently with the conditions of validity of elasticity theory, we consider here only those vibrational modes with wavelengths of the same order of the nanotube length and therefore we approximate $d^2\varphi_j/dz^2 \sim \mathcal{O}(L^{-2})$.

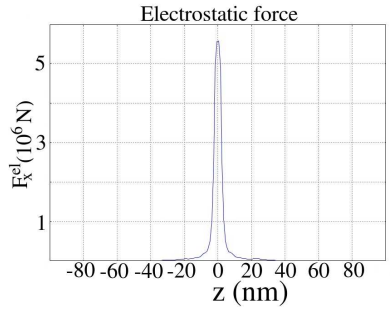

Figure 3.6: Electrostatic force distribution for a truncated cone-shaped STM tip with base radius R=20 nm, top radius 2 nm, height 50 nm which at equilibrium is d = 1 nm far from a cylinder with length L = 200 nm. The voltage drop between the STM tip and the nanotube is 1 V and the STM tip is put above the midpoint of the cylinder ($z_0 = 0$). The force vanishes outside a region centered around z_0 whose width is of the order of R (we would like the thank Juan Atalaya for the support with the finite-element calculation).

The correction term in Eq. (3.28) for typical values $R \sim 10^{-7}$, $L \sim 10^{-6}$, turns out to be very small. Therefore the local approximation for the electrostatic force, i.e. $Lf_j \approx F[Q(t)]\delta(z - z_0)$, is valid in the geometry of the system considered here.

As a further support of these analytical considerations, we calculated the electrostatic force LF from the numerical solution of the Poisson equation (obtained through the finite-element method) for the STM-nanotube system. The STM tip is modeled as a truncated cone with a fixed potential, while the leads are grounded. As shown in Fig. (3.6), the results of this calculation manifest a quite good agreement with the behaviour predicted by the physical considerations reported above.

CHAPTER 4

Cooling of nanomechanical resonators by thermally activated electron transport

In Chapter (3) we have discussed the conditions under which the coupling of mechanical and electronic degrees of freedom in the STM-nanotube system can give rise to a dynamical instability that drive the suspended nanotube to a regime a self-sustained periodic oscillations in which the transport of charge is significantly enhanced by the mechanical motion. From a general point of view, the onset of the electromechanical instability is possible because there is a transfer of energy from the electronic to the mechanical subsytem and, as a consequence of this process, the amplitude of the oscillations increases in time, until a balance bewteen the energy pumped and the energy dissipated per cycle is established.

One could then naturally wonder if this is the only effect that the electromechanical coupling can have or rather if there exist conditions under which the tunneling of electrons causes instead a net removal of energy from the mechanical subsystem. The analysis performed in Paper III and IV indicates that such conditions actually exist and that is possible to reduce the energy of the mechanical vibrations to a level very close to the value associated to the quantum mechanical ground state, i.e. $E_{gs} = \hbar\omega/2$.

The problem of defining an efficient procedure to actively cool macroscopic mechanical oscillators, especially in connection with the fundamental issue of the crossover between classical and quantum mechanics, generated a remarkable amount of work in the last years, particularly in the fields of nanoelectromechanical and optomechanical systems (see section (1.4) and references therein). The cooling mechanisms described in Paper III and IV can be considered as examples of experimentally feasible methods to drive a macroscopic oscillator to a state that is very close to its vibrational ground state. The description of the physical behaviour of the system in this regime demands a quantum-mechanical analysis such as the one performed to derive the results in Paper III and IV.

Moreover, we think that there are at least a further reason of interest for the results presented here, beyond the performance of our cooling procedure and the comparison with other methods proposed in the literatue. From a thermodynamics point of view, the suspended nanotube is a mechanical system interacting with a *nonequilibrium* environment, that is the one provided by the

tunneling current. Under nonequilibrium conditions, we cannot draw general (i.e. based only on the laws of thermodynamics) conclusions about the state of the system.

On the basis of these considerations, it might sounds quite surprising that the picture that emerges from the equations of motion for the mechanical system coupled to the nonequilibrium electronic environment is formally equivalent to that of a system interacting with a thermal bath at *equilibrium*. This behaviour has been found in a variety of electro- and opto-mechanical system under some general conditions of weak coupling and large separation between relevant time scales.

In this chapter, we devote sections (4.1) and (4.2) to discuss the general features of the cooling mechanism introduced in Paper III. The characterization of the mechanical state of the nanotube under the nonequilibrium conditions imposed by the tunneling current constitutes the main subject of Paper IV, which is briefly introduced in Sec. (4.3).

4.1 Nanotube dynamics in the quantum limit

As anticipated in the introduction above, we are now interested in the dynamics of the suspended nanotube in the quantum regime. The general way to proceed is to start from the Liouville-von Neumann equation of motion for the total density matrix of the system (which contains information about the nanotube, the STM and the leads), and then apply some suitable approximation in order to extract the information concerning only the dynamical state of the nanotube.

The density matrix formalism requires that the degrees of freedom of the system can be modeled in terms of Hamiltonian operators. For the mechanical degrees of freedom we already presented the classical hamiltonian function (3.3), that can be physically interpreted as the mechanical energy of the suspended nanotube. The standard way of quantizing it is to perform the canonical quantization of the normal mode amplitudes and their conjugated momenta, (x_j, π_j), that are mapped to the hermitean operators $(\hat{X}_j, \hat{P}_j)$ satisfying the canonical commutation relations

$$[\hat{X}_i, \hat{P}_j] = i\hbar\delta_{ij}, \tag{4.1}$$

where δ_{ij} is the Kronecker delta. For simplicity, we assume that the displacement of the nanotube is adequately described by the fundamental bending mode alone, that is the coupling of the other vibrational modes to the net charge on the nanotube is negligibly small (higher-frequency modes contribute nevertheless to the root-mean-square deviation of the nanotube center-of-mass position, as discussed in Paper IV). If this approximation is valid, the mechanical degrees of freedom of the system can be modeled by the Hamiltonian of a

quantum harmonic oscillator

$$H_m = \frac{\hat{P}^2}{2M} + \frac{M\omega^2}{2}\hat{X}^2. \tag{4.2}$$

Since the STM tip, the nanotube and the supporting leads are assumed to be in a normal metallic state, they can be simply modeled as gases of noninteracting electronic quasiparticles that, in the language of second quantization, can be represented by the following Hamiltonian operators

$$H_e = \sum_{q,\alpha} E_{q,\alpha} a^\dagger_{q,\alpha} a_{q,\alpha} + \sum_q \xi_q c^\dagger_q c_q = H_S + H_L + H_{e,NT}, \tag{4.3}$$

where $a^{(\dagger)}_{q,\alpha}$ and $c^{(\dagger)}_q$ are annihilation (creation) operators for electrons in the STM tip ($\alpha = S$), in the leads ($\alpha = L$), and in the nanotube, respectively. It is worth to remark that, while the theory of Fermi liquids is well suited to describe the electronic structure of ordinary metals, a number of theoretical works have argued about the non-Fermi liquid character of the electrons in one-dimensional nanowires and, in particular, in carbon nanotubes [63].

In the Hamiltonian (4.3) the suspended nanotube is considered as a normal metallic system with a continuous electronic spectrum. However, this approximation can be not justified if the quantization of the electronic levels is not negligible, as it has already pointed out in section (3.2).

In Paper IV we considered the case in which the average difference of the electronic states energies is largest than any other energy scale in the system, so that only a single (spin-degenerate) level is involved in the transport of charge. In this case, the operator describing the electronic degrees of freedom of the nanotube shown in Eq. (4.3) must be replaced by

$$H_{e,NT} = E_0 c^\dagger c \tag{4.4}$$

Then we turn to discuss the terms describing the coupling between mechanical and electronic degrees of freedom. The STM-nanotube system is characterized by two independent mechanisms of interaction, that is the electrostatic force hat affects the nanotube when it is charged and the modulation of the width of the tunneling barrier at the STM tip-nanotube junction due to the nanotube displacement.

We start discussing the electrostatic interaction first and come back to the expression of the electrostatic force presented in Eq. (3.20) within section (3.3) to perform some further analysis. Opening the square in Eq. (3.20), in the regime in which the nanotube can be only neutral or charged by a single electron, we can rewrite the electrostatic force as:

$$F = -\frac{NeC_L(V - V_C)}{2C_\Sigma^2}\left|\frac{\partial C_S}{\partial x}\right| - \frac{(C_L V)^2}{2C_\Sigma^2}\left|\frac{\partial C_S}{\partial x}\right|, \tag{4.5}$$

where V_C is the Coulomb blockade threshold voltage, $V_C = e/2C_L$. The factor $\chi(z, z_0)$ defined in Sec. (3.3) has been omitted in Eq. (4.5) since only the lowest-frequency bending mode is considered here and, with our choice of normalization, $\varphi_0(0) \approx 1$.

We point out that the expression of F in Eq. (4.5) can be seen as the sum of two contributions, one that depends only on x and another that depends on both x and N, the number extra electrons in the nanotube. The latter term provides a mechanism of interaction between mechanical and electronic degrees of freedom. The capacitance of the STM-nanotube junction can be expanded in Taylor series around the equilibrium position of the nanotube, i.e. $C_S[x] \approx C_S[0] + (\partial C_S/\partial x)_0 x + \ldots$, which suggests that the charge-dependent part of the electrostatic force can be formally derived from an effective potential energy which is linear in both x and N. The Hamiltonian operator that corresponds to this effective potential energy is given by

$$H_C = \frac{\Delta G_S^{\rightarrow}}{C_\Sigma} \hat{N}\hat{X} \equiv \mathfrak{F}_m \hat{N}\hat{X}. \tag{4.6}$$

We are aware that the procedure followed to derive the Hamiltonian (4.6) might present some ambiguity, since the classical function that corresponds to it (see Sec. 3.3) cannot be interpreted as the energy of a closed system, because the STM tip is held at fixed potential by an external voltage source. The operator defined in Eq. (4.6) should be therefore considered as an *effective* Hamiltonian that describes the electrostatic interaction in the system.

In Eq. (4.6) it has been recognized the fact that the electrostatic interaction turns out to be proportional to $\Delta G_S^{\rightarrow}$, that is the variation of the generalized Gibbs energy associated to the tunneling of one electron from the STM tip to the initially neutral nanotube. This simple relationship between $\Delta G_S^{\rightarrow}$ (that determines the rate of charge exchange between the STM tip and the nanotube) and the electrostatic force that might look rather unexpected. It is natural to wonder if this result hints us to something deep about the relationship between charge transport in the Coulomb blockade regime and mechanical displacement and probably it would be interesting to make some speculations along that direction. However, on the basis of the number of approximations on which this result follows, it seems unlikely to us that there could be some very deep meaning enclosed in it.

What is relevant for our purposes in the effective interaction term (4.6) is the possibility to control not only the strength, but also the sign of the coupling by varying the bias voltage above or below the threshold value V_C. It is important that there is a threshold value, but the fact that it coincides with the Coulomb blockade threshold is probably just accidental.

Nevertheless, the existence of a threshold value is expected to persist also if some additional control parameter is added to the STM-nanotube system is modified, for example in the form of a gate electrode inserted in the trench over which the nanotube is suspended (see Appendix B). That might be useful

to increase the experimental control over the system. As we show in Appendix B, the qualitative behavior of the system is not affected, but then the threshold value that discriminates the regimes in which the sign of $\mathfrak{F}_m$ is positive or negative does not coincide with the Coulomb blockade threshold value. A richer scenario of different dynamical/transport regimes can then be envisaged, which is summarized in the table below:

V	$< V_C$	$> V_C$
$< V_F$	no tunneling at $T = 0$ $\mathfrak{F}_m$ negative	tunneling yes $\mathfrak{F}_m$ negative
$> V_F$	no tunneling at $T = 0$ $\mathfrak{F}_m$ positive	tunneling yes $\mathfrak{F}_m$ positive

It is interesting that the existence of the threshold voltage for the force is strictly related to the quantized nature of the electron charge. This is in contrast with the phenomenon of the "shuttle-like" electromechanical instability illustrated in Chapter (3), for which the quantization of the electron charge is not essential, as shown in [72]. That can be understood from Eq. (4.5), which shows clearly that if e could take vanishingly small values, it would be not possible to control the sign of $\mathfrak{F}_m$. We stress that the total electrostatic force (i.e., Eq. (3.20)) does not change its orientation by varying the bias voltage, it is always attractive, as it should be since the charge distributions accumulated on the two sides of the STM-nanotube junction have always opposite signs, like on the plates of a capacitor.

We now proceed to describe the tunneling coupling, that can be included in our model through the "transfer Hamiltonian" [84]:

$$H_T = \sum_{q,q'} e^{i\hat{\varphi}} c_{q'}^{\dagger} \left[t_S(\hat{X}) a_{q,S} + t_L a_{q,L} \right] + \text{H.c.}, \tag{4.7}$$

where $t_S[\hat{X}]$ and t_L are the probability amplitudes for tunneling across the STM-nanotube and nanotube-leads tunnel junctions (they are supposed to be independent from the electron energy) and the operator $e^{i\hat{\varphi}}$ changes the number $\hat{N}$ of excess electrons on the nanotube by one, $e^{-i\hat{\varphi}} \hat{N} e^{i\hat{\varphi}} = \hat{N} + 1$. This charge-shift operator emphasises the quantized nature of the tunneling electrons and therefore provides a way to include Coulomb blockade effects [79]. The "phase" operator $\hat{\varphi}$ is the canonically conjugated to the number of extra electrons operator $\hat{N}$, since they obey the commutation relations:

$$[\hat{N}, \hat{\varphi}] = i. \tag{4.8}$$

Since t_S depends on the overlap between electronic states in the STM tip and the nanotube, it depends on the deflection of the tube through the operator $t_S \exp[\hat{X}/\lambda]$, where t_S is a constant and λ the tunneling length. In contrast,

the distance between the nanotube and the leads is fixed, so that t_L does not depend on the nanotube deflection.

It is worth to remark that the tunneling electrons produce fluctuactions in the momentum of the suspended nanotube. At the intuitive level, this fact is evident if we adopt a classical point of view and consider the electrons as particles impinging on the nanotube surface and transferring their momentum to it.

However, at the quantum level this picture is no longer valid, since the momentum of the tunneling electrons is not even defined, because of the lack of translational symmetry in the system. The issue of momentum transfer in the STM-nanotube system is rather subtle. A quantum-mechanical model to assess it (that treats the electrons in the tip as free particles) has been proposed by [85].

The role of current-induced momentum fluctuations has been discussed in several works about the performance of the STM as a sensitive displacement sensor [86–89]. In all these papers the fluctuations are estimated (mainly according to heuristic arguments) to be of the order of $\hbar/\lambda$. The analysis focuses on the noise in the measured tunneling current (through which it is possible to detect the displacement of a mechanical oscillator coupled to the STM) and particularly on that part whose origin can be found in the back-action caused by the momentum transfer associated to the tunneling electrons.

It is interesting to remark that the transfer Hamiltonian (4.7) incorporates the fact that the tunneling of electrons is responsible for fluctuations of the nanotube momentum, as it emerges clearly from the equation of motion for the nanotube momentum operator in Heisenberg picture:

$$i\hbar\frac{\hat{P}}{dt} = [\hat{P}, H] = [\hat{P}, H_T]. \tag{4.9}$$

4.2 Cooling by destructive interference

As discussed in the previous section, the electromechanical interaction in the STM-nanotube system arises from two independent mechanisms, one related to the *tunneling* coupling between the nanotube and the STM tip and the other due to the *electrostatic* [1] force that affects the nanotube when it is charged by one electron. The cooling effect described in Paper III and IV results from the interplay between these different mechanisms of coupling.

The analysis of the nanotube dynamics in the quantum regime can be conveniently performed representing the mechanical degrees of freedom in terms of quanta of vibrational energy (*vibrons*), which are described by the following annihilation and creation operators: $b/b^\dagger \equiv (\hat{X}/2\Delta x_{gs} + / - i\Delta x_{gs}\hat{P}/\hbar)$, where

[1] Due to the formal similarity between the electrostatic term in the Hamiltonian of our model and the interaction term used in the polaron problem, in Paper III and IV and in the following, the electrostatic coupling will be refererred to as the "polaronic" coupling.

$\Delta x_{gs} = \sqrt{\hbar/2M\omega}$ is the position uncertainty of the oscillator position in the ground state.

As it is shown, in Paper III, the "polaronic" term can be removed from the Hamiltonian by a suitable unitary transformation. As a result of this transformation, the tunneling amplitudes turn out to be dependent on the momentum operator and not only on the displacement. In the vibron representation, the transformed tunneling Hamiltonian is given by:

$$\tilde{H}_T = \sum_{k,q} t_{kq,S} e^{-(\varepsilon_t+\varepsilon_p)b+(\varepsilon_t-\varepsilon_p)b^\dagger} c_q^\dagger a_{k,S} + \text{H.c.} + \\ + \sum_{k,q} t_{kq,L} e^{-\varepsilon_p(b-b^\dagger)} a_{k,L} c_q + \text{H.c.}. \tag{4.10}$$

The tunneling Hamiltonian considered in Paper III and IV is obtained from Eq. (4.10) by linearizing the exponentials with respect to the vibron operators (see Eq. (6) in Paper III), which amounts to consider only single-vibron inelastic processes. This approximation is motivated by the fact that we are interested in the dynamics of the nanotube in a regime that is closed to its quantum-mechanical ground state, therefore only low-energy excitations (or, classically speaking, small amplitudes of oscillations) should play a relevant role.

The main idea on which the cooling effect discussed in Paper III and IV is based can be understood directly from the structure of the tunneling Hamiltonian shown in Eq. (4.10). The probability amplitude of inelastic electron tunneling processes through the STM tip-nanotube junction depends on the sum and the difference of the electromechanical coupling constants, which can be controlled externally by virtue of the voltage-dependence of the "polaronic" coupling constant ε_p. Therefore, if the voltage is set to a value for which $\varepsilon_p \sim \varepsilon_t$, according to Eq. (4.10), one would expect that the rate of inelastic processes involving vibron emission is significantly suppressed.

In the stationary regime, the effective unbalance between absorption and emission processes in favour of the former ones leads to a net decrease of the average number of vibrons, that is a phenomenon that, in some sense, can be interpreted as "cooling" of the mechanical system. The concept of cooling, although intuitively clear, should be perhaps used with some care in the present context, because the environment with which the mechanical system interacts here is far from thermodynamic equilibrium.

In order to fulfill the sort of "resonance" condition, $\varepsilon_p \sim \varepsilon_t$ that implies a net removal of energy from the oscillator, the "polaronic" coupling constant must be positive, $\varepsilon_p > 0$. It follows from Eq. (4.5) that the positive sign of ε_p corresponds to $\Delta G_S^{\rightarrow} > 0$, the condition for which the tunneling from the STM tip to the nanotube is suppressed at low temperatures. At this point, it is clear that for the tunneling current to work as an effective refrigerator of the mechanical system, it is necessary that the temperature of the STM tip is high enough to overcome the Coulomb blockade at the STM tip-nanotube junction.

However, in the regime of thermally-activated tunneling, the "backward" inelastic tunneling processes (i.e. those ones from the nanotube to the STM tip) should be taken into account. It is clear from Eq. (4.10) that they are detrimental for the performance of the cooling procedure because, as a consequence of time-reversal symmetry, the enhancement of absorption for "forward" processes would correspond to an equal increase of emission for the "backward" processes. No net decrease (and not even increase) of the average number of vibrons would be experienced in this case.

For this reason, in order to achieve the effective cooling of the mechanical degrees of freedom, it is crucial that the geometry of system implies that the rate of "backward" transitions is extremely lower than the rate of "forward" transitions through the nanotube-leads tunnel junction, that is $\Gamma_S \ll \Gamma_L$ or, equivalently, the STM tip-nanotube junction is much more resistive than the nanotube-leads junction.

We would like to stress that the cooling effect discussed here relies fundamentally on the quantum-mechanical nature of the electronic transitions. The possibility to achieve the necessary unbalance between vibron emission and absorption processes depends essentially on the fact that the respective rates are obtained as squares of probability amplitudes. To leading order in (t_S, ε_t, ε_p) the rates of single-vibron emission and absorption associated to inelastic electron tunneling processes through the STM tip-nanotube junction are given by:

$$\Gamma^{\leftrightarrow}_{S,\pm} = \Gamma^{\leftrightarrow}_{S}(\Delta G^{\leftrightarrow}_{S} \pm \hbar\omega)[\varepsilon_t^2 + \varepsilon_p^2 \pm 2\varepsilon_t\varepsilon_p]. \tag{4.11}$$

The first (second) term of (4.11) gives the probability for tunneling assisted by either absorption or emission of a vibron due to the tunneling ("polaronic") coupling alone, while the third term corresponds to the "interference" between these two mechanisms in the case of vibron emission ($-$) and absorption (+). In particular, $\varepsilon_p > 0$ if $\Delta G^{\rightarrow}_{S} > 0$ so that the interference is destructive (constructive) for tunneling accompanied by vibron emission (absorption). If $\Delta G^{\rightarrow}_{S} < 0$, the situation is reversed in the sense that $\varepsilon < 0$ and the interference is constructive (destructive) for emission (absorption).

A further comment can be made about Eq. (4.11). In principle, the rates for vibron emission/absorption processes are different not only for the $\varepsilon_{t,p}-$dependent part, but also for the mechanical energy exchanged in the two cases, $\pm\hbar\omega$, which affects the t ransition rates because of the energy-conservation constraint (see Eq. (3.11)). However, in all our considerations the temperature (of both the STM tip and the leads) is always assumed to be high over the scale defined by the quantum of mechanical energy, that is $T_S, T_L \gg \hbar\omega/k_B$.

In this regime, $\hbar\omega$ can be neglected with respect to $\Delta G^{\rightarrow}_{S}$, and therefore the presence of the mechanical degrees of freedom in Eq. (4.11) is manifested only in the $\varepsilon_{t,p}-$dependent part. In this sense the cooling effect described here does not depend on the conservation of energy during the tunneling processes. That feature is a distinctive feature, which makes it essentially different from all the procedures for active cooling that, in analogy with the basic principles

of laser cooling of trapped atoms, rely completely on electronic transitions promoted by the absorption of energy from the mechanical system (i.e., the difference in energy between the initial and final states matches exactly $\hbar\omega$).

In order to perform a quantitative analysis of the cooling effect expected on the basis of the physical considerations presented above, we followed the standard procedure to derive a quantum master equation for the reduced density matrix that describes only the mechanical degrees of freedom of the nanotube.

The starting point is the Lioville-von Neumann equation for the density matrix operator which represents the state of the *whole* system:

$$i\hbar\frac{d\rho}{dt} = [H, \rho(t)], \tag{4.12}$$

where H is the total Hamiltonian of the system, given by the sum of all the contributions introduced above, that is $H = H_S + H_L + H_m + H_{el,NT} + H_C + H_T$. It is convenient to apply the unitary transformation $U(t) = \exp(iH_0 t/\hbar)$, where $H_0 \equiv H_S + H_L + H_{el,NT} + H_C$ (i.e. switch to the "interaction picture"). The equation of motion for ρ then becomes $i\hbar d\rho_I/dt = [H_{TI}(t), \rho_I(t)]$, which can be recast in the following integral form

$$\frac{d\rho_I}{dt} = \frac{1}{i\hbar}[H_{TI}(t), \rho_I(-\infty)] - \frac{1}{\hbar^2}\int_{-\infty}^{t} dt^{'}[H_{TI}(t), [H_{TI}(t^{'}), \rho_I(t^{'})]], \tag{4.13}$$

which amounts to a second-order perturbative expansion in the tunneling amplitudes (i.e. "Born approximation"). The procedure that leads to the equations of motion for the mechanical subsystem can be summarized in the following points:

- Define the *reduced density matrix* operator:

$$\sigma = \mathrm{Tr}_{\mathrm{S+L}}[\rho]. \tag{4.14}$$

  The trace in Eq. (4.14) is performed over the electronic degrees of freedom of the STM tip and the leads, which are supposed to be weakly coupled to the nanotube. Any possible back-action effect of the nanotube on the STM tip and leads dynamics is not taken into account, which can be expressed by writing the total density matrix in the factorized form: $\rho \approx \sigma \otimes \rho_S \otimes \rho_L$, where ρ_S and ρ_L are equilibrium density matrices, i.e. $\rho_\alpha = Z^{-1}exp(-H_\alpha/k_B T_\alpha)$, where $\alpha = S, L$. The trace over the electronic degrees of freedom of the STM tip and the leads produces corresponding Fermi factors at temperatures T_S and T_L.

- Resolve σ with respect to the possible charge states of the nanotube, that is charged by one electron (1) or neutral (0). It means that the equation of motion for σ is multiplied by the operators $\hat{N}$ and $1 - \hat{N}$ and traced over the nanotube electronic degrees of freedom. This procedure results

in the equations of motion for the two density matrices $\sigma_1 \equiv \mathrm{Tr_e}[\hat{\mathrm{N}}\sigma]$ and $\sigma_0 \equiv \mathrm{Tr_e}[(1-\hat{\mathrm{N}})\sigma]$. These equations are non-Markovian, that is non-local in time.

- Similarly to what happens in the high-bias-voltage limit, in the high-temperature limit, enforced by the conditions $k_B T_S$, $k_B T_L \gg \hbar\omega$ the quantum master equations for $\sigma_{0,1}$ become local in time.

- Switch back to Schrödinger picture, which makes more transparent the analysis of the physical processes involved in the dynamics of $\sigma_{0,1}$.

The quantum master equations derived according to this procedure are given by:

$$\frac{d\sigma_1}{dt} = -\frac{i}{\hbar}[H_m,\sigma_1] + \frac{iF}{\hbar}[\hat{X},\sigma_1] - \Gamma_L^-\sigma_1 + \Gamma_S^+\left(\sigma_0 + \frac{1}{\lambda}\{\sigma_0,\hat{X}\} + \frac{1}{2\lambda^2}\{\sigma_0,\hat{X}^2\} + \frac{1}{\lambda^2}\hat{X}\sigma_0\hat{X}\right) -$$
$$- \Gamma_S^-\left(\sigma_1 + \frac{1}{\lambda}\{\sigma_1,\hat{X}\} + \frac{1}{\lambda^2}\{\sigma_1,\hat{X}^2\}\right) + \Gamma_L^+\sigma_0 + \mathcal{L}_\gamma\sigma_1 \tag{4.15}$$

$$\frac{d\sigma_0}{dt} = -\frac{i}{\hbar}[H_m,\sigma_0] + \Gamma_L^-\sigma_1 + \Gamma_S^-\left(\sigma_1 + \frac{1}{\lambda}\{\sigma_1,\hat{X}\} + \frac{1}{2\lambda^2}\{\sigma_1,\hat{X}^2\} + \frac{1}{\lambda^2}\hat{X}\sigma_1\hat{X}\right) -$$
$$- \Gamma_S^+\left(\sigma_0 + \frac{1}{\lambda}\{\sigma_0,\hat{X}\} + \frac{1}{\lambda^2}\{\sigma_0,\hat{X}^2\}\right) - \Gamma_L^+\sigma_0 + \mathcal{L}_\gamma\sigma_0, \tag{4.16}$$

where $\Gamma_\alpha^+ \equiv \Gamma_\alpha f_\alpha(E_0)$, $\Gamma_\alpha^- \equiv \Gamma_\alpha(1-f_\alpha(E_0))$. The operator $\mathcal{L}_\gamma$ describes the interaction with the *equilibrium* environment and, on the basis of general considerations on quantum dissipative systems, it can be written as [90]:

$$\mathcal{L}_\gamma[\sigma] \equiv -\frac{i\gamma}{2\hbar}[\hat{X},\{\hat{P},\sigma\}] - \frac{\gamma}{2\Delta x_{gs}^2}\coth\left(\hbar\omega/2k_BT_L\right)[\hat{X},[\hat{X},\sigma]]. \tag{4.17}$$

where$\gamma \equiv \omega/Q$ represents the rate of damping of the mechanical energy to the equilibrium environment, Q being the quality factor of the resonator, and $n_{th} = [\exp(\hbar\omega/k_BT)-1]^{-1}$ is the thermal average number of vibrons. Due to the geometry of the system, the thermal bath that determines the state of the nanotube at equilibrium can be identified with the phonon bath in the supporting leads. Therefore the temperature that enters the expression of n_{th}, must be intended as the temperature of the leads, that however, in the analysis presented in Paper III, is supposed to be the same as in the STM tip, i.e. $T_L = T_S \equiv T$.

In the high-temperature limit (T_S, $T_L \gg \hbar\omega/k_B$), the master equation becomes local in time and the dynamics of diagonal and off-diagonal elements decouple [65]. The analysis presented in Paper III focuses on the diagonal elements of the density matrix, denoted by $P_{0,1}(n,t) \equiv \langle n|\sigma_{0,1}(t)|n\rangle$, which provide the populations of the vibron states. They evolve in time according to

the equations of motion:

$$\frac{dP_0}{dt}(n,t) = \Gamma_L \left[1 - \frac{\varepsilon_p^2}{2}(1+2n)\right] P_1(n,t) + \Gamma_L \frac{\varepsilon_p^2}{2}(n+1)P_1(n+1,t) + \\ + \Gamma_L \frac{\varepsilon_p^2}{2} n P_1(n-1,t) - \Gamma_S[1+\varepsilon_t^2(1+2n)]P_0(n,t) + \mathcal{L}_\gamma[P_0(n,t)] \tag{4.18a}$$

$$\frac{dP_1}{dt}(n,t) = \Gamma_S \left[1 + \varepsilon_t\varepsilon_p + \frac{\varepsilon_t^2 - \varepsilon_p^2}{2}(1+2n)\right] P_0(n,t) + \\ + \Gamma_S \left(\varepsilon_t\varepsilon_p + \frac{\varepsilon_t^2+\varepsilon_p^2}{2} + \varepsilon_t\varepsilon_p\right) P_0(n+1,t) + \\ + \Gamma_S \left(\frac{\varepsilon_t^2+\varepsilon_p^2}{2} - \varepsilon_t\varepsilon_p\right) n P_0(n-1,t) - \Gamma_L P_1(n,t) + \mathcal{L}_\gamma[P_1(n,t)] \tag{4.18b}$$

The operator describing the relaxation to thermal equilibrium introduced in Eq. (4.17) assumes the following form in vibron representation:

$$\mathcal{L}_\gamma[P_\alpha(n)] \equiv \gamma(n+1)[(n_{th}+1)P_\alpha(n+1) - n_{th}P_\alpha(n)] - \\ - \gamma n[(n_{th}+1)P_\alpha(n) - n_{th}P_\alpha(n-1)], \tag{4.19}$$

where α =0,1. We remark that Eqs. (4.18a) and (4.18b) could be also directly derived as kinetic equations for the populations $P_{0,1}(n,t)$ based on the balance between the electronic transitions that populate the Fock state $|0/1,n\rangle$ and those that deplete it.

The stationary solution of Eqs. (4.18a) and (4.18b) can be found by means of a perturbative approach based on the smallness of the parameters ε_t^2, ε_p^2 and $1/Q$. The same method has been applied in both Paper III and IV, therefore it is worth to present it in some detail.

The problem of finding the stationary solution of linear systems of equations such as Eqs. (4.18a) and (4.18b) can be formulated in general as:

$$(\mathcal{L}_0 + \varepsilon\mathcal{L}_1) f(\xi) = 0, \tag{4.20}$$

where $\mathcal{L}_0$, $\mathcal{L}_1$ are linear operators defined in some vector space and ε a small dimensionless parameter. The independent variable ξ can be continuous or discrete. The perturbative approach to the problem represented by Eq. (4.20) is based on the search for a solution in the form of a power series in the small parameter ε, that is:

$$f(\xi) = f^{(0)}(\xi) + \varepsilon f^{(1)}(\xi) + \varepsilon^2 f^{(2)}(\xi) + \mathcal{O}(\varepsilon^3). \tag{4.21}$$

By replacing the perturbative expansion shown in Eq. (4.21) into Eq. (4.20) and imposing that terms at the same order in ε must be equal, it should be possible

to determine $f(\xi)$ at any desired level of accuracy. It is worth to remark that the power series shown in Eq. (4.21) does not imply that the zero-order term, $f^{(0)}(\xi)$, does not depend at all on ε, but rather that any deviation from $f^{(0)}(\xi)$ is proportional to some power of ε, therefore it can be considered as a correction to $f^{(0)}(\xi)$ of the order of (at most) ε, that is small if ε is small. In other terms, most of the physical character that can be attributed to the solution $f(\xi)$ is expected to be captured by the zero-order term $f^{(0)}(\xi)$.

However, we can see immediately that this procedure encounters some trouble if $\mathcal{L}_0$ and $\mathcal{L}_1$ are non-invertible, such as in the case of Eqs. (4.18a) and (4.18b). For example, substituting the zero-order term, $f^{(0)}(\xi)$ into Eq. (4.20), we obtain the equation $\mathcal{L}_0 f^{(0)}(\xi) = 0$, that surely has some non-trivial solution, since $\mathcal{L}_0$ is non-invertible, however it is not sufficient to determine $f^{(0)}(\xi)$ (i.e. all the functions in the kernel of $\mathcal{L}_0$ satisfy the equation).

In order to derive an equation that constraints the form of $f^{(0)}(\xi)$, it is necessary to consider the perturbative expansion of $f(\xi)$ up to the first order in ε. Substituting the Ansatz $f(\xi) = f^{(0)}(\xi) + \varepsilon f^{(1)}(\xi)$ into Eq. (4.20), to first order in ε we obtain the equation

$$\mathcal{L}_0 f^{(1)} = -\mathcal{L}_1 f^{(0)} \tag{4.22}$$

Let us now consider a left eigenvector of $\mathcal{L}_0$ corresponding to the eigenvalue 0 and denote it by $g_L(\xi)$, that is $g_L(\xi)\mathcal{L}_0 = 0$. Multiplying from left by g_L both sides of Eq. (4.22), we get

$$g_L \mathcal{L}_1 f^{(0)} = 0 \tag{4.23}$$

If the left eigenvector g_L is such that (g_L,$f^{(0)\dagger}$) are not linearly dependent ($f^{(0)\dagger}$ being the conjugate transpose of $f^{(0)}$), then Eq. (4.23) provides the wanted condition that makes possible to determine $f^{(0)}$. The existence of a g_L that is not linear dependent with respect to $f^{(0)\dagger}$ is not guaranteed *a priori*. For example, if $\mathcal{L}_0$ is Hermitian, then g_L coincides with the conjugate transpose of $f^{(0)}$, therefore Eq. (4.23) does not help to find $f^{(0)}$.

Fortunately, this is not the case for Eqs. (4.18a) and (4.18b), from which it results that the operator $\mathcal{L}_0$ has a block-diagonal structure, each block being defined by the 2×2 matrix:

$$\begin{pmatrix} -\Gamma_S & \Gamma_L \\ \Gamma_S & -\Gamma_L \end{pmatrix}.$$

The zero-order approximation of the unknown functions $\overline{P}_0(n)$, $\overline{P}_1(n)$ can be written in the form

$$\overline{P}_1(n) = \frac{\Gamma_S}{\Gamma_S + \Gamma_L}\overline{p}(n) \qquad \overline{P}_0(n) = \frac{\Gamma_L}{\Gamma_S + \Gamma_L}\overline{p}(n), \tag{4.24}$$

where the function $p(n)$ is presented in Eq. (9) in Paper III. In order to determine the function $p(n)$, the (infinite-dimensional) matrix corresponding to the

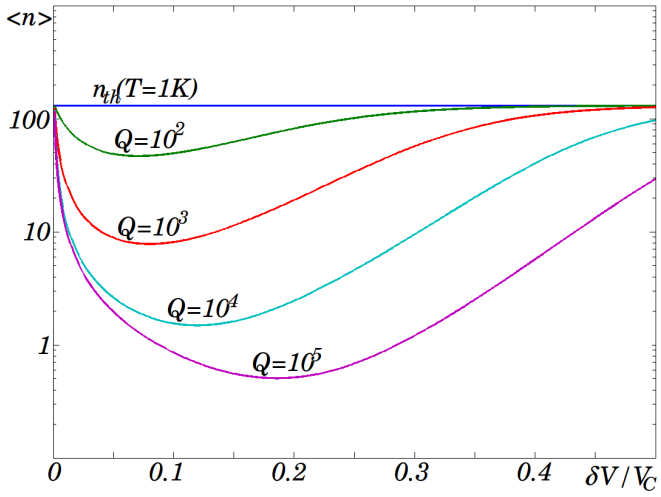

Figure 4.1: Average number of vibrons $\langle n\rangle$ plotted against the difference $\delta V = V_C - V$ between the Coulomb blockade threshold voltage V_C and the bias voltage V. Each curve corresponds to a different quality factor of the oscillator, while the straight line gives the thermal average number of vibrons at the temperature of $T = 1$ K. Other parameters used were: V_C= 2 mV, R_S = 2.5 MΩ, R_L = 250 kΩ, ε_t = 0.27, $\varepsilon_p(\propto \delta V) = 0.0 - 0.3$.

operator $\mathcal{L}_0$ can be multiplied by a row vector whose elements are all zeros except for the two (one for each charge state) at a given $n-$th position which are ones, that is $(\ldots 0 \ldots 0_{n-1}0_{n-1}1_n1_n0_{n+1}0_{n+1}\ldots)$. The resulting equation is a finite-difference equation of the form: $\mathcal{F}(n+1) - \mathcal{F}(n) = 0$ ($\mathcal{F}$ being a certain functional of $p(n)$, i.e. $\mathcal{F} \equiv \mathcal{F}[p_n]$), which implies $\mathcal{F} =$ constant. Since $\mathcal{F}(0) = 0$, it follows that $\mathcal{F}(n) = 0$ for every n, which corresponds to Eq. (8) in Paper III.

By means of the stationary probability distributions $\overline{P}_0(n)$ and $\overline{P}_1(n)$, we can determine the average number of vibrons that characterizes the mechanical state of the nanotube in the stationary regime resulting from the interaction with the nonequilibrium electronic environment: $\langle n\rangle = \sum_m m[\overline{P}_0(m) + \overline{P}_1(n)]$.

The expression of $\langle n\rangle$ is presented in Eq. 4.25, while $\langle n\rangle$ is plotted as a function of the bias voltage (for different values of the quality factor) in Fig. (4.1)

$$\langle n\rangle = \frac{\varepsilon_p^2 + (\varepsilon_t - \varepsilon_p)^2 + \omega n_{th}/(\Gamma_S Q)}{\varepsilon_p^2 + (\varepsilon_t + \varepsilon_p)^2 + \omega(n_{th}+1)/(\Gamma_S Q)} \tag{4.25}$$

In the limit $Q \to \infty$ in which the system is basically decoupled from the equilibrium environment, the stationary state of the nanotube is determined only by the vibron processes associated to the electronic transitions. From Eq. (4.25) it follows that the best performance of the cooling mechanism presented here (i.e. the minimum of $\langle n\rangle$) is achieved for $\varepsilon_p(\delta V^*) = \varepsilon_t/\sqrt{2}$ and the minimum average number of vibrons is given by $\langle n\rangle_{min} \approx 0.2$, that is a probability of nearly 80% to find the system in the vibrational ground state.

4.3 Cooling in the zero-bias limit

In Paper IV we investigated the conditions under which the suspended nanotube is effectively cooled through the same mechanism introduced in Paper 3 when the electronic tunneling transitions are promoted exclusively by the temperature drop between the STM tip and the leads, i.e. $T_S \gg T_L$ and both the STM tip and the leads are electrically grounded.

Although no electrostatic field is present between the STM tip and the leads, since $V = 0$, the electrostatic (or "polaronic") electromechanical coupling still exist, originated by the fact that when a "hot" electron tunnels from the STM tip to the nanotube, it creates a polarization charge of opposite sign in the STM tip. The electron is supposed to remain inside the nanotube for a time interval sufficiently long to assure that the electrostatic interaction with the polarization charge is not negligible.

The contribution to the total energy in this case can be evaluated analytically by means of a simple electrostatic model: two wires of lengths L and R (i.e. the effective radius of the STM tip) situated at distance d and charged by uniform distributions of charge with opposite sign. The result of this estimate is shown in Eq. (2) of Paper IV: the attractive electrostatic force (and therefore, the "polaronic" coupling constant) is inversely proportional to the $d - \hat{u}(z,t)$, where $\hat{u}(z,t)$ is the quantum field that describes the displacement of the nanotube. Expanding the force in Taylor series with respect to the small parameter $\hat{u}/d$, we obtain an Hamiltonian operator describing an interaction linear in the displacement and witn strength that can be controlled through the distance d, that is moving the STM tip farther or closer to the suspended nanotube.

The relevant electronic transitions that contribute to determine the stationary state of the suspended nanotube interacting with the nonequilibrium electronic environment are shown in Fig. (4.2). The temperature drop from the STM tip to the leads activate transitions from/to the thermally populated electronic states in the STM tip and the leads and the single level of the nanotube, characterized by energy E_0. The combination of electrostatic and tunneling coupling implies that, for $\varepsilon_p \simeq \varepsilon_t$ when electrons tunnel inelastically from the STM tip to the nanotube, they mainly cause the absorption of vibrons, whereas the emission is promoted for transitions in the opposite direction, that in the regime of thermally-activated transport occurs at the same rate as the "forward" processes. The effective cooling of the system is achieved if the rate of tunneling from the nanotube to the leads is significantly higher than the rate of tunneling from the STM tip to the nanotube. The quantitative analysis of the nanotube dynamics can be performed following the same approach outlined in Sec. (4.1). In order to describe the dynamics of its mechanical degrees of freedom, it is convenient to formulate the problem in terms of the operator $\sigma_+ \equiv \sigma_0 + \sigma_1$. A closed set of equations of motion is then obtained by introducing the operator $\sigma_- \equiv \sigma_0 - \sigma_1$, which accounts for the correlations between

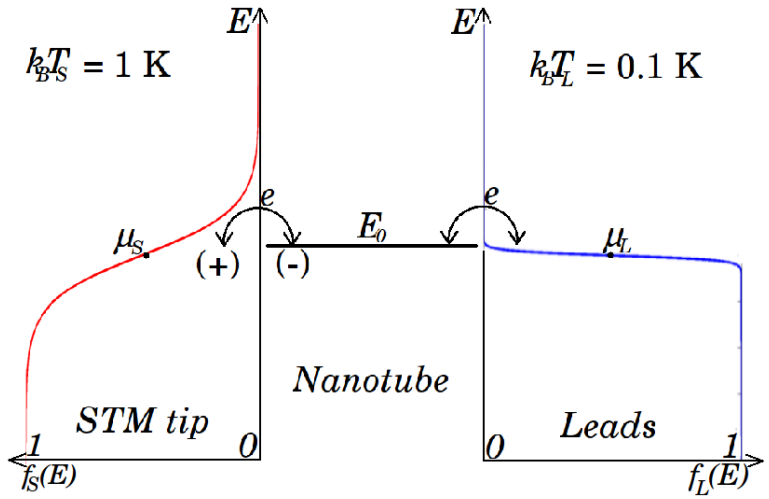

Figure 4.2: Schematic picture of the electronic transitions through the STM-nanotube system in the zero-bias limit. The (+) and (-) refer to the inelastic tunneling processes that leads to the emission (+) and absorption (-) of one vibron (see text).

the charge states of the nanotube. After shifting the origin of the reference frame to the equilibrium position of the "+" oscillator (defined by $\mathrm{Tr_m}(\mathrm{P}\sigma_+)$), the time evolution of σ_+ and σ_- results to be determined by the equations:

$$\frac{d\sigma_+}{dt} = -i\omega[H_m,\sigma_+] - i\omega\varepsilon_p\frac{\Delta\Gamma_\Sigma}{2\Gamma_\Sigma}[\hat{X},\sigma_+] - i\omega\frac{\varepsilon_p}{2}[\hat{X},\sigma_-] + \varepsilon_t^2\frac{\Gamma_S}{2}\left(\frac{1}{2}\{\hat{X}^2,\sigma_+\} + \hat{X}\sigma_+\hat{X}\right) + \\ + \varepsilon_t^2\frac{\Delta\Gamma_S}{2}\left(\frac{1}{2}\{\hat{X}^2,\sigma_-\} - \hat{X}\sigma_-\hat{X}\right) + \mathcal{L}_\gamma\sigma_+ \tag{4.26a}$$

$$\frac{d\sigma_-}{dt} = -i\omega[H_m,\sigma_-] - i\omega\varepsilon_p\frac{\Delta\Gamma_S}{\Gamma_\Sigma} - i\omega\frac{\varepsilon_p}{2}[\hat{X},\sigma_+] - \\ - \left(\Gamma_\Sigma\sigma_- + \varepsilon_t\Gamma_S\{\hat{X},\sigma_-\} + \frac{3}{4}\varepsilon_t^2\Gamma_S\{\hat{X}^2,\sigma_-\} - \varepsilon_t^2\frac{\Delta\Gamma_S}{2}\hat{X}\sigma_-\hat{X}\right) - \\ - \left(\Delta\Gamma_\Sigma\sigma_+ + \varepsilon_t\Delta\Gamma\{\hat{X},\sigma_+\} + \frac{3}{4}\varepsilon_t^2\Delta\Gamma_S\{\hat{X}^2,\sigma_+\} - \varepsilon_t^2\frac{\Gamma_S}{2}\hat{X}\sigma_-\hat{X}\right) + \mathcal{L}_\gamma\sigma_-, \tag{4.26b}$$

The operators H_m and $\hat{X}$ in Eqs. (4.26a) and (4.26b) are dimensionless, having been expressed in units of the fundamental scales $\hbar\omega$ and Δx_{gs}. The stationary state of the oscillator can be conveniently described through the "Wigner function representation" [91,92] of the operators $\overline{\sigma}_+$ and $\overline{\sigma}_-$ (that is, the stationary solutions of Eqs. (4.26a) and (4.26b)), which is defined as:

$$W_\pm(x,p,t) = \int_{-\infty}^{+\infty}\frac{d\xi}{\pi}e^{-i2p\xi}\langle x-\xi|\sigma_\pm(t)|x+\xi\rangle \tag{4.27}$$

The linear transformation introduced in Eq. (4.27) maps the quantum-mechanical operators to classical function of the position and momentum, $\hat{\mathcal{A}} \to \mathcal{A}(x,p)$,

where hereafter (x, p) will be always intended to be dimensionless (see Paper IV). In particular, the operator $\sigma_+(t)$, that describes the mechanical degrees of freedom of the nanotube, corresponds to the quasi-distribution function $W_+(x, p, t)$, for which the "quasi-" prefix reflects the fact that this function is negative in some regions of the phase space, and hence it cannot be interpreted as a probability density.

A pair of dynamical equations for the Wigner functions $W_\pm(x, p, t)$ is obtained by applying the transformation defined in Eq. (4.27) to all the terms in Eqs. (4.26a) and (4.26b), which results in the mappings

$$[\hat{P}^2, \sigma_\pm] \to -2\frac{i}{\hbar} p\partial_x W_\pm \tag{4.28}$$

$$[\hat{X}^2, \sigma_\pm] \to -2i\hbar x\partial_p W_\pm \tag{4.29}$$

$$\{\hat{X}^2, \sigma_\pm\} \to 2\left[x^2 - \frac{1}{4}\partial_p^2\right] W_\pm \tag{4.30}$$

$$\hat{X}\sigma_\pm\hat{X} \to \left[x^2 + \frac{1}{4}\partial_p^2\right] W_\pm \tag{4.31}$$

$$[\hat{X}, \sigma_\pm] \to i\partial_p W_\pm \tag{4.32}$$

$$\{\hat{X}, \sigma_\pm\} \to 2xW_\pm \tag{4.33}$$

$$[\hat{X}, [\hat{X}, \sigma_\pm]] \to -\partial_p^2 W_\pm \tag{4.34}$$

$$[\hat{X}, \{\hat{P}, \sigma_\pm\}] \to 2i\partial_p(pW_\pm), \tag{4.35}$$

where $\{\hat{A}, \hat{B}\} = \hat{A}\hat{B} + \hat{B}\hat{A}$ denotes the anticommutator of the operators $\hat{A}$ and $\hat{B}$. The Wigner functions $\overline{W}_\pm(x, p)$ associated to the stationary state of the oscillator coupled to the nonequilibrium electronic environment can be obtained from Eqs. (4.26a) and (4.26b) by imposing $\partial W_\pm(x, p, t)/\partial t = 0$ and they turn out to be

$$\begin{aligned}\omega(p\partial_x - x\partial_p)\overline{W}_+ = {} & \varepsilon_p\omega\frac{\Delta\Gamma_\Sigma}{\Gamma_\Sigma}\partial_p\overline{W}_+ + \frac{\varepsilon_p\omega}{2}\partial_p\overline{W}_- + \Gamma_S\frac{\varepsilon_t^2}{4}\partial_p^2\overline{W}_+ + \\ & \Delta\Gamma_S\frac{\varepsilon_t^2}{4}\partial_p^2\overline{W}_+ + \gamma\partial_p(p\overline{W}_+) + \coth(\hbar\omega/2kT_L)\frac{\gamma}{2}\partial_p^2\overline{W}_+ \end{aligned} \tag{4.36a}$$

$$\begin{aligned}\omega(p\partial_x - x\partial p)\overline{W}_- = {} & \frac{\omega\varepsilon_p}{2}\partial_p\overline{W}_+ - \left(\Delta\Gamma_\Sigma + 2\varepsilon_t\Delta\Gamma_S x - 2\varepsilon_t^2\Delta\Gamma_S x^2 - \frac{1}{4}\partial_p^2\right)\overline{W}_+ - \\ & - \left(\Gamma_\Sigma + 2\varepsilon_t\Gamma_S x - 2\varepsilon_t^2\Gamma_S x^2 - \frac{1}{4}\partial_p^2\right)\overline{W}_- + \gamma\partial_p(p\overline{W}_-) + \\ & \coth(\hbar\omega/2kT_L)\frac{\gamma}{2}\partial_p^2\overline{W}_-, \end{aligned} \tag{4.36b}$$

where $\Gamma_\Sigma \equiv \Gamma_S + \Gamma_L$, $\Delta\Gamma_\Sigma = \Delta\Gamma_S + \Delta\Gamma_S$, $\Delta\Gamma_\alpha \equiv \Gamma_\alpha(f_\alpha(E_0) - (1 - f_\alpha(E_0)))$, f_α being the Fermi-Dirac distribution of the STM tip ($\alpha = S$) and the leads ($\alpha = L$). It should be noticed that, in contrast to the kinetic description for the dynamics of the vibron populations (i.e. Eqs. (4.18a) and (4.18b)) discussed

in Paper III and Sec. (4.1), in Eqs. (4.36a) and (4.36b), all the processes, that is both "forward" and "backward" electronic transitions have been taken into account. The regime of thermally activated charge transport from the STM tip to the leads is defined by imposing $f_S(E_0) \simeq 1/2$, $f_L(E_0) \simeq 0$, $\Gamma_S/\Gamma_L \ll 1$.

The perturbative methode described in Sec. (4.1) can be adoperated in order to solve Eqs. (4.36a) and (4.36b). Corrections to the solution found through this procedure are at most of the order of the small parameters (ε_t^2, ε_p^2, Q^{-1}). After the change of variables, $A \equiv \sqrt{(}x^2 + p^2)$, $\varphi = \arctan(x/p)$, the perturbative solutions of Eqs. (4.36a) and (4.36b) result to be: $\overline{W}_+^0 = w(A)$, $\overline{W}_-^0 = -(\Delta\Gamma_\Sigma/\Gamma_\Sigma)w(A)$, where the function $w(A)$ in the regime of thermally-activated-single electron transport turns out to have a Gaussian shape (see Fig. (2) in Paper IV for comparison with the Wigner functions corresponding to the quantum ground state and the thermal equilibrium distribution function), $w(A) = Z^{-1}\exp[-(A/\theta)^2]$, where θ is given by:

$$\theta^{-2} = \frac{\frac{\varepsilon_p\varepsilon_t}{1+\Gamma_\Sigma^2} + \frac{1}{4Q\Gamma_S}}{\frac{\varepsilon_p^2}{1+\Gamma_\Sigma^2} + \frac{\varepsilon_t^2}{4} + \frac{\coth(\hbar\omega/2k_BT_L)}{2Q\Gamma_S}}. \tag{4.37}$$

Due to the Gaussian form of the quasi-distribution function $w(A)$, the quantity $\sqrt{\theta}$ provides also the root-mean-square fluctuations of the nanotube center-of-mass position (only the fundamental bending mode is taken into account).

In Fig. (4.3) the nonequilibrium-environment-induced fluctuations $\sqrt{\theta}$ are compared to the zero-point fluctuations that the oscillator has in the ground state and to the thermal equilibrium fluctuations (at the leads temperature T_L). For any value of the "polaronic" coupling constant ε_p, the nonequilibrium-induced fluctuations are significantly smaller than the thermal ones even at moderate quality factors and approach the value of the quantum fluctuations as Q increases. This behavior can be considered as an effective cooling of the mechanical degrees of freedom. In spite of the Gaussian form of the quasi-distribution function $w(A)$, the fluctuations represented by θ preserve their nonequilibrium character even in the limit in which the nanotube is completely decoupled by the equilibrium environment, that is $Q \to \infty$. In this case the stationary state of the oscillator is determined only by the interplay between the two mechanisms of electromechanical coupling, represented by the parameters ε_t and ε_p. It follows from Eq. (4.37) that the "cooled" state, characterized by fluctuations of the nanotube center-of-mass position that are smaller than the thermal ones, can be established only if both the coupling mechanisms are present in the system. If one of the two interactions is negligible in with respect to the other, the numerator at the right-hand-side of Eq. (4.37) $-$ which can be intepreted as an effective damping term on the basis of Einstein's relation between diffusion coefficient and viscosity$-$ vanishes, causing the broadening of quasi-distribution function $w(A)$, even beyond the width that characterizes the thermal distribution function. This behavior is in

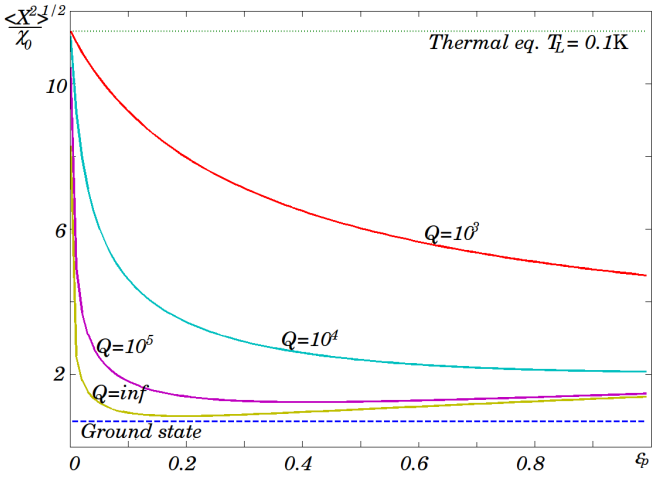

Figure 4.3: Comparison between the root-mean-square fluctuations of the center-of-mass nanotube position, $\sqrt{\langle X^2\rangle}$ (only the fundamental bending mode is considered), calculated with the Wigner functions corresponding to the ground state of the oscillator, the thermal equilibrium state at temperature T_L and the stationary state induced by the nonequilibrium electronic environment as a function of the "polaronic" coupling constant ε_p for different quality factors. Values of the relevant parameters: $\omega = 10^9$ Hz, $\Gamma_S = 10^7$ Hz, $\Gamma_L = 10^9$ Hz, $\varepsilon_t = 0.27$.

striking contrast with the equilibrium case, in which diffusion and damping are always both present, by virtue of the fluctuation-dissipation theorem.

We conclude this section with a few remarks about the problem of experimental detection of the cooling effect described here.

In the STM-nanotube system the physical quantity that is more natural to considered as experimentally accessible parameter carrying information about the mechanical state of the oscillator is the tunneling current. To leading order in the small parameters (ε_t, ε_p, Q^{-1}), the current obtained through the perturbative approached described in Sec. (4.1), is given by:

$$I = I_0[1 + \varepsilon_t^2\,(1 + 2\langle n\rangle)], \tag{4.38}$$

where $I_0 = e\Gamma_S$ with $\Gamma_S \approx k_B T/e^2 R_S$ (in the case of sub-Coulomb threshold bias and equal temperatures in the STM tip and the leads). If $k_B T \gg e\delta V^*$ then Γ_S remains independent of voltage in a certain voltage interval, where the differential conductance will be completely determined by the derivative of the average number of vibrons with respect to voltage, i.e. $\partial I/\partial V \cong 2I_0\varepsilon_t^2\partial\langle n\rangle/\partial V$. Therefore, the cooling effect will be reflected in the structure of the $dI/dV - V$ curves and accessible for experimental investigation. The presence of regions of negative differential conductance in the $dI/dV - V$ curves measured for suspended carbon nanotubes has been already reported experimentally [60] and generally attributed to the effects of inelastic electron tunneling processes [65].

In order to detect experimentally the cooling effect predicted above, the

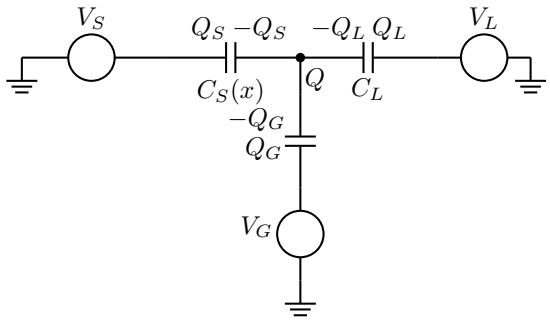

Figure 4.4: STM-carbon nanotube system with a gate electrode capacitively coupled to the nanotube.

most direct approach consists in the measurement of the root-mean-square fluctuations of the nanotube center-of-mass position, i.e. $\sqrt{\langle X^2 \rangle}$. Regarding this point, it is has been pointed out since a long time ago that the STM (combined with a current amplifier) can provide the basic building block for a quantum-limited position displacement sensor [86].

The tunneling current that can be measured at the output of such a device contains information about the displacement of the mechanical system under investigation but, at the same time, perturbs it with a very small back-action force, being this mainly due to the random momentum transfer associated with the tunneling electrons. The reduced back-action makes it possible for the STM-based displacement sensor to achieve a sensitivity that is several orders of magnitude larger than that one of conventional (e.g. capacitive) electromechanical transducers.

4.4 Appendix B

If the $x-$dependence of the gate capacitance is taken into account, following the procedure described in Sec. (3.3), one obtains a more complicated expression for the electrostatic force, which, for arbitrary values of the voltages V_S, V_L and V_G, is given by

$$F = \frac{[Q + C_L(V_L - V_S) + C_G(x)(V_G - V_S)]^2}{2C_\Sigma(x)} \frac{\partial C_S}{\partial x} - \frac{[Q + C_L(V_L - V_G) + C_S(x)(V_S - V_G)]^2}{2C_\Sigma(x)} \frac{\partial C_G}{\partial x} \tag{4.39}$$

The second term in Eq. (4.39) can be obtained from the first one by swapping the indexes $STM \rightarrow\leftarrow G$. The threshold value for the charge-dependent part of the electrostatic force can be calculated straightforwardly from Eq. (4.39) by

applying the condition $F(V_F) = 0$ and it turns out to be

$$V_F = \frac{1}{1 - \frac{C_S}{C_L+C_G}\frac{\partial C_G}{\partial x}\left|\frac{\partial C_S}{\partial x}\right|^{-1}} V_C - \frac{\frac{e}{2(C_L+C_G)} + \frac{C_L+C_S}{C_L+C_G}V_G}{1 - \frac{C_S}{C_L+C_G}\frac{\partial C_G}{\partial x}\left|\frac{\partial C_S}{\partial x}\right|^{-1}} \frac{\partial C_G}{\partial x}\left|\frac{\partial C_S}{\partial x}\right|^{-1} \tag{4.40}$$

In the limit $|\partial C_S/\partial x| \gg |\partial C_G/\partial x|$ we recover the result $V_F = V_C$ that has been used throughout the Thesis and in the Papers.

CHAPTER 5

Summary

The work presented in this thesis concerned the theoretical analysis of some phenomena that are expected to characterize the physical behavior of those systems in which the dynamics of mechanical and electronic degrees of freedom are strongly correlated, such as a suspended carbon nanotube (or, more generally, nanowire) in tunneling contact with the tip of a STM and its supporting leads.

Regarding the nanotube/nanowire remark, it is pertinent to remark that the analysis presented in this thesis, even though carbon nanotubes are mentioned throughout, is basically not dependent on the specific material properties of the movable part of the nanoelectromechanical system. Therefore, nothing prevents that phenomena assimilable to the electromechanical instability and the cooling effect presented here could be found, generally, in a large class of mechanical systems, characterized by different material properties and geometries.

The "shuttle-like" electromechanical instability in suspended-nanowired-based NEMS, which is described in Chapter 3 and in Papers I and II provides an example of such phenomena. The general conditions under which the instability arises and the development of the instability in limit-cycle-like oscillations are the same as in the conventional, point-like shuttle system. However, our analysis shows that the extended structure of the suspended nanowire considered here (in contrast to the "point-like" structure in the shuttle case) provides a more complicated (and richer) scenario for the dynamics of the system.

In particular, the results presented in Paper I suggest that, no matter how many vibrational modes are unstable, the stationary state that towards which the system evolves is characterized by the excitation of only *one* eigenmode. The other modes do not contribute to the self-sustained oscillations that the nanowire performs in the stationary regime.

In order to operate this selective excitation in a controllable way, the possibility to exploit the accuracy in the positioning of the STM tip has been investigated in Paper II. The results presented there indicate that the tuning of the electromechanical coupling of different modes originated by their different spatial profile can be sufficient to promote the selective instability of single vibrational modes.

In relation with the general problem of the characterization and control of the quantum dynamics of nanomechanical (although, in some sense, "macroscopic") oscillators, we investigated the conditions under which the electromechanical coupling in the STM tip-nanotube system can be exploited in order to produce an effective cooling of the mechanical degrees of freedom, down to a state as close as possible to the quantum ground state, that is, characterized by the minimum number of vibrational excitations.

As a first result of this analysis, it turns out the no effective cooling can occur if the bias voltage is above a certain threshold value, that in the geometry of the STM tip-nanotube system, is very close to the Coulomb blockade threshold value, which determines the rate of tunneling processes at low temperatures. Therefore, an alternative source of energy must be available in order to activate the tunneling transitions, including the inelastic processes that, if a suitable unbalance between the vibron emission and vibron absorption rate is established, remove energy from the mechanical system. The stationary state that originates from this effective cooling mechanism can be characterized by an average number of vibrons lower than 1 (0.2 is the best achievable), which means that the ground state is approached.

The cooling mechanism described here presents some peculiar features that mark the difference with respect to most of the other proposed scheme for ground state cooling of nanomechanical resonators. For example, it does not rely on the constraint of energy conservation that must be satisfied by the inelastic tunneling transition. In this sense, the tunneling here is seen just as a stochastic process, no coherence effects related to the wave-like nature of the electrons are involved. At the same time, the whole mechanism of cooling can be seen as a kind of quantum interference process, because the probability amplitudes depend on the sum and difference of the parameters that express the strength of the two mechanisms of electromechanical coupling that characterize the system, i.e. the position-dependent tunneling amplitude between the STM tip and the nanotube and the electrostatic force.

Independently of the performance in terms of minimum average number of vibrons achievable, the cooling mechanism described here is interesting from another (and more general) point of view, that is the analysis of the effect that the interaction with a far-from-equilibrium environment produces on the mechanical state of the suspended nanowire. In the zero-bias limit, in which the electronic transitions are activated only by the temperature drop from the STM tip to the supporting leads, the result of our analysis might appear slightly puzzling at the intuitive level. In absence of temperature gradient, the nanowire is in thermal equilibrium with the leads. When a higher temperature is applied to the STM tip, electronic tunneling processes transfer energy to and from the suspended nanotube. In the stationary regime, the mechanical system is in a state that corresponds to an effective temperature that is *lower* than the temperature of the STM tip (and of the leads), instead of simply intermediate between the STM tip and leads temperatures.

The analysis of the system from the thermodynamical point of view is still going on, besides the results presented in this thesis, in order to clarify in what sense and to what degree we can interpret the stationary state resulting from the coupling with the nonequilibrium environment as some sort of "effective equilibrium" state. Interestingly, a necessary condition for the system to experience the effective cooling, is that both the mechanisms of electromechanical coupling are present. If only one of them is active, its effect is to increase the diffusion of the system in energy space. The intepretation of the resulting quasi-distribution function as a state of effective thermal equilibrium appears dubious, since for a system interacting with a "true" equilibrium thermal bath, diffusion *and* damping (i.e. fluctuation and dissipation) are always both present.

The experimental investigation of the phenomena examined in this thesis (both in the pumping and cooling regimes) seems not a trivial task. Among the issues that should be dealt with carefully in order to observe such effects, there are the requirement of very high quality factors and a quite accurate spatial control of the in the local injection of tunneling current through the nanotube. Nevertheless, the tremendous at which the refinement of nanofabrication methods and the development of new measurement techniques proceed, suggest the idea that the experimental test of the phenomena described in this thesis is not completely unrealistic.

We can find at least two reasons which can motivate the interest in the experimental realization of this effect. At the purely scientific level, the selectivity associated to the simultaneous excitation of several vibrational modes provides an interesting example of how "simple" behaviors can emerge out of the dynamics of rather "complicated" systems.

From a more practical perspective, one might conceive several ways to exploit the large separation between the frequencies of the vibrational modes and the pronounced selective character of the electromechanical instability, for example to design sensors that do not need a time-varying driving signal in order to work (the STM tip could be replaced by something that could be patterned on a substrate, such as an atomic point contact). For some applications, the fact that the electromechanical instability described here requires a DC bias voltage might present some advantages over more conventional excitation schemes based on a resonant mechanism.

The possibility to transfer some of the knowledge acquired by purely curiosity-driven studies into practical realizations is one of the most relevant points in any discussion concerning the relationship between science and technology, that in the case of NEMS represent literally the two sides of the same coin. Although in principle the ability to *exploit* the natural phenomena for our aims does not improve our *understanding* the phenomena themselves, we consider positively the perspective that the research on NEMS in the forthcoming years will probably oriented to a large extent towards the development of novel devices for quite mundane purposes.

More NEMS-based applications can generate more extensive knowledge and deeper understanding of the fundamental principles underlying their physical behavior. That not only provides us with new challenging problems, but also induce us to look at old problems with new eyes. For example, the works presented in this thesis suggest that, in spite of the fact that thermodynamics and quantum mechanics have been elaborated and tested for more than one hundred years and have provided the basic tools to solve countless problems even outside the domain of physics, their application to the "intermediate" (neither "microscopic" nor "macroscopic") and sometimes seemingly bizarre world of nanoelecromechanical systems oblige us to reconsider them once again from their (solid?) foundations. Incidentally, thermodynamics and quantum mechanics are perhaps those ones which, more than any other branch of physics, have constantly led the mankind to confront with the limits of its comprehension of the natural phenomena.

It is not excluded that we will come to doubt (or even partially reject) some piece of well-established knowledge matured in different (more "micro-" or "macro-") contexts. Something like a journey for which neither the destination nor the return date are fixed.

In other words, an opportunity to grow, maybe wiser, but not necessarily older.

"*Ah, but I was so much older then*
I'm younger than that now"

My Back Pages, Bob Dylan (1964).

Acknowledgements

There are many people that I would like to thank not only for their professional and practical support, but most of all, to have made me enjoy the time I spent in Sweden so far, in spite of the darkness at 3.00 pm in the winter and the irreproducibile (by me) variety of vowels in the Swedish language.

First, I would like to thank my supervisor Leonid Y. Gorelik for the variety of concepts and perspectives related to physics that I had the opportunity to learn through him, and my examiner Mats Jonson, for the constant support. A collective thank should then be adressed to all the people that I met in these years in the Condensed Matter Theory group that for the stimulating atmosphere that everyone contributes to create in all the discussions during the lunch and coffee breaks, being them physics- or not physics oriented. Among them, I feel that a special thank should be reserved to Gustav Sonne, with whom I had the pleasure to share the office during the last five years.

Finally, I would like to express a word of gratitude towards all the people that I met in these years in the Physics and Chemistry departments, mainly due to my participation to the Faculty of Science research platform "Nanoparticle in interactive environments". The possibility to interact with people with different scientific and personal backgrounds and to share with them some great experiences such as the summer schools in Seoul and Tokyo has decisively contributed to the quality of my time in Sweden.

So long, and thanks for all the fish!

† Translation (from http://www.faqs.org/periodicals/200901/2122679441.html):
"I'd like not to pass away / Before I have had the chance to know / The black dogs who live afar / In Mexico asleep dreamlessly night and day / The monkeys whose bare asses show / Devourers of the tropics as they are / The silver spiders / With nests garnished with bubbles / I'd like not to pass away / Without knowing if the moon / Which poses as a doubloon / Has a pointy side / If the sun is cold / If the four seasons / Are really only four [...]
I'd like not to die / Before the invention of / Eternal roses / The two-hour day / The ocean on the mountain / The mountain in the ocean / The end of all distress / Colour-printing in the press / All the children being happy / And so much more stuff / That slumbers in the heads of / Ingenious engineers / Amused arborists / Solicitous socialists / Urban urbanists / And thoughtful thinkers [...]"

BIBLIOGRAPHY

[1] M. P. Blencowe, "*Nanoelectromechanical systems*", Contemporary Physics **46**, 249 (July-August, 2005).

[2] M. Blencowe, "*Quantum electromechanical systems*", Phys. Rep. **395**, 159 (2004).

[3] K. L. Ekinci and M. L. Roukes, "*Nanoelectromechanical systems*", Review of scientific instruments **76**, 061101 (2005).

[4] A. D. Armour, M. P. Blencowe, and Y. Zhang, "*Classical dynamics of a nanomechanical resonator coupled to a single-electron transistor*", Phys. Rev. B **69**, 125313 (2004).

[5] Y. M. Blanter, O. Usmani, and Y. V. Nazarov, "*Single-Electron Tunneling with Strong Mechanical Feedback*", Phys. Rev. Lett. **93**, 136802 (2004).

[6] M. P. Blencowe, J. Imbers, and A. D. Armour, "*Dynamics of a nanomechanical resonator coupled to a superconducting single-electron transistor*", New Journal of Physics **7**, 236 (2005).

[7] A. N. Cleland, *Foundations of nanomechanics*. Springer-Verlag, 2003.

[8] M. Desquesnes, S. V. Rotkin, and N. R. Aluru, "*Calculation of pull-in voltages for carbon-nanotube-based nanoelectromechanical switches*", Nanotechnology **13**, 120 (2002).

[9] X. Li, T. Ono, and Y. Wang, "*Ultrathin single-crystalline-silicon cantilever resonators: fabrication technology and significant specimen size effect on Young's modulus*", Appl. Phys. Lett. **83**, 3081 (2003).

[10] A. K. Naik, M. S. Hanay, W. K. Hiebert, X. L. Feng, and M. L. Roukes, "*Towards single-molecule nanomechanical mass spectrometry*", Nature Nanotechnlogy **4**, 445 (2009).

[11] M. C. Cross and R. Lifshitz, "*Elastic wave transmission at an abrupt junction in a thin plate with application to heat transport and vibrations in mesoscopic systems*", Phys. Rev. B **64**, 085324 (2001).

[12] Z. Hao, A. Erbil, and F. Ayazi, "*An analytical model for support loss in micromachined beam resonators with in-plane flexural vibrations*", Sensors and Actuators A **109**, 156 (2003).

[13] A. N. Cleland and M. L. Roukes, "*External control of dissipation in a nanometer-scale radiofrequency mechanical resonator*", Sensors and Actuators A **72**, 256 (1998), no. 3.

[14] F. R. Blom, S. Bouwstra, M. Elwenspoek, and J. H. J. Fluitman, "*Dependence of the quality factor of micromachined silicon beam resonators on pressure and geometry*", Journal of Vacuum Science and Technology **10**, 19 (1992).

[15] L. Sekaric, M. Zalalutdninov, R. B. Bhiladvala, A. T. Zehnder, J. M. Parpia, and H. G. Craighead, "*Operation of nanomechanical resonant structures in air*", Appl. Phys. Lett. **81**, 2641 (2002).

[16] P. Mohanty, D. A. Harrington, K. L. Ekinci, Y. T. Yang, M. J. Murphy, and M. L. Roukes, "*Intrinsic dissipation in high-frequency micromechanical resonators*", Phys. Rev. B **66**, 085416 (2002).

[17] B. H. Houston, D. M. Photiadis, M. H. Marcus, J. A. Bucaro, X. Liu, and J. F. Vignola, "*Thermoelastic loss in microscale oscillators*", Appl. Phys. Lett. **80**, 1300 (February, 2002).

[18] R. Lifshitz and M. L. Roukes, "*Thermoelastic damping in micro- and nanomechanical systems*", Phys. Rev. B **61**, 5600 (2000).

[19] A. D. Martino, R. Egger, and A. O. Gogolin, "*Phonon-phonon interactions and phonon damping in carbon nanotubes*", Phys. Rev. B **79**, 205408 (2009).

[20] C. Zener, *Elasticity and anelasticity of metals*. The University of Chicago Press, Chicago, 1948.

[21] A. S. Nowick and B. S. Berry, *Anelastic relaxation in crystalline solids*. Academic Press, 1972.

[22] L. Y. Gorelik, A. Isacsson, M. V. Voinova, B. Kasemo, R. I. Shekhter, and M. Jonson, "*Shuttle mechanism for charge transfer in Coulomb blockade nanostructures*", Phys. Rev. Lett. **80**, 4526 (May, 1998).

[23] R. I. Shekhter, Y. M. Galperin, L. Y. Gorelik, A. Isacsson, and M. Jonson, "*Shuttling of electrons and Cooper pairs*", J. Phys.: Condens. Matter **15**, R441 (2003).

[24] R. I. Shekhter, L. Y. Gorelik, M. Jonson, Y. M. Galperin, and V. M. Vinokur, "*Nanomechanical shuttle transfer of electrons*", J. Comput. Theor. Nanos. **4**, 860 (August, 2007).

[25] L. D. Landau and E. M. Lifshitz, *Statistical Physics*. Pergamon, 1980.

[26] A. Isacsson, L. Y. Gorelik, M. V. Voinova, B. Kasemo, R. I. Shekhter, and M. Jonson, "*Shuttle instability in self-assembled Coulomb blockade nanostructures*", Physica B **225**, 150 (1998).

[27] S. Strogatz, *Nonlinear dynamics and chaos: with applications to physics, biology, chemistry and engineering*. Perseus Books Group, 2001.

[28] M. T. Tuominen, R. V. Krotkov, and M. L. Breuer, "*Stepwise and hysteretic transport behavior of an electromechanical charge shuttle*", Phys. Rev. Lett. **83**, 3025 (1999).

[29] Y. Majima, K. Nagano, and A. Okuda, "*Displacement current staircase in mechanical single-electron turnstiles*", Jpn. J. Appl. Phys. **41**, 5381 (2002).

[30] K. Nagano, A. Okuda, and Y. Majima, "*Observation of Coulomb staircase of both tunneling current and displacement current in nanomechanical double barrier tunneling structures*", Appl. Phys. Lett. **81**, 544 (2002).

[31] A. Erbe, R. H. Blick, A. Tilke, A. Kriele, and J. P. Kotthaus, "*A mechanically flexible tunneling contact operating at radio frequencies*", Appl. Phys. Lett. **73**, 3751 (1998).

[32] A. Erbe, C. Weiss, W. Zwerger, and R. H. Blick, "*Nanomechanical resonator shuttling single electrons at radio frequencies*", Phys. Rev. Lett. **87**, 096106 (2001).

[33] D. V. Scheible, A. Erbe, and R. H. Blick, "*Tunable coupled nanomechanical resonators for single-electron transport*", New J. Phys. **4**, 86 (2002).

[34] D. R. Koenig, E. M. Weig, and J. P. Kotthaus, "*Ultrasonically driven nanomechanical single-electron shuttle*", Nature Nanotechnlogy **3**, 482 (2008).

[35] H. Park, J. Park, A. K. L. Lim, E. H. Anderson, A. P. Alivisatos, and P. L. McEuen, "*Nanomechanical oscillations in a single-C60 transistor*", Nature **407**, 57 (2000).

[36] A. V. Moskalenko, S. N. Gordeev, O. F. Koentjoro, P. R. Raithby, R. W. French, F. Marken, and S. E. Savel'ev, "*Nanomechanical electron shuttle consisting of a gold nanoparticle embedded within the gap between two gold electrodes*", Phys. Rev. B **79**, 241403(R) (2009).

[37] T. Nord and A. Isacsson, "*Impact of van der Waals forces on the classical shuttle instability*", Phys. Rev. B **69**, 035309 (2004).

[38] W. D. Ristenpart, J. C. Bird, A. Belmonte, F. Dollar, and H. A. Stone, "*Non-coalescence of oppositely charged drops*", Nature **461**, 377 (2009).

[39] A. J. Leggett, "*Testing the limits of quantum mechanics: motivation, state of play, prospects*", J. Phys.: Condens. Matter **14**, R415 (2002).

[40] V. B. Braginsky and F. Y. Khalili, *Quantum measurement*. Cambridge University Press, 1992.

[41] A. A. Clerk, M. H. Devoret, S. M. Girvin, F. Marquardt, and R. J. Schoelkopf, "*Introduction to quantum noise, measurement, and amplification*", Rev. Mod. Phys. **82**, 1155 (2010).

[42] A. D. O'Connell, M. Hofheinz, M. Ansmann, R. C. Bialczak, M. Lenander, E. Lucero, M. Neeley, D. Sank, H. Wang, M. Weides, J. Wenner, J. M. Martinis, and A. N. Cleland, "*Quantum ground state and single-phonon control of a mechanical resonator*", Nature **464**, 697 (2010).

[43] K. Schwab, E. A. Henriksen, J. M. Worlock, and M. L. Roukes, "*Measurement of the quantum of thermal conductance*", Nature **404**, p974 p974 974 (2000).

[44] I. Wilson-Rae, P. Zoller, and A. Imamoğlu, "*Laser cooling of a nanomechanical resonator mode to its quantum ground state*", Phys. Rev. Lett. **92**, 075507 (2004).

[45] J. Eschner, G. Morigi, F. Schmidt-Kaler, and R. Blatt, "*Laser cooling of trapped ions*", J. Opt. Soc. Am. B **20**, 1003 (2003).

[46] P. J. Koppinen and I. J. Maasilta, "*Phonon cooling of nanomechanical beams with tunnel junctions*", Physical Review Letters **102**, 165502 (2009).

[47] S. Zippilli, G. Morigi, and A. Bachtold, "*Cooling carbon nanotubes to the phononic ground state with a constant electron current*", Phys. Rev. Lett. **102**, 096804 (March, 2009).

[48] S.-H. Ouyang, J. Q. You, and F. Nori, "*Cooling a mechanical resonator via coupling to a tunable double quantum dot*", Phys. Rev. B **79**, 075304 (2009).

[49] F. Pistolesi, "*Cooling a vibrational mode coupled to a molecular single-electron transistor*", J. Low Temp. Phys. **154**, 199 (2009).

[50] I. Martin, A. Shnirman, L. Tian, and P. Zoller, "*Ground-state cooling of mechanical resonators*", Phys. Rev. B **69**, 125339 (2004).

[51] A. Naik, O. Buu, M. D. LaHaye, A. D. Armour, A. A. Clerk, M. P. Blencowe, and K. C. Schwab, "*Cooling a nanomechanical resonator with quantum back-action*", Nature **443**, 193 (2006).

[52] K. C. Schwab and M. L. Roukes, "*Putting mechanics into quantum mechanics*", Physics Today **58**, 36 (July, 2005).

[53] D. Qian, G. J. Wagner, W. K. Liu, M.-F. Yu, and R. S. Ruoff, "*Mechanics of carbon nanotubes*", Appl. Mech. Rev. **55**, 495 (2002).

[54] R. Saito, G. Dresselhaus, and M. S. Dresselhaus, *Physical properties of carbon nanotubes*. Imperial College Press, 1998.

[55] M. Monthioux and V. L. Kuznetsov, "*Who should be given the credit for the discovery of carbon nanotubes?*", Carbon **44**, 1621 (2006).

[56] S. Iijima, "*Helical microtubules of graphite carbon*", Nature **354**, 56 (1991).

[57] N. W. Ashcroft and N. D. Mermin, *Solid state physics*. Brooks/Cole, 1976.

[58] A. K. Hüttel, M. Pott, B. Witkamp, and H. S. J. van der Zant, "*Nanoelectromechanics of suspended carbon nanotubes*", New Journal of Physics **10**, 095003 (2008).

[59] M. S. Dresselhaus and P. C. Eklund, "*Phonons in carbon nanotubes*", Advances in Physics **49**, 705 (2000).

[60] B. J. LeRoy, S. G. Lemay, J. Kong, and C. Dekker, "*Electrical generation and absorption of phonons in carbon nanotubes*", Nature **432**, 371 (November, 2004).

[61] S. Sapmaz, P. Jarillo-Herrero, Y. M. Blanter, C. Dekker, and H. S. J. van der Zant, "*Tunneling in suspended carbon nanotubes assisted by longitudinal phonons*", Phys. Rev. Lett. **96**, 026801 (2006).

[62] V. Sazonova, Y. Yaish, H. Üstünel, D. Roundy, T. A. Arias, and P. L. McEuen, "*A tunable carbon nanotube electromechanical oscillator*", Nature **431**, 284 (2004).

[63] W. Izumida and M. Grifoni, "*Phonon-assisted tunnelling in interacting suspended single-wall carbon nanotubes*", New J. Phys. **7**, 244 (2005).

[64] B. Witkamp, M. Poot, and H. S. J. van der Zant, "*Bending-mode vibration of a suspended nanotube resonator*", Nano Lett. **6**, 2904 (2006).

[65] A. Zazunov, D. Feinberg, and T. Martin, "*Phonon-mediated negative differential conductance in molecular quantum dots*", Phys. Rev. B **73**, 115405 (2006).

[66] K. Flensberg, "*Electron-vibron coupling in suspended nanotubes*", New J. Phys. **8**, 5 (January, 2006). There is an erratum.

[67] M. M. J. Treacy, T. W. Ebbesen, and J. M. Gibson, "*Exceptionally high Young's modulus observed for individual carbon nanotubes*", Nature **381**, 678 (June, 1996).

[68] D. Garcia-Sanchez, A. S. Paulo, M. J. Esplandiu, F. Perez-Murano, L. Forró, A. Aguasca, and A. Bachtold, "*Mechanical detection of carbon nanotube resonator vibrations*", Phys. Rev. Lett. **99**, 085501 (2007).

[69] B. Lassagne, Y. Tarakanov, J. Kinaret, D. Garcia-Sanchez, and A. Bachtold, "*Coupling mechanics to charge transport in carbon nanotube mechanical resonators*", Science **325**, 1107 (2009).

[70] G. A. Steele, A. K. Hüttel, B. Witkamp, M. Poot, H. B. Meerwaldt, L. P. Kouwenhoven, and H. S. J. van der Zant, "*Strong coupling between single-electron tunneling and nanomechanical motion*", Science **325**, 1103 (2009).

[71] B. J. LeRoy, S. G. Lemay, J. Kong, and C. Dekker, "*Scanning tunneling spectroscopy of suspended single-wall carbon nanotubes*", Appl. Phys. Lett. **84**, 4280 (May, 2004).

[72] L. M. Jonsson, L. Y. Gorelik, R. I. Shekhter, and M. Jonson, "*Electromechanical instability in suspended carbon nanotubes*", Nano Lett. **5**, 1165 (March, 2005).

[73] L. M. Jonsson, L. Y. Gorelik, R. I. Shekhter, and M. Jonson, "*Electromechanical instabilities of suspended carbon nanotubes - multi mode excitations*", New J. Phys. **9**, 90 (April, 2007).

[74] L. M. Jonsson, F. Santandrea, L. Y. Gorelik, R. I. Shekhter, and M. Jonson, "*Self-organization of irregular nanoelectromechanical vibrations in multimode shuttle structures*", Phys. Rev. Lett. **100**, 186802 (2008).

[75] F. Santandrea, "*Selective Excitations of Transverse Vibrational Modes of a Carbon Nanotube through a "Shuttle-Like" Electromechanical Instability*", Physics Research International **2010**, 493478 (2010).

[76] I. O. Kulik and R. I. Shekhter, "*Kinetic phenomena and charge discreteness effects in granulated media*", Sov. Phys. JEPT **41**, 308 (1975).

[77] H. Grabert and M. Devoret, eds., *Single Charge Tunneling - Coulomb Blockade Phenomena in Nanostructures*. Plenum Press, New York, 1992.

[78] K. K. Likharev, "*Single-electron devices and their applications*", Proc. IEEE **87**, 606 (1999).

[79] H. Grabert, G.-L. Ingold, M. H. Devoret, D. Esteve, H. Pothier, and C. Urbina, "*Single electron tunneling rates in multijunction circuits*", Zeitschrift für physik B **84**, 143 (1991).

[80] F. Pistolesi and S. Labarthe, "*Current blockade in classical single-electron nanomechanical resonator*", Phys. Rev. B **76**, 165317 (2007).

[81] A. N. Koroktov, M. R. Samuelsen, and S. A. Vasenko, "*Effects of overheating in a single-electron transistor*", Journal of Applied Physics **76**, 3623 (1994).

[82] H. Reiss, *Methods of thermodynamics*. Dover, 1996.

[83] L. D. Landau and E. M. Lifshitz, *Electrodynamics of continuous media*. Butterworth-Heinemann, Oxford, 1998.

[84] D. K. Ferry and S. M. Goodnick, *Transport in nanostructures*. Cambridge University Press, 1997.

[85] B. Yurke and G. P. Kochanski, "*Momentum noise in vacuum tunneling transducers*", Phys. Rev. B **41**, 8184 (1990).

[86] M. F. Bocko and K. A. Stephenson, "*Vacuum tunneling probe: a nonreciprocal, reduced-back-action transducer*", Phys. Rev. Lett. **61**, 726 (1988).

[87] K. A. Stephenson, M. F. Bocko, and R. H. Koch, "*Reduced-noise nonreciprocal transducer based upon vacuum tunneling*", Phys. Rev. A **40**, 6615 (1989).

[88] M. F. Bocko, "*The scanning tunneling microscope as a high-gain low-noise displacement sensor*", Review of Scientific Instruments **61**, 3763 (1990).

[89] C. Presilla, R. Onofrio, and M. F. Bocko, "*Uncertainty-principle noise in vacuum-tunneling transducers*", Phys. Rev. B **45**, 3735 (1992).

[90] H.-P. Breuer and F. Petruccione, *The theory of open quantum systems*. Oxford University Press, 2002.

[91] E. Wigner, "*On the quantum correction for thermodynamic equilibrium*", Physical Review **40**, 749 (1932).

[92] M. Hillery, R. F. O'Connell, M. O. Scully, and E. P. Wigner, "*Distribution functions in physics: fundamentals*", Physics Reports **106**, 121 (1984).